



Room 14-0551  
77 Massachusetts Avenue  
Cambridge, MA 02139  
Ph: 617.253.5668 Fax: 617.253.1690  
Email: docs@mit.edu  
<http://libraries.mit.edu/docs>

## **DISCLAIMER OF QUALITY**

Due to the condition of the original material, there are unavoidable flaws in this reproduction. We have made every effort possible to provide you with the best copy available. If you are dissatisfied with this product and find it unusable, please contact Document Services as soon as possible.

Thank you.

**Some pages in the original document contain pictures, graphics, or text that is illegible.**

THE MESOSTRIATAL SYSTEM IN  
THE PRIMATE

by

Laura Feigenbaum Langer

B.A., Harvard University

SUBMITTED TO THE DEPARTMENT OF BRAIN  
AND COGNITIVE SCIENCES IN PARTIAL  
FULFILLMENT OF THE REQUIREMENTS FOR THE  
DEGREE OF

DOCTOR OF PHILOSOPHY

at the

MASSACHUSETTS INSTITUTE OF TECHNOLOGY

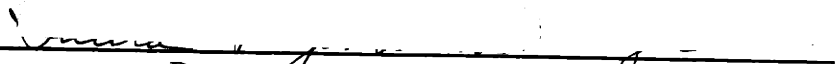
September 1989

JUN 7 1990

SCHERING-  
PLOUGH LIBRARY

Copyright (c) 1989 Massachusetts Institute of Technology

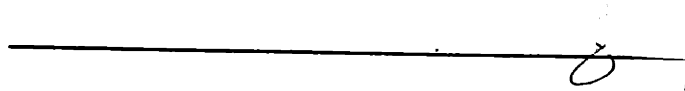
Signature of Author



Department of Brain and Cognitive Sciences

September 1, 1989

Certified by



Dr. Ann M. Graybiel

Thesis Supervisor

Accepted by



Dr. Emilio Bizzi

Head, Department of Brain and Cognitive Sciences

MASS. INST. TECH.  
SEP 20 1989

# The Mesostriatal System in the Primate

by

Laura Feigenbaum Langer

Submitted to the Department of Brain and Cognitive Sciences on September 1, 1989 in partial fulfillment of the requirements for the degree of Doctor of Philosophy.

## Abstract

The neuropil of the striatum is characterized by chemically distinct macroscopic compartments related to the spatial arrangement of most striatal projection neurons, interneurons and to the disposition of striatal afferents as well. This macroscopic compartmentalization was first defined histochemically in tissue sections within the adult striatum after staining for acetylcholinesterase [AChE] activity. Zones of low AChE staining, about 0.5-0.8 mm wide, called "striosomes", appear in the midst of an AChE-rich neuropil. A number of anatomically identifiable markers related to dopaminergic function in the striatum have also been shown to observe this striosomal compartmentalization. Ligand binding selective for dopamine receptor subtypes, immunostaining for tyrosine hydroxylase (TH), the synthetic enzyme of the catecholamines, and immunohistochemically detectable dopamine have uneven distributions in which the markers are particularly concentrated either in or out of zones corresponding to striosomes. Axonal transport studies in the rat and cat suggest that these compartmentalized marker distributions may reflect the presence of subsystems within the dopamine-containing mesostriatal pathways terminating preferentially in the striosomal or in the matrix compartments of the striatum.

In an attempt to identify the particular patterns of striatal termination of fibers from the dopamine-containing cell groups A8-A9-A10, we placed deposits of anterograde tracer (<sup>35</sup>S-methionine, WGA-HRP, fast blue and/or PHA-L) into different parts of the nigral cell complex in 25 squirrel monkeys (44 hemispheres) and compared the nigrostriatal labeling observed in such cases with the distribution of striosomes identified there with the aid of histochemical and immunohistochemical staining carried out on serially adjoining sections. Our results suggest that, in the primate, spatially separate parts of the dopamine-containing cell complex of the midbrain project, respectively, to striosomes and to the extrastriosomal matrix of the striatum. The A8 cell group and part of the pars

mixta were implicated as sources of a strikingly selective innervation of the extrastriosomal matrix. At least the lateral part of the main horizontal band of the pars compacta of the substantia nigra with its ventrally descending finger-like extensions was identified as projecting strongly to striosomes. The differential striatal projections of the medial part of the main horizontal band and of the overlying rostral pars mixta are more difficult to determine because injection sites at these rostral levels of the nigral complex are likely to affect both subdivisions. A major implication of our observations is that in the primate, the activity of such dopamine-containing afferents of the striatum may be different in striosomes and matrix by virtue of different regulation of striosome-projecting and matrix-projecting parts of the A8-A9-A10 cell complex. As a consequence, in any particular district of the striatum, neural processing (for example, of inputs from the neocortex) could be under the influence of different and perhaps even independent dopaminergic systems in adjoining striosomal and nonstriosomal zones.

Thesis Supervisor: Dr. Ann M. Graybiel  
Title: Professor of Neuroanatomy



## Acknowledgements

There are many people I would like to thank for giving me the encouragement, support and assistance that helped and guided me through my predoctoral years.

I owe my initial enthusiasm for neuroscience to Dr. James R. Stellar, who introduced me to the world of neuroscience research. This enthusiasm was further nurtured by Dr. Walle J. H. Nauta, who I want to thank for many supportive and encouraging discussions as well as for being a member of my thesis committee, and by Dr. Ann M. Graybiel, my thesis advisor. I especially want to thank Ann not only for providing me with a stimulating and challenging environment in which to work but also for being a source of constant patience, guidance and caring; her emotional support during both the painful and the happy times is cherished. The encouragement of these three individuals, and their great enthusiasm and love for teaching was, and continues to be, my source of "neuroscience inspiration".

The excellent technical help and guidance I received from Henry F. Hall, Diane Major, Glenn Holm, Judy Rankin and Yona Dornay is very much appreciated. Thanks goes to Mary Nastuk, Steve Wertheim, Elizabeth Connors, Fu-Chin Liu and Bruce Quinn for their advice, assistance and good humor as well as to Alice Flaherty for making hours of autoradiography more fun through cheerful darkroom chats.

In my interactions with each of the other members of my thesis committee, Dr. Richard J. Wurtman, Dr. Emilio Bizzi, and Dr. James H. Fallon, I received much encouragement and for their caring and support I feel grateful.

The patience and understanding of my husband, Dr. Robert Langer, have been instrumental to the completion of this thesis. It is with my deepest respect, love and admiration that I thank him for his support and encouragement.

My thesis work was funded by the Whitaker Health Sciences Fund and NIH 2 R01 NS 25529-01A1 (to AMG).

## **Dedication**

*This thesis is dedicated to the memory of my sister Dr. Susan Feigenbaum  
Levene and my mother Dorothy Lampert Feigenbaum.*

## Table of Contents

<b>Abstract</b>	<b>2</b>
<b>Acknowledgements</b>	<b>4</b>
<b>Table of Contents</b>	<b>6</b>
<b>List of Figures</b>	<b>7</b>
<b>1. Introduction: The Dopamine-Containing Neurons of the Mesostratial System in the Primate</b>	<b>9</b>
<b>2. The Mesostratial Projection I: Autoradiographic Results</b>	<b>42</b>
<b>3. The Mesostratial Projection II: Anterograde and Retrograde Results with Horseradish Peroxidase, Fast Blue and <i>Phaseolus vulgaris</i>-leucoagglutinin [PHA-L]</b>	<b>141</b>
<b>References</b>	<b>184</b>

## List of Figures

<b>Figure 1-1:</b> TH-positive neurons in the substantia nigra of the rat, cat and monkey.	19
<b>Figure 1-2:</b> TH-positive neurons in the nigral complex of the squirrel monkey.	22
<b>Figure 1-3:</b> Enhanced autoradiographic labeling in striosomes and in the matrix.	28
<b>Figure 1-4:</b> Sections through the nigral complex stained for AChE, TH- and CaBP-like immunoreactivity.	34
<b>Figure 1-5:</b> TH-like immunoreactivity in the human striatum.	37
<b>Figure 2-1:</b> Injection sites resulting in no striatal labeling.	50
<b>Figure 2-2:</b> Injection sites eliciting labeling of the matrix compartment.	52
<b>Figure 2-3:</b> Injection sites eliciting enhanced labeling of striosomes predominantly within the caudate nucleus.	54
<b>Figure 2-4:</b> Injection sites eliciting enhanced labeling of striosomes in both the caudate nucleus and putamen.	56
<b>Figure 2-5:</b> Injection sites eliciting labeling in the nucleus accumbens.	58
<b>Figure 2-6:</b> Injection sites resulting in mixed and homogeneous patterns of labeling.	60
<b>Figure 2-7:</b> Chartings of autoradiographic labeling observed along pipette tracks.	63
<b>Figure 2-8:</b> Striatal labeling of the matrix in case S3.	70
<b>Figure 2-9:</b> Drawing delineating zones for densitometry: case S3.	72
<b>Figure 2-10:</b> Striatal labeling of the matrix in case S5.	74
<b>Figure 2-11:</b> Drawing delineating zones for densitometry: case S5.	76
<b>Figure 2-12:</b> Injection site: case S3.	78
<b>Figure 2-13:</b> Injection site: case S5.	80
<b>Figure 2-14:</b> Enhanced labeling of striosomes: case S10R.	85
<b>Figure 2-15:</b> Drawing delineating zones for densitometry: case S10R.	87
<b>Figure 2-16:</b> Injection site: case S10R.	89
<b>Figure 2-17:</b> Enhanced labeling of striosomes: case S18L.	91
<b>Figure 2-18:</b> Enhanced labeling of striosomes: case S18L [light-field].	93
<b>Figure 2-19:</b> Injection site: case S18L.	95
<b>Figure 2-20:</b> Enhanced labeling of striosomes: case S20L.	98
<b>Figure 2-21:</b> Injection site: case S20L.	100
<b>Figure 2-22:</b> Enhanced labeling of striosomes in the putamen: case S11L.	103
<b>Figure 2-23:</b> Drawing delineating zones for densitometry: case S11L.	105
<b>Figure 2-24:</b> Injection site: case S11L.	107
<b>Figure 2-25:</b> Injection site [VTA]: case S19, rostral.	110
<b>Figure 2-26:</b> Injection site [VTA]: case S19, caudal.	112
<b>Figure 2-27:</b> Striatal labeling: case S19L.	114
<b>Figure 2-28:</b> Striatal labeling: case S19R.	116
<b>Figure 2-29:</b> Schematic representations of possible modes of termination.	129

<b>Figure 3-1:</b>	Injection sites: Cases with WGA-HRP.	148
<b>Figure 3-2:</b>	Injection sites: Cases with FB.	150
<b>Figure 3-3:</b>	Injection sites: Cases with PHA-L.	152
<b>Figure 3-4:</b>	Chartings of labeling along the pipette tracks: WGA-HRP and FB.	154
<b>Figure 3-5:</b>	Striatal labeling with WGA-HRP: case S14L.	156
<b>Figure 3-6:</b>	Striatal labeling with WGA-HRP: case S16L.	158
<b>Figure 3-7:</b>	Retrogradely labeled cells in striosomes: fast blue.	164
<b>Figure 3-8:</b>	PHA-L-labeled striatal fibers: single fibers in the matrix.	168
<b>Figure 3-9:</b>	PHA-L-labeled striatal fibers: in and out of striosomes.	170
<b>Figure 3-10:</b>	PHA-L-labeled striatal fibers: a dense plexus in the matrix.	172
<b>Figure 3-11:</b>	PHA-L injection site photograph: case S23R.	174

## **Chapter 1**

### **Introduction:**

# **The Dopamine-Containing Neurons of the Mesostriatal System in the Primate**

The relationship between the dopamine-containing neurons in the midbrain and neurons in the striatum has been a matter of intense interest ever since the pathogenesis of Parkinson's disease was linked to the degeneration of dopamine-containing neurons in the nigral complex (Barbeau, 1986; Eadie, 1963; Greenfield and Bonsaquet, 1953; Hassler, 1938; Jellinger, 1986). It is now known that different sets of dopamine-containing neurons are affected in different clinical disorders (Barbeau, 1986; Jellinger, 1986; Hirsch et. al., 1988; Uhl et. al., 1985). For example, in idiopathic Parkinson's disease and in certain other parkinsonian syndromes, including parkinsonism induced by metabolites of 1-methyl-4-phenyl-1,2,3,6-tetrahydropyridine (MPTP), the nigrostriatal pathway is much more severely affected than the mesolimbic pathway (Burns et. al., 1983; Deutch et. al., 1986; German et. al., 1988; Hirsch et. al., 1988; Jellinger, 1986; Uhl et. al., 1985). There are also other neurons damaged in these parkinsonian disorders, including neurons in the locus coeruleus and pedunculopontine region (Barbeau, 1986; Forno and Alvord, 1974; Hirsch et. al., 1987); however, the most consistent and severe damage in Parkinson's disease and MPTP-induced parkinsonism is in the nigral complex itself (Barbeau, 1986; Jellinger, 1986; Deutch et. al., 1986; Burns et. al., 1983). The implication of these patterns of degeneration is that the profound deficit in voluntary movement and other motor disabilities that are the hallmarks of parkinsonism are probably specifically attributable to dysfunction of the

nigrostriatal innervation. Accordingly, examining the functional relationship between these midbrain neurons and the striatum will necessarily add depth to current views of how the input-output processing of the striatum ultimately affects the control of voluntary motoric behavior.

### **The Anatomical Organization of the Substantia Nigra**

The neuroanatomical characteristics of the substantia nigra have been extensively described; however, these descriptions differ as to the types, sizes and even the distribution of neurons which make up the substantia nigra. The following account summarizes the most consistent anatomical characteristics from a range of articles and from personal observations. The classification of neuronal types and groups within the substantia nigra have been based on the study of material stained 1) for classic cytologic histology (e.g. Nissl stains or hematoxylin and eosin), 2) by the Golgi method, 3) by methods localizing neurotransmitter-specific elements [for example, for dopamine-containing neurons: histofluorescent methods and immunohistochemical localization of tyrosine hydroxylase (a catecholamine synthesizing enzyme) and/or dopamine], 4) by any of the preceding methods in conjunction with retrograde or anterograde tract tracing.

The substantia nigra is commonly divided into at least two regions, the pars compacta and the pars reticulata, on the basis of cell type and density. A third subdivision of the substantia nigra, dorsolateral to the pars compacta, called the pars lateralis, is recognized by many investigators, although it is most often considered to be part of the pars reticulata. A fourth subdivision, the pars mixta, specific to primates, is usually not distinguished from the pars compacta; however, the diversity of cell types and projections originating from this somewhat segregated part of the substantia nigra, dorsal to the pars compacta, suggests that it should be considered as a separate nigral region.

*The substantia nigra, pars compacta:* The pars compacta is made up of numerous densely packed neurons. In Nissl-stained sections, these neurons are characterized by dense staining of the Nissl substance within the cytoplasm, a pale nucleus, rarely centrally located within the cell body, and a darkly staining nucleolus (Poirier et. al., 1983; Domesick et. al., 1983). In addition, most of the neurons of the pars compacta contain the neurotransmitter dopamine (Anden et. al., 1964; Arsenault et. al., 1988). They are also the principal source of nigrostriatal afferents. According to Fallon and coworkers (Fallon et. al., 1978), two functionally distinct groups of neurons within the pars compacta may be distinguished; in the rat, the dorsally-situated and horizontally-oriented neurons appear to project prominently to allocortical regions and the more ventrally located neurons with dorsoventrally-oriented dendrites innervate the striatum. In the cat and monkey an analogous organization of layers has not been characterized, but there is substantial evidence for the existence of segregated groups of neurons in the pars compacta with functionally-distinct patterns of projection; these subdivisions will be discussed in a following section.

*The substantia nigra, pars reticulata:* There is no clearly definable border between the pars compacta and the more ventrally situated pars reticulata. These two regions are generally differentiated by their cell density. Compared to the pars compacta, there are far fewer neurons in the pars reticulata [at least 50% fewer in the rat and cat and an estimated 88% fewer in the monkey (Poirier et. al., 1983)] and the pars reticulata is more diffusely organized. The cell bodies of neurons within the pars reticulata are embedded in a dense network of fibers; these prominent fibers may be observed in sections immunostained to reveal gamma-aminobutyric acid (GABA), substance P and enkephalin (Smith et. al., 1987; McLean et. al., 1985; Mai et. al., 1986). In Nissl-stained sections, the neurons of



the pars reticulata are more lightly stained than those in the pars compacta neurons (Poirier et. al., 1983; Domesick et. al., 1983). The majority of these neurons may also be distinguished by their expression of GABA- and GAD-like immunoreactivity (Mugnaini and Oertel, 1985; Smith et. al., 1987).

The main projections of the neurons of the pars reticulata are to thalamic nuclei, the superior colliculus and the midbrain tegmentum. In the rat, the neurons of origin of the nigrothalamic, nigrotectal and nigrosegmental pathways are organized into distinct longitudinal zones (Faull and Mehler, 1978). Similarly in the monkey, these nigrofugal neurons are segregated into distinct cell groups (Beckstead and Frankfurter, 1982; Francois et. al., 1984). The nigrothalamic neurons are predominantly located in the rostral two-thirds of the pars reticulata (Beckstead and Frankfurter, 1982) and appear to be arranged in the form of clusters (Parent et. al., 1983a). The nigrotectal neurons are the least numerous of the nigrofugal neurons and are located laterally within the pars reticulata and also within the pars lateralis and pars mixta (Francois et. al., 1984). The nigrosegmental cells are most abundant in the caudal part of the pars reticulata (Beckstead and Frankfurter, 1982). There are also some nigrostriatal neurons located within the pars reticulata but they are thought to account for less than 2% of the nigrostriatal innervation in the primate brain (Francois et. al., 1984).

*The substantia nigra, pars lateralis:* Dorsolateral to the pars reticulata is the pars lateralis, often not differentiated from the pars reticulata. The neurons of the pars lateralis are very similar to those of the pars reticulata in terms of their shape and staining characteristics (Poirier et. al., 1983; Juraska et. al., 1977; Hanaway et. al., 1970). When this nigral subdivision has been described, it is distinguished by its sparseness of neurons and the larger size of its neurons compared to the neurons of the pars reticulata (Francois et. al., 1985; Rioch, 1929). In the cat, it has been

shown to be rich in somatostatin-immunoreactive fibers (Graybiel and Elde, 1983). In addition, in the monkey, the pars lateralis contains almost exclusively nigrotectal neurons (Francois et. al., 1985; Beckstead and Frankfurter, 1982).

*The substantia nigra, pars mixta:* In the monkey, dorsal and caudal to the pars compacta is a loosely organized collection of neurons which have been described in many studies but are rarely distinguished from the pars compacta (Arsenault et. al., 1988; Crosby and Woodburne, 1943; Davis and Huffman, 1968; Kusama and Mabuchi, 1970). This group of neurons may also be analogous to those neurons described in the human brain as belonging to the pars gamma and all or part of the pars beta of the pars compacta (Olszewski and Baxter, 1954). According to Francois and colleagues (Francois et. al., 1984), this region consists of a mixture of cells cytologically similar to neurons of the pars compacta and the pars reticulata, containing "an approximately equal number of nigrostriatal, nigrothalamic and nigrotectal neurons (and probably other neuronal efferent populations)" (Francois et. al., 1984); due to its mixture of nigrofugal cells, these authors suggest that the pars mixta be recognized as distinct from the pars compacta.

*The cytology of the substantia nigra:* The preceding anatomical subdivisions were based largely on nigral connectivity and some cellular morphological characteristics; however, it is necessary to point out that there are large variations in the literature concerning the types and sizes of nigral neurons. For example, the diameters of neurons reported range from  $8\mu\text{m}$  (Hanaway et. al., 1970) to  $74\mu\text{m}$  (Juraska et. al., 1977) in the rat and similarly,  $12\text{-}99\mu\text{m}$  in the monkey (Schwyn and Fox, 1974). Many investigators have attempted to distinguish different types of neurons on the basis of cytological characteristics such as the density of Nissl staining or the size of the cell body, however, the results of these studies vary significantly.

Generally, two or three "types" of neurons are described. For example, Domesick and coworkers (Domesick et. al., 1983) reported, in Nissl-stained material in the rat, the existence of two types of cells: one type distinguished by darkly stained Nissl substance (putative dopamine-containing) with neuronal diameters of 22-40 $\mu$ m and another group of more lightly staining (non-dopaminergic) neurons, 18-35 $\mu$ m wide. Hanaway and coworkers (Hanaway et. al., 1970) also described two nigral cell types, a small (8-11  $\mu$ m) and medium-sized (12-17 $\mu$ m) population of neurons, as did Hajdu and coworkers (Hajdu et. al., 1973), reporting neuronal diameters of 8-25 $\mu$ m. Poirier, Giguere and Marchand (Poirier et. al., 1983) reported four different types of neurons with mean diameters ranging from 7 to 29 $\mu$ m. However, the last three studies are at odds with other reports, based largely on Golgi-stained material, of neuronal diameters minimally up to 40 $\mu$ m in the rat. For example, Gulley and Wood (Gulley and Wood, 1971) and Juraska and coworkers (Juraska et. al., 1977) described three types of neurons. According to Gulley and Wood, these groups were represented by large (25-40 $\mu$ m), medium (15-20 $\mu$ m) and small (10-12 $\mu$ m) neurons. Juraska and coworkers also described large (45-74 $\mu$ m), medium (19-46 $\mu$ m) and small (11-20 $\mu$ m) neurons; apparently even with the Golgi method, authors do not agree on the maximal size of the neurons observed.

In the cat and monkey, such variations in neuronal size and type also exist. Poirier and colleagues (Poirier et. al., 1983) recognized, as in the rat, four types of neurons: the compacta-, reticulata-, intermediary- and globular-type neurons. In all three species the compacta-type was most abundant (85% of the total population in the monkey, 58% in the cat and 44% in the rat) compared to the other three types. In contrast, Hirosawa (Hirosawa, 1968) in the monkey and Rinvik and Grofova (Rinvik and Grofova, 1970) in the cat recognized only a single, neuronal cell type. Schwyn and Fox (Schwyn and Fox, 1974) describing Golgi-

stained neurons and electron micrographs indicated that they believed they could distinguish three types of neurons on the basis of cell size, but that there were no substantial cytological differences to clearly differentiate them.

It is not clear why there are such large discrepancies in the literature concerning the types and sizes of nigral neurons. Due to the wide variety of reported sizes of neurons, it would appear that the size of the neuron is the least valuable, distinguishing feature of any particular group of nigral neurons. The most consistent picture that emerges from these studies is that generally neurons within the region of the pars compacta can be distinguished from the neurons of the pars reticulata based on certain cytological characteristics, such as the pattern Nissl staining within the cell body (Domesick et. al., 1983; Gulley and Wood, 1971; Poirier et. al., 1983), but these neuronal groups may be best differentiated by their neurotransmitter content, as described previously. Those neurons observed to be dissimilar to the majority of neurons either in the pars compacta or pars reticulata, such as the rare, "achromatic" cells (Schwyn and Fox, 1974), the small, globular-type neurons (Poirier et. al., 1983) and the small, short-axoned neurons (Francois et. al., 1979) are generally believed to be interneurons.

### **The Mesencephalic Dopamine Neuron System**

In addition to the topographical subdivisions of the substantia nigra, as described above, the mesencephalic dopamine neurons within the region of the substantia are also classified into subdivisions. The segregation of monoaminergic cells into distinct groups was first described by Dahlstrom and Fuxe in the early 1960's (Dahlstrom and Fuxe, 1964). The midbrain dopamine-containing neurons were termed the A8, A9 and A10 cell groups corresponding to the retrorubral area (dorsal and caudal to the pars compacta), the substantia nigra, pars compacta, proper and the ventral tegmental area (medial to the pars compacta), respectively.

In other species these cell groups have also been referred to as C8, C9, and C10 (Hubbard and DiCarlo, 1974; DiCarlo et. al., 1973) [for catecholamine neurons in the squirrel monkey] or M8, M9 or M10 (Garver and Sladek, 1975) [to distinguish catecholamine neurons in the macaque monkey]. In addition, it was believed that from these cell groups two major projection systems could be distinguished: a nigrostriatal projection (originating from A9 and terminating exclusively in the striatum) and a mesolimbic projection (originating from A10 and terminating within a variety of limbic forebrain structures). It soon became evident, however, from studies with anterograde and retrograde tract tracing methods, that the "mesolimbic" and "nigrostriatal" distinctions were not absolute: for example, the striatum does not receive "exclusive" input from the A9 cell group; cell group A8 projects strongly to the striatum and A10 neurons also appear to project to at least the ventral part of the caudate-putamen complex.

Most recently, the dopamine-containing neurons of the midbrain have come to be viewed more as a single continuous band of cells with somewhat overlapping and widespread terminal fields. The mesencephalic projection systems are generally referred to in terms of their fields of terminal projections: the mesostriatal, mesocortical (or mesolimbocortical), mesodiencephalic and mesopontine systems. These systems reflect the distribution of fibers from the A8-A9-A10 cell complex to, respectively, 1) the caudate nucleus, putamen, nucleus accumbens and globus pallidus, 2) the forebrain limbic and cortical areas [olfactory bulb, anterior olfactory nuclei, olfactory tubercle, islands of Calleja, lateral septal nucleus, interstitial nucleus of the stria terminalis, piriform cortex, amygdala, ventral entorhinal cortex, hippocampus, suprarhinal cortex, pregenual anteromedial cortex, perirhinal cortex and temporal association cortex], 3) the subthalamic nucleus and lateral habenula, and 4) the locus coeruleus (Bjorklund and Lindvall, 1984).

Within these mesencephalic projection systems there are also non-dopamine-containing neurons (Thierry et. al., 1980; Van der Kooy et. al., 1981; Swanson, 1982; Loughlin and Fallon, 1983). For example, as many as 15% of the neurons within the ventral tegmental area which project to the nucleus accumbens may be non-dopaminergic (Swanson, 1982); however, less than 5% of the mesencephalic neurons projecting to the caudate nucleus and putamen appear to be non-dopamine-containing (Van der Kooy et. al., 1981). The mesostriatal afferents are apparently predominantly ipsilateral. There is some evidence for the existence of a very minor contralateral mesostriatal projection, but the majority of these projection fibers originate largely within the ventral tegmental area (Royce, 1978; Fass and Butcher, 1981; Loughlin and Fallon, 1982). In the following sections, the discussion will be limited to those mesostriatal connections between the A8-A9-A10 cell complex and the caudate nucleus, the putamen and the nucleus accumbens.

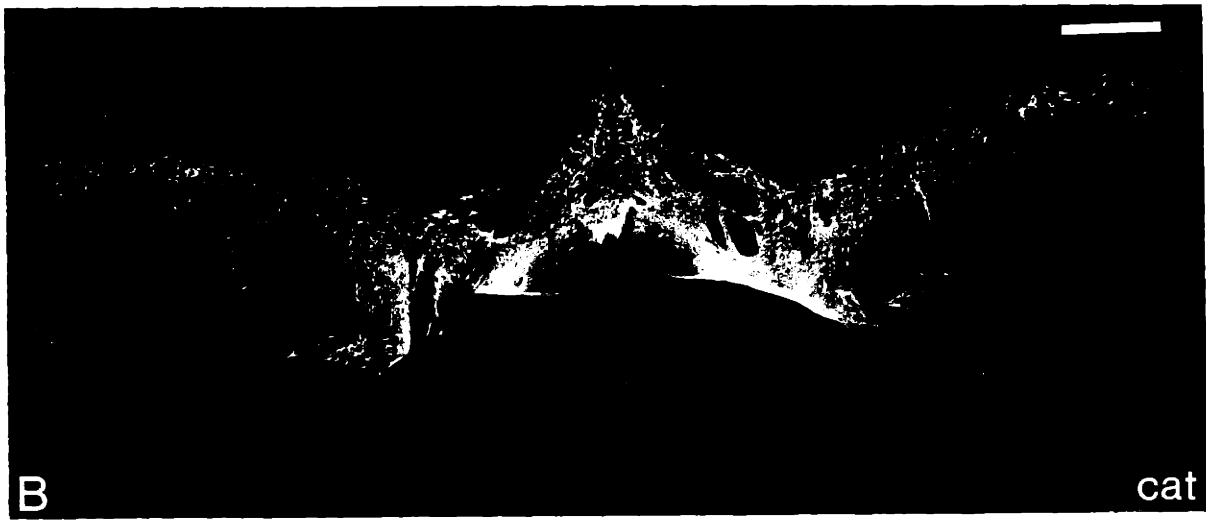
*Cell group A10: the ventral tegmental area.* The ventral tegmental area, or cell group A10, is particularly developed in the rat brain. These neurons form a very large cell complex extending from the midline region, at the level of the mammillary bodies, following the caudal part of the third ventricle, to midline regions at the level of the raphe nuclei. Midway from its most rostral extent, the cells of the ventral tegmental area extend far laterally, intermingling with the neurons of the pars compacta as shown in Fig. 1. In the cat and monkey these cells have a similar anteroposterior distribution, however, the cell group is somewhat smaller and more medially confined [see Fig. 1]. Among the three species, the ventral tegmental area appears to be the least extensive in the monkey. The catecholaminergic neurons of cell group A10 are generally restricted to an almost triangular region at the midline, medial to the pars compacta, and are bordered laterally by the fibers of the oculomotor nerve [see Fig. 2]. Some neurons

of the A10 cell group are intermingled with these oculomotor nerve root fibers. In the caudal part of the ventral tegmental area, the medio-lateral width (in frontal sections) of the triangular region diminishes; this group of cells is bordered ventrally by the interpeduncular nucleus and dorsally by the oculomotor nucleus. In most cytological descriptions, the neurons of the ventral tegmental area may be distinguished from the pars compacta neurons by their somewhat lessened intensity of catecholamine histofluorescence (Hubbard and DiCarlo, 1974; DiCarlo et. al., 1973) and their smaller and rounder appearance (Arsenault et. al., 1988; Francois et. al., 1985; Garver and Sladek, 1975; Poirier et. al., 1983).

*Cell group A9: the pars compacta.* The pattern of distribution of the dopamine-containing neurons of the pars compacta varies among species. [See Fig. 1]. In the rat, the dopaminergic neurons form a dense, cellular layer in the dorsal and medial parts of the substantia nigra [see also (Hokfelt et. al., 1984a)]. In the cat, these cells appear to be more widely distributed throughout the substantia nigra, although some distinct groups of densely-packed neurons may be observed, for example, in the caudomedial part of the pars compacta (Jimenez-Castellanos and Graybiel, 1987a). As shown in Fig. 1, the organization of the dopamine-containing neurons in the squirrel monkey appears more complex than was found in either the rat or the cat. There is a dense band of cells particularly in the dorsomedial pars compacta which extends laterally in progressively caudal parts of the nigra, maintaining a position lateral to the medial lemniscus at its most caudal extent [see Fig. 2]. Many of these densely-packed cells are oriented dorsoventrally and grouped into elongated finger-like zones, where numerous cells appear to extend their dendritic processes ventrally into the region of the pars reticulata. A generally similar organization of neurons within the pars compacta has also been demonstrated in the human brain, designated as the pars alpha (Hassler, 1938;

**Figure 1-1:** TH-positive neurons in the substantia nigra of the rat, cat and monkey. Coronal sections through the rostral part of the substantia nigra in the rat (A), cat (B) and monkey (C) illustrate differences in the distribution of neurons and neuropil immunostained for tyrosine hydroxylase in the three species. These sections were photographed as reverse-contrast images so that neurons appear white against a dark background. Scale bar = 1 mm.



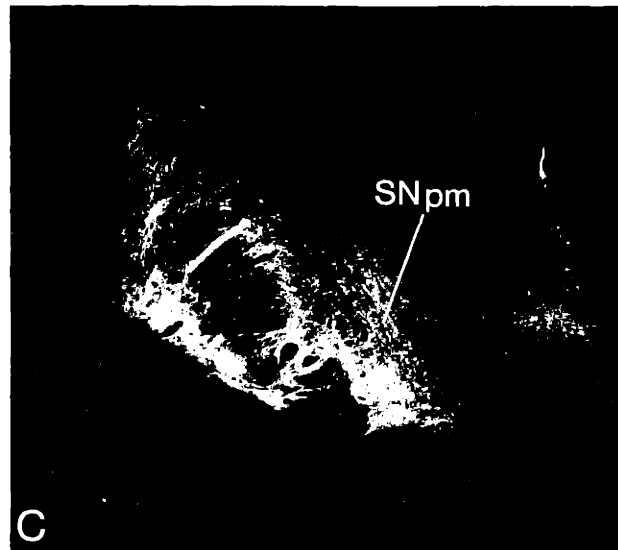
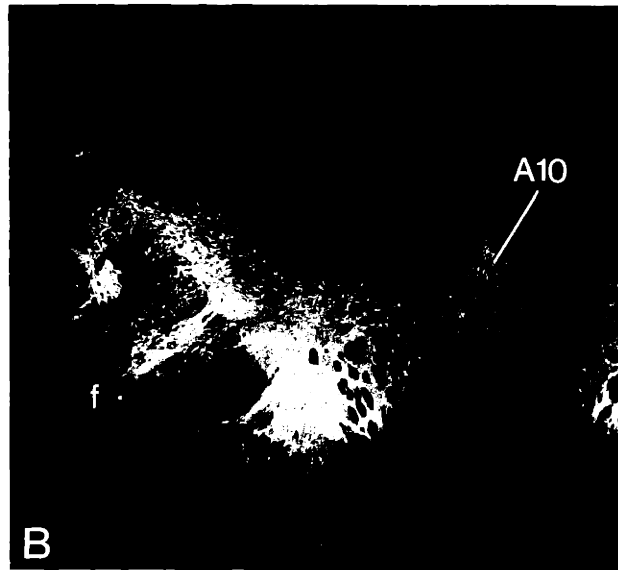
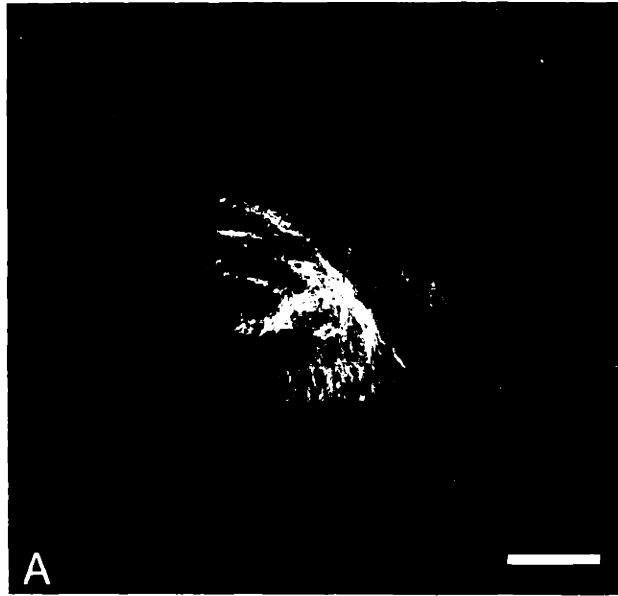


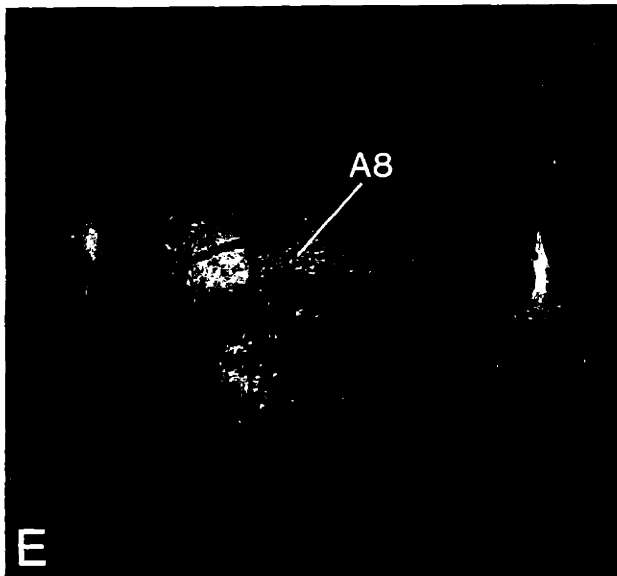
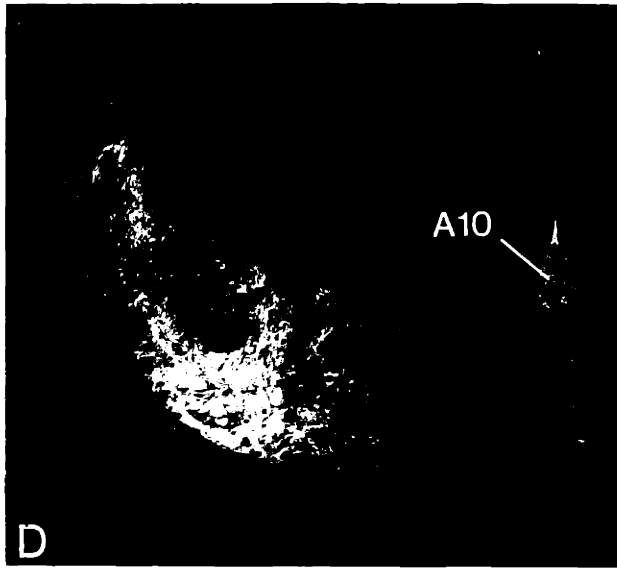
Olszewski and Baxter, 1954; Nobin and Bjorklund, 1973). In addition, dorsal to the dense, horizontal band of cells is a group of loosely-organized dopamine-containing neurons. These are the neurons of the pars mixta of the monkey, and as mentioned above, perhaps includes the pars beta and gamma of the human (see below).

*Cell group A8: the retrorubral area.* In the rat, cat and monkey, the most caudally located dopamine-containing neurons are found within the retrorubral area. In the rat, this cell group was designated as A8 (Dahlstrom and Fuxe, 1964). It is a loosely-organized collection of neurons, dorsal (in the rat and cat) and medial (in the monkey) to the caudalmost neurons of the pars compacta. At the level of the red nucleus in the rat and cat, these neurons form a dorsal band of cells, extending mediolaterally from the midline dopamine-containing neurons of the ventral tegmental area to the lateralmost part of the brainstem. In the monkey, these neurons are intermingled with the lateral part of the decussation of the brachium conjunctivum, medial to the fibers of the medial lemniscus. In their most caudal extent, they are scattered among the neurons of the pedunculopontine nucleus [see Fig. 2 and also Arsenault et. al, 1988].

There exists some controversy over whether a distinction between the A8 and A9 cell groups should be made. For example, Hubbard and DiCarlo (Hubbard and DiCarlo, 1974) found that in the primate brain, the cell groups A8 and A9 were indistinguishable on the basis of histofluorescence and other cytological characteristics. These authors suggest that cell groups C8 and C9 should be considered as a single entity. Hanaway and coworkers (Hanaway et. al., 1970) in the rat brain also recognized these cell groups as a single entity and described the A8 cell group as the caudal part of the pars compacta. However, Garver and Sladek (Garver and Sladek, 1975) described the histofluorescence of the M8 cells as

**Figure 1-2:** TH-positive neurons in the nigral complex of the squirrel monkey. Reverse-contrast photographs show the distribution of TH-positive neurons and neuropil in five rostrocaudally ordered sections [(A) rostral, (E) caudal] through the nigral complex of the squirrel monkey. The distance between sections is approximately 0.75 mm. A10, cell group A10 (ventral tegmental area); f, ventrally descending finger-like extensions; SNpm, substantia nigra, pars mixta; A8, cell group A8 (retrosubthalamic area). Scale bar = 1 mm.





being "somewhat smaller and duller" than the cells of M9 and Arsenault and coworkers (Arsenault et. al., 1988) described the dopamine-immunoreactive neurons of the monkey retrorubral area as displaying "a more intense immunostaining" and having a smaller cell body size and shorter dendrites than the other midbrain dopamine-containing neurons. It is also known that both the A8 and A9 cell groups project predominantly to the striatum (Ungerstedt, 1971; Beckstead et. al., 1979; Fallon and Moore, 1978) and that references to the pars compacta will often include the neurons of both cell group A8 and A9 (Poitras and Parent, 1978; Hanaway et. al., 1970). In the human brain, at least part of the A8 cell group corresponds to the pars gamma and pars beta of the pars compacta; it is therefore considered part of the pars compacta, even though it is distinguished from the dense layer of cells, most likely analogous to the A9 cell group, which is designated as the pars alpha (Nobin and Bjorklund, 1973; Olszewski and Baxter, 1954). Whether or not fine cytological distinctions are made between the cell groups A8 and A9, most authors agree that these dopamine-containing cells are part of a "continuous cell system" (Schofield and Everitt, 1981) and that, at least, the retrorubral area "can be regarded as a caudal extension of the substantia nigra" (Bjorklund and Lindvall, 1984).

If the cell groups A8 and A9 are to be considered as separate regions, then one confusing issue remains: are the dopamine-containing neurons of the pars mixta part of cell group A8 or A9? In most descriptions and atlases of the primate substantia nigra the dorsally placed neurons of the pars mixta are rarely distinguished from the substantia nigra, pars compacta (Arsenault et. al., 1988; Crosby and Woodburne, 1943; Davis and Huffman, 1968; Kusama and Mabuchi, 1970; Olszewski and Baxter, 1954; Schwyn and Fox, 1974; Snider and Lee, 1961) except by Francois et. al (Francois et. al., 1984; Francois et. al., 1985). However,

most studies describing the dopamine-containing neurons in the primate brain label as cell group A8 those neurons which correspond to the region of the pars mixta (Hubbard and DiCarlo, 1974; DiCarlo et. al., 1973; Garver and Sladek, 1975) Similarly, the region corresponding to A8 in the human brain also includes the region of the pars mixta (Nobin and Bjorklund, 1973). A logical conclusion from these two lines of evidence (as well as the preceding discussion of cell groups A8 and A9) would be that the dopamine-containing neurons of the pars mixta are analogous to cell group A8 (or are at least part of cell group A8) and that the A8 cell group (including the pars mixta) is an extension of the pars compacta.

### **Other Anatomical Subdivisions of the Primate Substantia Nigra**

In this section, and the following section, recent evidence on the organization of the nigrostriatal and striatonigral connections will be presented in order to reveal the complex and heterogeneous network of the striato-nigro-striatal system.

*Heterogeneity within the Nigrofugal System:* As described previously, the nigrothalamic, nigrotectal and nigrotegmental neurons within the pars reticulata are distributed topographically into segregated functional groups. Within the pars compacta, there is also evidence for the segregation of functionally distinct groups of neurons projecting to the striatum. Parent and colleagues (Parent et. al., 1983b; Smith and Parent, 1986) have shown that nigrostriatal neurons in the primate brain project almost exclusively to either the caudate nucleus or putamen and that these distinct groups of projection neurons can be shown to originate from interdigitating clusters within the pars compacta. They have also demonstrated that caudatonigral and putaminonigral fibers are well segregated within the substantia nigra. Caudatonigral fibers appear to innervate the rostral two thirds of the pars reticulata; the putaminonigral fibers are restricted to the caudal third of the pars reticulata. In addition, some striatonigral fibers apparently also terminate

within the pars compacta in relation to the clustering of neurons projecting to either the caudate nucleus or the putamen, suggesting the existence of a segregated, but reciprocally linked relationship between some of the striatonigral fibers and the nigrostriatal cell clusters (Parent et. al., 1983b; Smith and Parent, 1986).

Groups of nigrostriatal neurons may also be distinguished by distinctive patterns of termination within the caudate nucleus and putamen. When anterograde tracers are injected into the region of the substantia nigra, patchy terminal labeling has been observed within the striatum of the rat, cat and monkey (Beckstead, 1985; Feigenbaum and Graybiel, 1988; Gerfen et. al., 1987a; Jimenez-Castellanos and Graybiel, 1985; Jimenez-Castellanos and Graybiel, 1986; Jimenez-Castellanos and Graybiel, 1987b; Langer and Graybiel, 1989; Moon-Edley and Herkenham, 1983; Wright and Arbuthnott, 1981). In the monkey [see Fig. 3], the A8 cell group and part of the pars mixta projects predominantly to the extrastriosomal matrix. The midline A10 neurons terminate almost exclusively within the nucleus accumbens, and at least the lateral part of the main horizontal band of the pars compacta with its ventrally descending finger-like extensions projects strongly to the striosomal compartment. These findings suggest that there exist segregated mesostriatal terminals which may be in a position to differentially regulate the other well-known compartmentalized inputs and outputs of the striatum (Graybiel, 1984a) [see below].

*Neurochemical Heterogeneity:* The following discussion does not presume to be a full accounting of all the possible neurotransmitter-specific elements within the substantia nigra, however, it represents the results of many different studies which have contributed to the current understanding of the neurochemical composition of the substantia nigra and its relationship to nigral input-output organization.

What is known of the neurochemical heterogeneity within the substantia



**Figure 1-3:** Enhanced autoradiographic labeling in striosomes and in the matrix. Transverse sections through the striatum in two different animals illustrate distinct patterns of autoradiographic labeling elicited by an injection of  $^{35}\text{S}$ -methionine in the lateral part of the main horizontal band of the substantia nigra, pars compacta (A) and with an injection infiltrating neurons of the substantia nigra, pars mixta and the rostral part of cell group A8 (B). Both photographs are dark-field images so that autoradiographic labeling appears white. In (A), the densest fiber labeling is in striosomes of the caudate nucleus and the dorso-medial part of the putamen. In (B), most of the mesostriatal label is in the extrastriosomal matrix, leaving striosomes in the caudate nucleus and putamen as dark images; there is also substantial mesostriatal labeling in the ventral part of the striatum. The injection sites in these cases (S8R and S5) are shown in chapter two (Figs. 2-2 and 2-3). IC, internal capsule; AC, anterior commissure. Scale bar = 1 mm.



nigra is largely based on evidence related to the putative neurochemical input to the substantia nigra as well as its intrinsic neurochemical components. The substantia nigra receives input from the striatum and nucleus accumbens, the pallidum, the subthalamic nucleus, the amygdala, the lateral preoptico-hypothalamic region, the raphe nuclei, the pedunculopontine nucleus and the cerebral cortex (Graybiel and Ragsdale, 1979). The majority of these inputs, except from the striatum, are directed predominantly to the pars compacta. The input to the substantia nigra from the cerebral cortex, most likely from the prefrontal cortex to the pars compacta (Kunzle, 1978), is believed to be glutamatergic (Kornhuber et. al., 1984). Connections from the raphe nuclei to the pars reticulata (Parent et. al., 1981) and the pars compacta (Bobillier et. al., 1976; Azmitia and Segal, 1978) contain serotonin. The principal neurochemical input from the pedunculopontine nucleus is believed to be cholinergic (Beninato and Spencer, 1986; Graybiel, 1977; Henderson and Greenfield, 1987; Moon-Edley and Graybiel, 1983; Scarnati et. al., 1986); it is also known that many dopamine-containing neurons (Butcher and Marchand, 1978) and nigral interneurons (Henderson, 1981) contain acetylcholinesterase. At least part of the pallidonigral input, predominantly to the neurons of the pars compacta, appears to contain substance P and GABA (Brownstein et. al., 1977; Hattori et. al., 1973; Jessell et. al., 1978; Kanazawa et. al., 1977; Kanazawa et. al., 1980). The neurochemical composition of the inputs from the subthalamic nucleus, amygdala and the hypothalamic region are less well characterized; however, somatostatin-immunoreactive fibers have been observed within the pars lateralis and may be derived from the subthalamic nucleus (Chesselet and Graybiel, 1983a; Graybiel and Elde, 1983). As described previously, the majority of the intrinsic neurons of the pars compacta are distinguished by their content of dopamine (Anden et. al., 1964;

Dahlstrom and Fuxe, 1964); many neurons within the pars reticulata appear to contain GABA or enkephalin (Mugnaini and Oertel, 1985; Nagai et. al., 1983; Oertel et. al., 1982; Waters et. al., 1988; Emson et. al., 1980; Inagaki and Parent, 1984; Inagaki et. al., 1986; Gaspar et. al., 1983; Smith et. al., 1987; Taquet et. al., 1982). In the rodent, cholecystokinin and neurotensin have been shown to be colocalized in a subpopulation of the mesencephalic dopamine-containing neurons predominantly in the ventral tegmental area, although these have not yet been identified in the primate (Hokfelt et. al., 1980; Hokfelt et. al., 1984b; Zaborszky et. al., 1985).

Of all the afferent connections, the most prominent input to the substantia nigra, predominantly to the pars reticulata (Schwyn and Fox, 1974; Szabo, 1979), is from the striatum. Striatonigral fibers have been shown to contain GABA, substance P and dynorphin (Brownstein et. al., 1977; Chesselet and Graybiel, 1983b; Fonnum et. al., 1978; Gale et. al., 1977; Haber and Watson, 1985; Hattori et. al., 1973; Hong et. al., 1977; Jessell et. al., 1978; Kanazawa et. al., 1977; Kanazawa et. al., 1980; Kim et. al., 1971; Nagy et. al., 1978; Oertel et. al., 1981; Palkovits et. al., 1984; Quirion et. al., 1985; Walaas and Fonnum, 1980; Zamir et. al., 1984). Enkephalin-immunoreactive fibers also pervade the pars reticulata, and some of these fibers may be found in the pars compacta; however, the origin of this enkephalinergic input is uncertain (Bouras et. al., 1984; Chesselet and Graybiel, 1983b; Chesselet and Graybiel, 1983a; Haber and Elde, 1982; Inagaki and Parent, 1984; Inagaki and Parent, 1985).

Many neurotransmitter-related compounds within the substantia nigra have been shown to be organized in a non-homogeneous manner. For example, the substance P-positive and enkephalin-positive nigrofugal fibers appear to be distributed within the substantia nigra in a highly heterogeneous manner.

particularly in the primate brain (Inagaki and Parent, 1984; Inagaki and Parent, 1985; Waters et. al., 1988); the significance of these fiber patterns remains somewhat obscure, but it is possible that they represent distinct anatomical subdivisions. For example, when Jimenez-Castellanos and Graybiel (Jimenez-Castellanos and Graybiel, 1987b) described histochemically-distinct zones of acetylcholinesterase (AChE) within the pars compacta, they not only showed that the regions of AChE-rich and AChE-poor neuropil corresponded to clusters of neurons seen in tyrosine hydroxylase-immunostained and Nissl-stained material, but they were also able to demonstrate that these clusters of neurons were related to distinct groups of neurons projecting preferentially to either the caudate nucleus or the putamen (Jimenez-Castellanos and Graybiel, 1989a).

Similarly, there are regional subdivisions within the substantia nigra which have been demonstrated by autoradiographic binding for sigma receptors and the dopamine receptors D1 and D2 (Besson et. al., 1988; Graybiel et. al., 1989a; Beckstead et. al., 1988; Dubois et. al., 1986; Martres et. al., 1985). A particular zone, referred to as the densocellular zone in the cat, is known to project predominantly to the striosomal compartment of the striatum (Jimenez-Castellanos and Graybiel, 1987a), (also see below); this same zone shows heightened labeling of sigma binding, whereas D1 binding appears reduced in this region compared to other parts of the substantia nigra (Graybiel et. al., 1989a). Heterogeneous sigma and D1 binding have also been observed in the primate brain (Besson et. al., 1988), (Graybiel, personal communication).

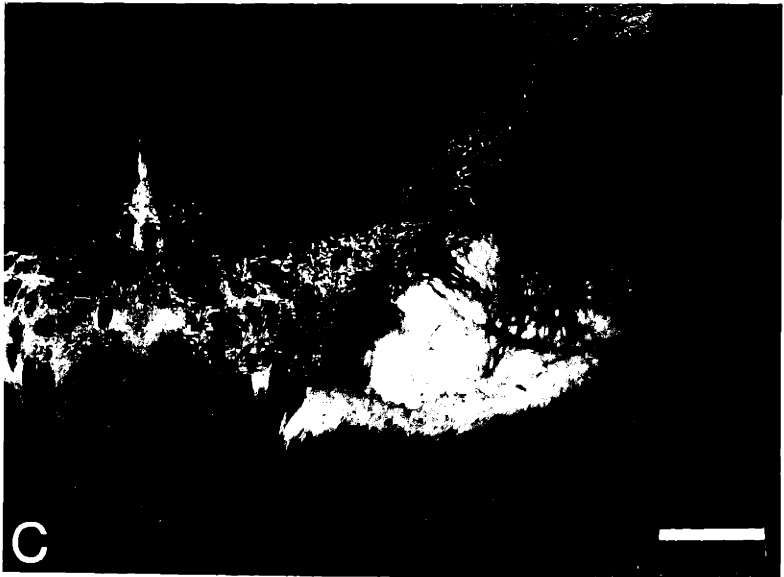
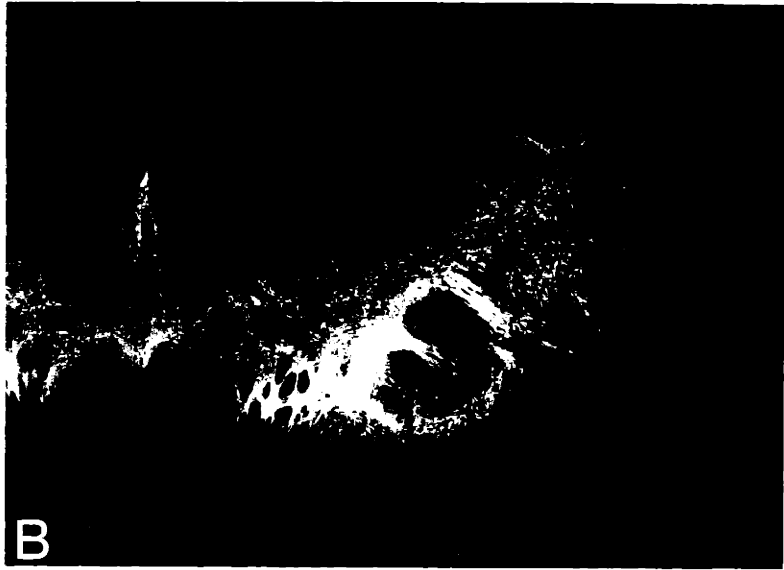
Calcium-binding protein (CaBP)-like immunoreactivity is another example of an intrinsic compound that has been shown to be distributed heterogeneously in the substantia nigra (Gerfen et. al., 1985); at least in the rat, neurons within the region of the pars compacta that express CaBP-like immunoreactivity appear to

correspond to those neurons which project to the striatal matrix. In the primate, CaBP-like immunoreactivity in the neuropil is predominantly distributed in the pars reticulata, with sharply diminished immunoreactive labeling in the pars compacta (Gerfen et. al., 1985), [personal observations, see Fig. 4]. A relationship between these CaBP-rich or CaBP-poor nigral zones and the striatal compartments have not yet been shown; however, we have observed many labeled neurons in the region of cell group A8, suggesting that this matrix-projecting subdivision has CaBP-positive neurons as in the rat.

### **Mesostriatal Compartmentalization**

*Experimental evidence:* The striatum is a complex, heterogeneous system of functional circuits with a distinct topography and compartmentalization related to its afferent, efferent and intrinsic connectivity as well as to the distribution of the substrates of its neurochemical machinery. Originally striatal compartmentalization was observed in the immature striatum. Patches of dopamine-containing afferents were observed in striatal tissue from rabbits and rats at the time of birth (Tennyson et. al., 1972; Olson et. al., 1972). In the mature striatum highly fluorescent, dopamine-containing patches could also be identified in rats pretreated with the tyrosine hydroxylase inhibitor  $\alpha$ -methylparatyrosine (Olson et. al., 1972). Subsequently, Kunzle (Kunzle, 1975; Kunzle, 1978) demonstrated a patchy termination of corticostriatal fibers in the monkey and Pert and colleagues (Pert et. al., 1976) described a patchy distribution of opioid binding sites within the rat striatum. Shortly thereafter, Graybiel and Ragsdale (Graybiel and Ragsdale, 1978) reported that within the cat, monkey and human striatum, in sections stained for AChE activity, distinct AChE-poor zones embedded in a surrounding AChE-rich matrix could be detected; these AChE-poor zones were called striosomes and have since been shown to correspond to differentially high or low concentrations

**Figure 1-4:** Sections through the nigral complex stained for AChE, TH- and CaBP-like immunoreactivity. Three adjacent coronal sections through the substantia nigra illustrate the heterogeneous pattern of staining observed in sections stained for (A) AChE activity and (C) CaBP-like immunoreactivity in relation to the location of dopamine-containing neurons detected by TH-like immunoreactivity (B). Scale bar = 1 mm.



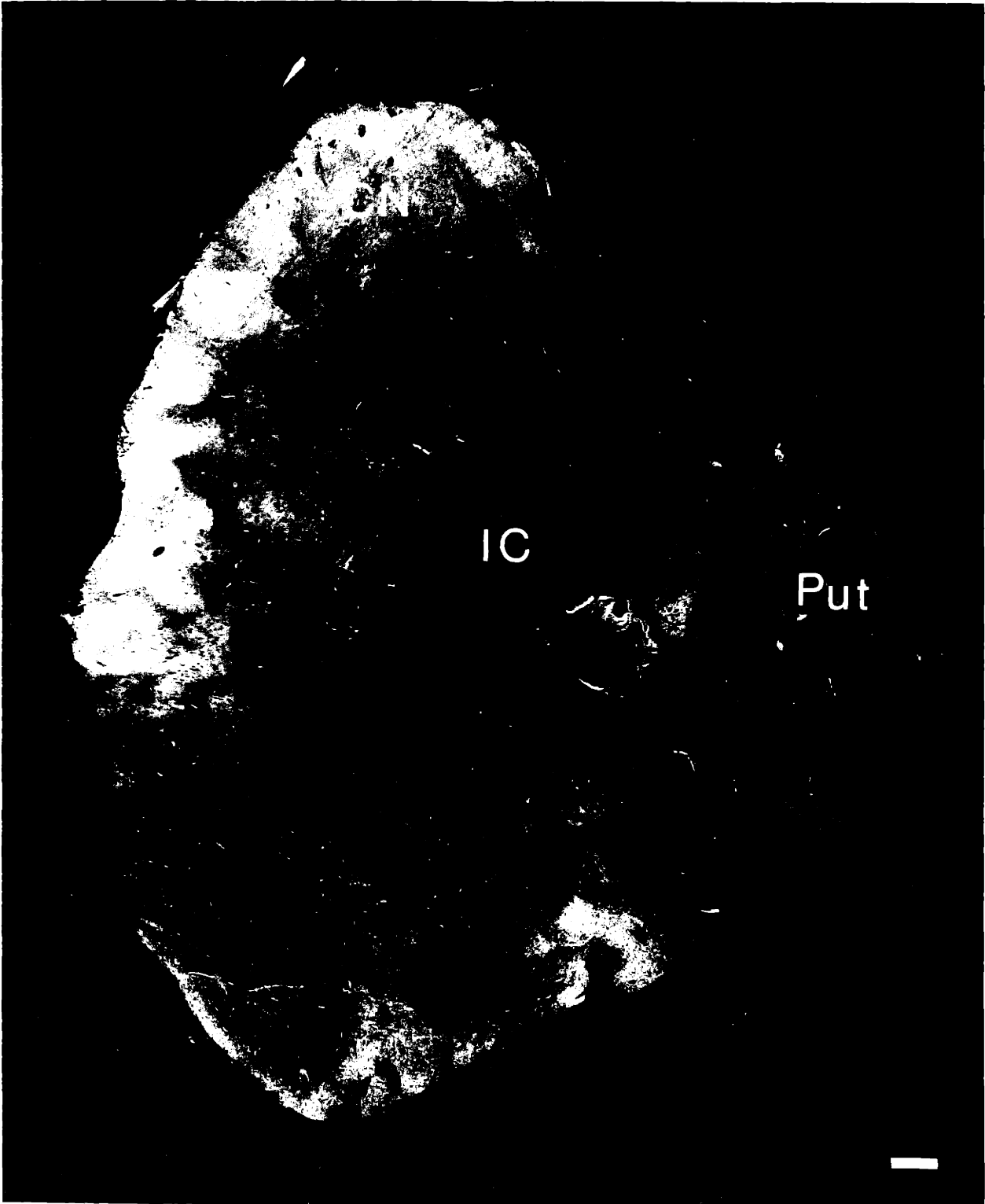


of most of the neurotransmitters and/or related enzymes and associated binding sites found within the striatum (Graybiel and Ragsdale, 1983; Graybiel, 1984a; Graybiel, 1989).

Striatal compartmentalization related to the dopaminergic projections has been demonstrated by axonal transport studies (Moon-Edley and Herkenham, 1983; Beckstead, 1987a; Gerfen et. al., 1987a; Jimenez-Castellanos and Graybiel, 1985; Jimenez-Castellanos and Graybiel, 1986; Jimenez-Castellanos and Graybiel, 1987b; Feigenbaum and Graybiel, 1988; Langer and Graybiel, 1989; Wright and Arbuthnott, 1981), as described above, as well as by the localization of dopamine receptor-selective ligand binding sites and immunohistochemically-identified dopaminergic fibers and terminals. For example, ligand binding selective for D1 receptor types are preferentially concentrated within zones corresponding to striosomes, whereas D2 binding sites are more concentrated within the surrounding matrix (Beckstead, 1987b; Beckstead et. al., 1988; Besson et. al., 1988; Joyce et. al., 1986). Immunostaining for tyrosine hydroxylase has also been shown to be unevenly distributed within the striatum [see Fig. 5]; zones of reduced tyrosine hydroxylase-like immunoreactivity, corresponding to striosomes, are surrounded by neuropil which shows heightened tyrosine hydroxylase-like immunoreactivity (Graybiel et. al., 1987; Ferrante and Kowall, 1987). The differential binding site distributions appear to reflect an important spatial segregation of pharmacologically-distinct dopaminergic interactions; the heterogeneous pattern of tyrosine-hydroxylase immunostaining could indicate the presence of dopaminergic subsystems distinguished by differences in enzymatic regulation or neuronal activity (Graybiel et. al., 1987).

*Trans-striatal channeling:* The functional circuitry of the striatum is organized as a system of discrete channels apparently differentiating among broad

**Figure 1-5:** TH-like immunoreactivity in the human striatum. A transverse section through the human striatum immunostained for tyrosine hydroxylase shows the heterogeneous pattern of staining observed. The section was photographed in reverse-contrast: zones of reduced staining, corresponding to striosomes, appear as dark images and are surrounded by zones of enhanced staining, appearing white. CN, caudate nucleus; Put, putamen; IC, internal capsule. Scale bar = 1 mm.



IC

Put

—

classes of information regionally and locally. These different functional compartments are composed of segregated subunits of afferent and efferent connections. Sensory and motor cortex project mainly to the matrix compartment (Donoghue and Herkenham, 1986; Ragsdale and Graybiel, 1981; Alexander et. al., 1988) whereas striosomes receive inputs from prefrontal and insulotemporal cortex, as well as the basolateral amygdala (Ragsdale and Graybiel, 1989a; Ragsdale and Graybiel, 1988a). This separation of information coming into the striatum would suggest that striosomal ordering minimally segregates channels having more to do with the processing of primary sensorimotor information from other channels that appear to be more limbic-related or associational. Because the striosomes are spaced quite regularly, on the order of 0.4 to 0.8 mm apart, they could influence much of the matrix (Graybiel, 1984a). They could thus "condition" the matrix, perhaps in relation to learning circuits in the striatum.

This duality of function also exists at the level of the outputs. The matrix is the principal origin of striatal outflow, which also is distinctly sensorimotor (Graybiel and Ragsdale, 1979; Jimenez-Castellanos and Graybiel, 1989b; Gimenez-Amaya and Graybiel, 1988; Gimenez-Amaya and Graybiel, 1989; Graybiel, 1989). By contrast, so far, the only projection from striosomes appears to be to the medial part of the substantia nigra, pars compacta (Jimenez-Castellanos and Graybiel, 1989b; Gerfen, 1985). This evidence suggests that the striatal output from the striosomes could act as a feedback regulator for the extensive dopaminergic projections to both the striosomes and the matrix. The segregation of dopaminergic input to these two compartments, as previously described, would result in a modulatory system attuned to the separate channels of striatal processing.

Because the matrix is also known to receive some limbic-associated inputs, for

example from the cingulate gyrus and parts of the amygdala (Donoghue and Herkenham, 1986; Ragsdale and Graybiel, 1988a; Ragsdale and Graybiel, 1989a), an absolute compartmental segregation of sensorimotor and limbic-associated functions is not likely (Graybiel, 1989). However, due to the segregation of at least some of the striatal input and output, there is obviously some compartmental, striosomal segregation of sensorimotor and limbic-related information; this arrangement suggests that segregated dopamine-containing striatal afferents would be in a position to act, at least partly independently, as local tuning mechanisms for these compartmentalized channels of information flow through the striatum.

*Potential clinical implications:*

The importance of the connection between the substantia nigra and the striatum has largely come from extensive work on the pathogenesis of Parkinson's disease. As described previously, in Parkinson's disease, the dopamine-containing neurons of the substantia nigra degenerate (Barbeau, 1986; Hassler, 1938; Jellinger, 1986) and extensive cell loss has been observed in a brain from a patient with a parkinsonian syndrome induced by MPTP toxicity (Ballard et. al., 1980). Recent studies on cell loss in Parkinson's disease and in MPTP-treated animals report that cell death in the nigral complex is not uniform (Burns et. al., 1983; Deutch et. al., 1986; German et. al., 1988; Hirsch et. al., 1988). Apparently, only a specific subset of dopamine-containing neurons are selectively vulnerable to Parkinson's disease and MPTP toxicity (Deutch et. al., 1986; German et. al., 1988; Hirsch et. al., 1988). There is even some evidence indicating that these preferentially vulnerable subsets may be distinguished by how they terminate within the striatum. For example, in MPTP-treated dogs, striosome- and matrix-projecting cell groups within the nigral complex appear to be differentially affected (Wilson et. al., 1987; Turner et. al., 1988), indicating the potential importance of identifying functionally distinct cell

groups within the dopamine-containing regions of the midbrain with respect to their mesostriatal termination.

## Chapter 2

# The Mesostriatal Projection I: Autoradiographic Results

### Abstract

Mesostriatal projections were labeled in 23 squirrel monkeys (40 hemispheres) by injecting the anterograde tracer,  $^{35}\text{S}$ -methionine, into different parts of the dopamine-containing A8-A9-A10 cell complex of the midbrain. The locations of injection sites were plotted in relation to subdivisions of the cell complex visible in sections immunostained for tyrosine hydroxylase. Anterograde labeling in the striatum was charted with respect to histochemically defined striosome and matrix compartments identified in serial sections stained for met-enkephalin-like immunoreactivity or for acetylcholinesterase or butyrylcholinesterase activity. Two strikingly different compartmental patterns of mesostriatal projection were found. Fields of dense labeling in both the caudate nucleus and the putamen, interrupted by pockets of sparse labeling, were observed with deposits involving cell group A8, cell group A10 and/or the dorsally situated "pars mixta" of Francois et. al., 1985. Where striosomes could be identified as such in adjoining histochemically stained sections, the sparsely labeled zones were aligned with them. By contrast, a pattern of focally dense labeling in the caudate nucleus and putamen with much weaker labeling surrounding the densely labeled zones was found with injection sites centered in the horizontal band and associated ventrally extending fingers of the substantia nigra pars compacta. Many of the pockets of dense labeling could be shown to correspond to striosomes. We conclude that the A8-A9-A10 cell complex of the primate contains spatially distinct subdivisions with preferential projections directed respectively toward the striosome and matrix compartments of the striatum.

Based on Langer and Graybiel, Brain Research, 1989, in press.

## Introduction

In the human and in experimental animals, a number of anatomically identifiable markers related to dopaminergic function in the striatum observe striosomal compartmentalization (Graybiel, 1986a; Besson et. al., 1988; Marshall et. al., 1985; Joyce et. al., 1986; Ferrante and Kowall, 1987; Graybiel et. al., 1987; Voorn, 1988; Beckstead, 1987b). Ligand binding selective for dopamine receptor subtypes, immunostaining for tyrosine hydroxylase (TH), the synthetic enzyme of the catecholamines and immunohistochemically detectable dopamine have uneven distributions in which the markers are particularly concentrated either in or out of zones corresponding to striosomes, identifiable by acetylcholinesterase [AChE] histochemistry. Many of these distinctions appear early in development and undergo apparent rearrangements during maturation (Olson et. al., 1972; Tennyson et. al., 1972; Kent et. al., 1982; Voorn et. al., 1988a; Graybiel, 1984b; Newman-Gage and Graybiel, 1988).

Axonal transport studies in the rat (Gerfen, 1985; Gerfen et. al., 1987a; Moon-Edley and Herkenham, 1983) and cat (Beckstead, 1987a; Jimenez-Castellanos and Graybiel, 1986; Jimenez-Castellanos and Graybiel, 1987a) suggest that these compartmentalized marker distributions may reflect the presence of subsystems within the dopamine-containing mesostriatal pathways terminating preferentially in the striosomal or in the matrix compartments of the striatum. In these species, fibers originating in cell group A8 terminate predominantly in the extrastriosomal matrix (Deutch et. al., 1984; Gerfen, 1985; Jimenez-Castellanos and Graybiel, 1987a; Moon-Edley and Herkenham, 1983; Jimenez-Castellanos and Graybiel, 1985). By contrast, at least one subdivision of the substantia nigra pars compacta, a visibly cell-dense zone in the cat (Jimenez-Castellanos and Graybiel, 1987a), and a ventrally situated zone in the rat (Gerfen et. al., 1987a), apparently projects selectively to striosomes.



Guided by these observations, we placed deposits of anterograde tracer into different parts of the A8-A9-A10 cell complex of the squirrel monkey and compared the nigrostriatal labeling observed in such cases with the distribution of striosomes identified there with the aid of histochemical and immunohistochemical staining carried out on serially adjoining sections. We hoped not only to identify the particular patterns of striatal termination of fibers from cell group A8 and the densely cellular parts of the substantia nigra pars compacta (cell group A9), but also to learn whether the large dorsally situated "pars mixta" of the nigral complex, specifically identified in the primate brain (Francois et. al., 1985; Francois et. al., 1984), had compartmentally targeted nigrostriatal projections. Accordingly, we analyzed the tracer deposits in the midbrain in relation to its chemoarchitecture as seen in sections stained for TH-like immunoreactivity (Arsenault et. al., 1988; Jimenez-Castellanos and Graybiel, 1987b; Jimenez-Castellanos and Graybiel, 1989a)

## Materials and Methods

Unilateral (n=5) or bilateral (n=32) injections of 3-10 nl of the anterograde tracer  $^{35}\text{S}$ -methionine (New England Nuclear; as a 200  $\mu\text{Ci}/\mu\text{l}$  solution in 0.9% saline delivered by air-pressure from glass pipettes) were placed under stereotaxic guidance (Emmers and Akert, 1963; Gergen and MacLean, 1962) into sites within the A8-A9-A10 cell complex of the midbrain of 23 adult squirrel monkeys (*Saimiri Sciureus*) [40 hemispheres] tranquilized with ketamine hydrochloride (Ketaset, 40 mg/kg IM) and anesthetized with Nembutal (50 mg/kg IP). A vertical approach was used for almost all (n=31) injections. To control for possible contamination along the pipette track, and to circumvent a midline approach in one animal, 6 injections were made by an oblique approach. Injections made with a vertical approach in which there was extensive contamination along the track (n=11) were included for corroborative and comparative purposes only.

After 2-4 day survivals (and in 4 animals, 10-14 days) the animals were deeply anesthetized with Nembutal and were perfused transcardially with 500 ml of 0.9% saline followed by 1.5 liters of 4% paraformaldehyde and 5% sucrose in 0.1 M dibasic phosphate buffer and 0.9% saline (pH 7.4, PBS) and then by 1.5 liters of PBS containing 5% sucrose. Brains were blocked stereotaxically in the frontal plane, washed overnight in PBS containing 20% sucrose and cut in the frontal plane into 40 $\mu$ m sections on a freezing microtome.

Adjoining sets of sections through the striatum were stained, respectively, for (a) acetylcholinesterase (Geneser-Jensen and Blackstad, 1971; Graybiel and Ragsdale, 1978), with acetylthiocholine iodide as substrate and ethopropazine hydrochloride (Parsidol, Warner-Lambert) as the pseudocholinesterase inhibitor, (b) butyrylcholinesterase [BuChE] (Graybiel and Ragsdale, 1980), with butyrylthiocholine iodide in the presence of the cholinesterase inhibitor BW284c51 (Burroughs Wellcome), and (c) met-enkephalin (ENK)-like immunoreactivity by protocol B of Graybiel and Chesselet (Graybiel and Chesselet, 1984) with antiserum kindly provided by Dr. R. Elde, diluted 1:1000. The single-cycle peroxidase-antiperoxidase (PAP) method (Sternberger, 1979) followed for the immunohistochemistry included the following steps: 1) Pretreatment with normal goat serum (1:30), hydrogen peroxide (3%), and Triton X-100 (0.2%); 2) primary antiserum incubation; 3) goat anti-rabbit IgG (1:50); 4) rabbit PAP (1:30); 5) diaminobenzidine (DAB, Sigma) reaction. Series of sections through the midbrain were stained for tyrosine hydroxylase-like immunoreactivity by the protocol according to Graybiel et. al. (Graybiel et. al., 1987) with Eugene Tech antiserum diluted 1:240, for AChE activity and for Nissl substance with cresylecht violet. Control procedures for AChE and BuChE staining involved incubating selected sections in routine acetylthiocholinesterase solution in the presence of BW284c51 or

routine butyrylthiocholinesterase solution with ethopropazine added. As a control for specificity of immunohistochemical reactivity, selected sections were processed without antiserum in the primary incubation.

For autoradiography, closely-spaced sections were mounted out of 0.9% saline, defatted and dipped in Kodak NTB-2 emulsion diluted 1:1 with 0.1% Drefit. Following exposure times of two days to eight weeks, slides were developed in Kodak D-19 and stained through the emulsion with cresylecht violet (Cowan et. al., 1972; Hendrickson et. al., 1972). The distribution of autoradiographic labeling in the striatum was analyzed with lightfield and darkfield optics, and mapped, when possible, in relation to the distribution of striosomal figures visible in the sections immunostained for met-enkephalin or stained for BuChE. The locations of the <sup>35</sup>S-methionine injection sites were studied in sections exposed for short (1-3 days) durations as well as in sections exposed for the same length of time as the striatal material (up to eight weeks). This procedure helped in identifying the centers of the deposits. Regional landmarks in the A8-A9-A10 region were identified in adjoining sections stained for TH-like immunoreactivity and for AChE activity (Arsenault et. al., 1988; Jimenez-Castellanos and Graybiel, 1987a; Jimenez-Castellanos and Graybiel, 1987b). All injection sites were charted with respect to TH-positive neurons (see Figs.1-6) and any visible labeling along the pipette track was also charted (Fig. 7).

In four cases densitometry measurements of striosomal and matrical labeling were made on single sections, corresponding to those shown in Figs. 8, 10, 14, 22; the zones that were measured in these sections are shown in Figs. 9, 11, 15 and 23, respectively. A *BIOCOM* computer-generated densitometry measurement was made from sections viewed with darkfield optics with a 4X objective. The computer generated a gray level intensity reading of specific zones corresponding to

each visible striosomal region (zones indicated by borders drawn in Figs. 9, 11, 15 and 23) or matrical regions (specific zones drawn within matrical regions are shown in Figs. 9, 11, 15 and 23). The mean gray level density measurement and corresponding standard deviation for striosomal, matrical and, in two cases, homogeneous regions in the ventral part of the caudate nucleus (S11L) and the ventral part of both the caudate nucleus and putamen (S5), as well as means and standard deviations for control regions (corresponding to the mean of two readings from unlabeled cortical areas and two readings from the glass slide without tissue) were calculated for each section. (See Table I). The statistical significance of the differences between means was determined by a two-sample t test (Rosner, 1986). The gray level density measurement is proportional to the absolute optical density based on the following relationship (Biocom User's Manual, 1989):

$$\text{Optical Density} = -\log [\text{Gray Level Measured} / \text{Maximum Transmission}]$$

However, the absolute optical density cannot be determined in these examples because "maximum transmission" cannot be defined with darkfield optics (i.e. light is not being transmitted). The gray level density measurement is, therefore, the only accurate way to represent the differences in the density of striatal labeling compared to control regions when viewed with darkfield optics.

## Results

Most of the injection sites in this study were centered within the A8-A9-A10 cell complex and resulted in compartmentalized patterns of striatal labeling. When all of the cases were taken together, there was a predictable relationship between the location of injection sites and the type of striatal labeling observed. For example, the A8 cell group and at least part of the pars mixta appear to predominantly innervate the extrastriosomal matrix whereas at least part of the

main horizontal band of the pars compacta and the ventrally descending finger-like extensions appear to project strongly to striosomes. Neurons located within the medial parts of the main horizontal band of the pars compacta may also project to striosomes, although all medially-placed injections in this study also involved, to some extent, neurons of the A8-pars mixta complex and/or the ventral tegmental area; striatal labeling of regions corresponding to both striosomes and matrix (mixed, regionally-distinct compartmentalization or homogeneity) was observed after such medial injections in the nigral complex.

### **Injection sites**

Of the 40 different stereotaxically-placed injections of  $^{35}\text{S}$ -methionine (40 hemispheres, 23 squirrel monkeys), the centers of 35 injections were found to be either completely or partially confined to the substantia nigra pars compacta, pars mixta, the ventral tegmental area or the retrorubral area (A8) as determined by charting these sites relative to the distribution of tyrosine hydroxylase-immunostained cell bodies. These injection sites are illustrated in Figs. 1-6; the centers of injections, determined by short exposure times (2-4 days), as well as the periphery of injections, seen after three to four week exposure times (similar to striatal tissue exposure times) are both indicated in the drawings.

Injection sites that were not located within the region of the nigral complex were centered within various regions of the hypothalamus (not illustrated;  $n=5$ ) and did not detectably infiltrate neurons of the A8-A9-A10 cell complex (Cases S2, S6R, S6L, S22L, and SF1R). These injections resulted in no perceptible striatal labeling. In some cases ( $n=7$ ; S8L, S9R, S12L, S14L, S16L, S16R and SF2R) the deposits of tracer were observed within or close to the region of the nigral complex, but very few nigral neurons appeared to have been labeled. The centers of these injections were either located on the extreme periphery of the nigral region and/or

## Figures 1 through 6: Chartings of Injection Sites

In the following figures, the locations of injection sites in the nigral complex are indicated semi-schematically in drawings of seven rostrocaudally ordered transverse sections through the midbrain of the squirrel monkey. The drawings were made from seven sections spaced approximately 0.5 mm apart. The outline of the substantia nigra, shown as dotted lines, was determined by the location of neurons and neuropil observed in serially adjacent sections immunostained for TH. Within the zones marked by the dotted lines are solid outlines showing the location of densely-packed TH-positive neurons and neuropil, corresponding to the pars compacta. The second and third sections also show the location of the oculomotor fibers lateral to the midline. In the seventh section, the horizontal fibers of the decussation of the brachium conjunctivum are shown as solid lines.

The injection sites have been grouped separately according to their locations in the nigral complex and the striatal labeling observed: injections eliciting no striatal labeling (Fig. 1); injections which resulted in labeling predominantly the extrastriosomal matrix (Fig. 2); injections which elicited enhanced striosomal labeling predominantly in the caudate nucleus (Fig. 3) or in parts of both the caudate nucleus and the putamen (Fig. 4); injection sites which resulted in labeling the most ventral part of the caudate nucleus and the putamen as well as the nucleus accumbens (Fig. 5); and injections eliciting regionally selective, mixed and homogeneous patterns of labeling (Fig. 6). The center and peripheral areas of each injection site are shown by dark and light stippled overlays, respectively. Each case is identified by its case number. OT, optic track; LGN, lateral geniculate nucleus; III, oculomotor nucleus; MGN, medial geniculate nucleus. Scale bar = 1 mm.

**Figure 2-1:** Injection sites resulting in no striatal labeling.

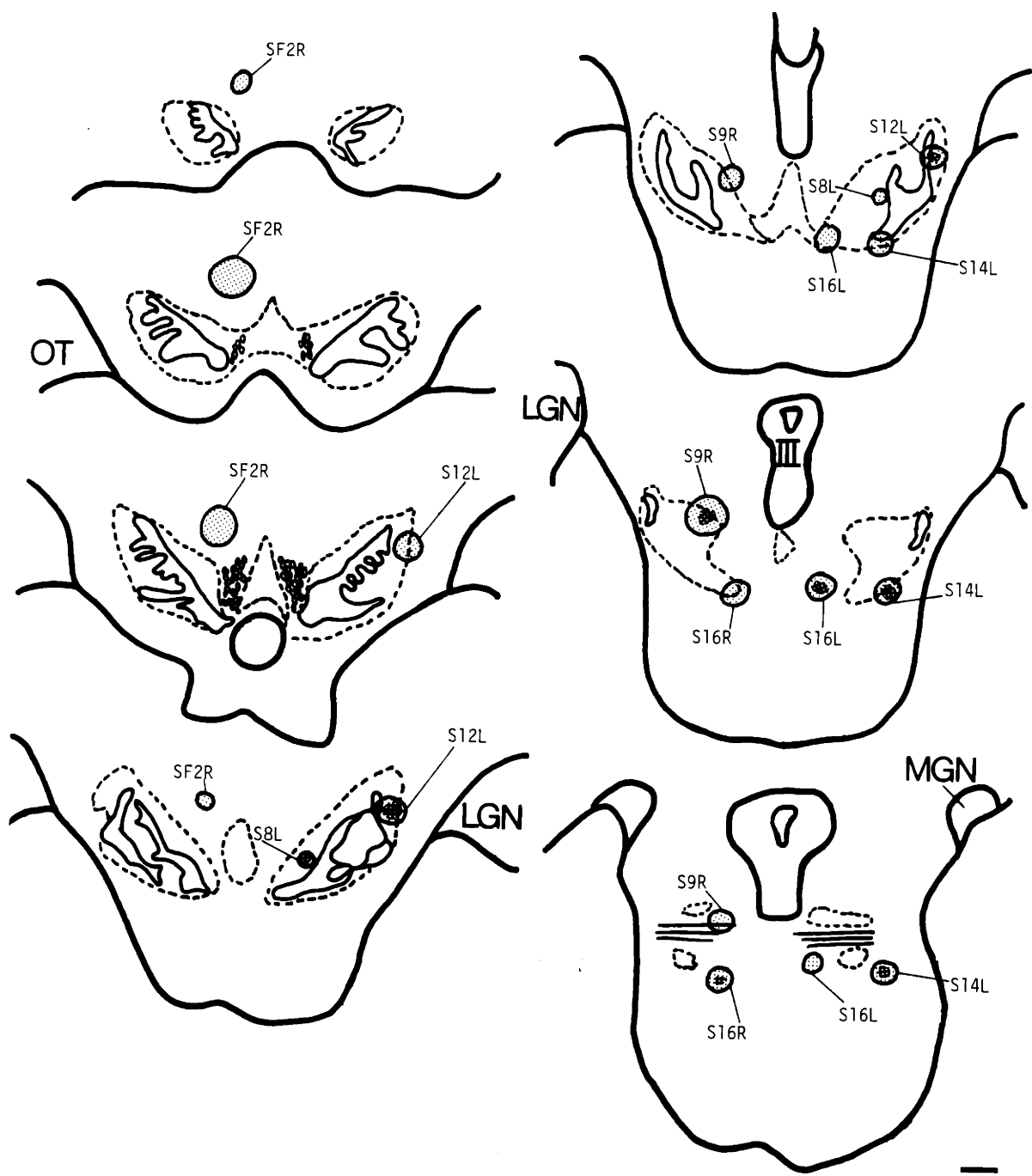




**Figure 2-2:** Injection sites eliciting labeling of the matrix compartment.

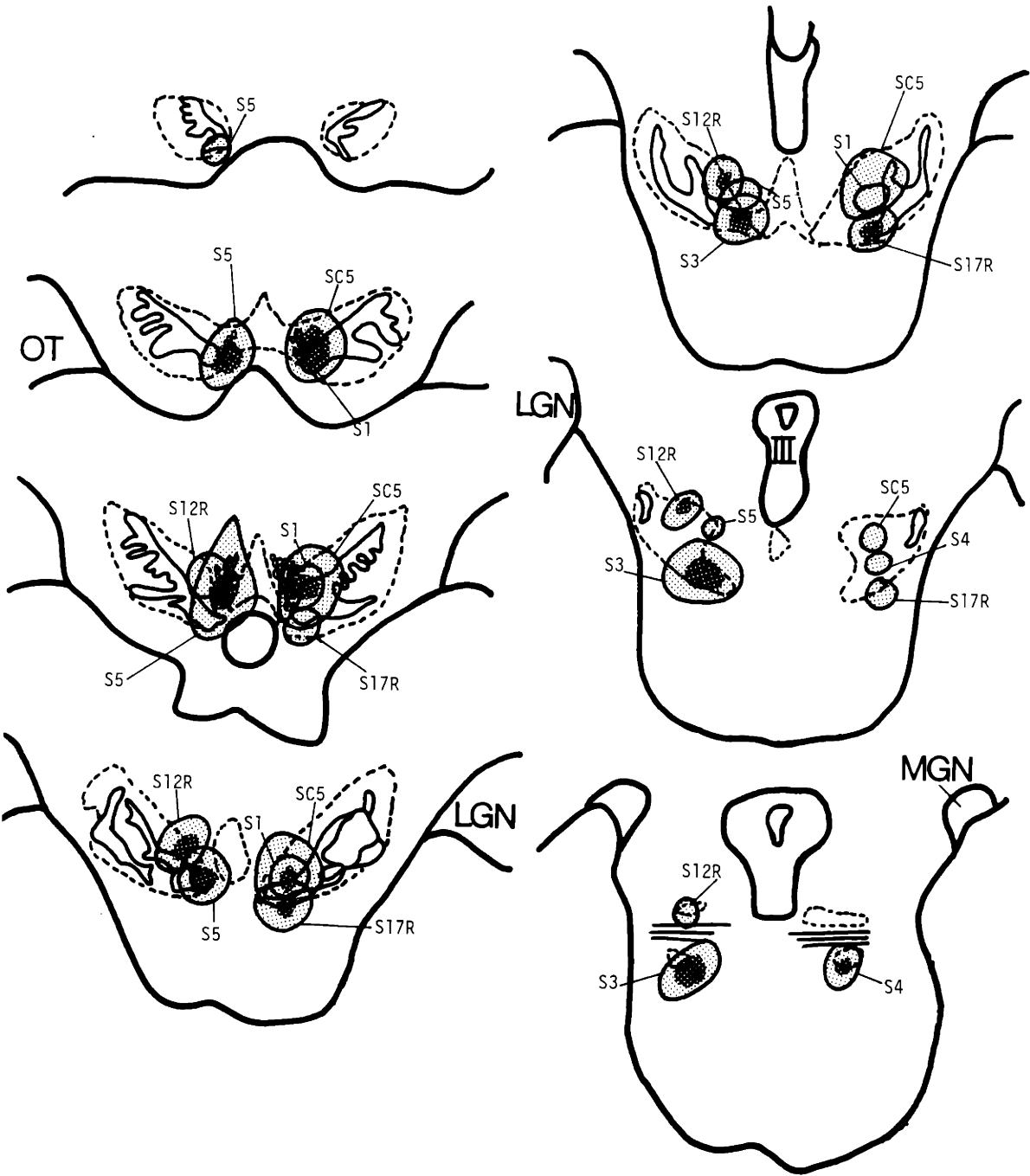


**Figure 2-3:** Injection sites eliciting enhanced labeling of striosomes predominantly within the caudate nucleus.

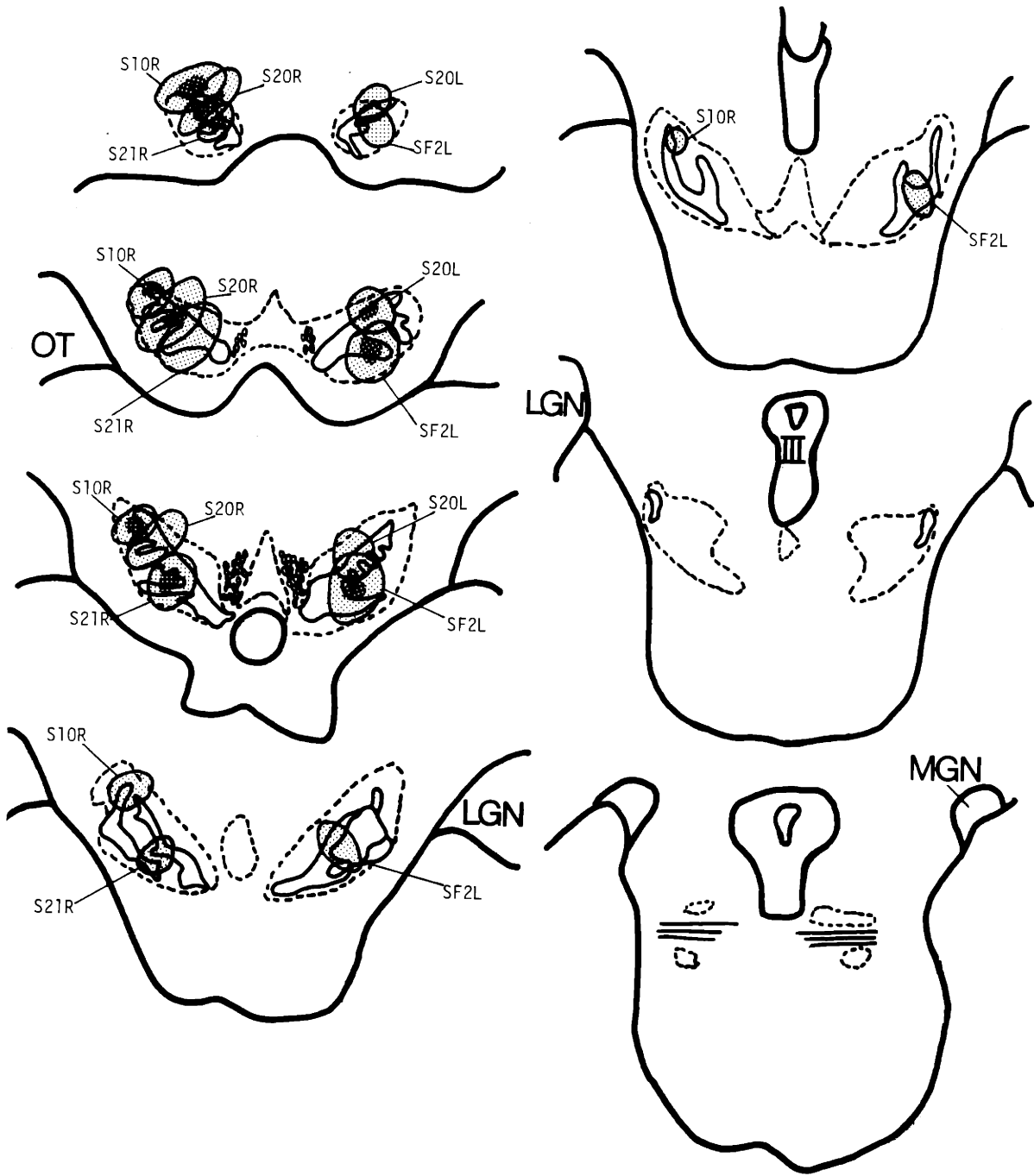


**Figure 2-4:** Injection sites eliciting enhanced labeling of striosomes in both the caudate nucleus and putamen.

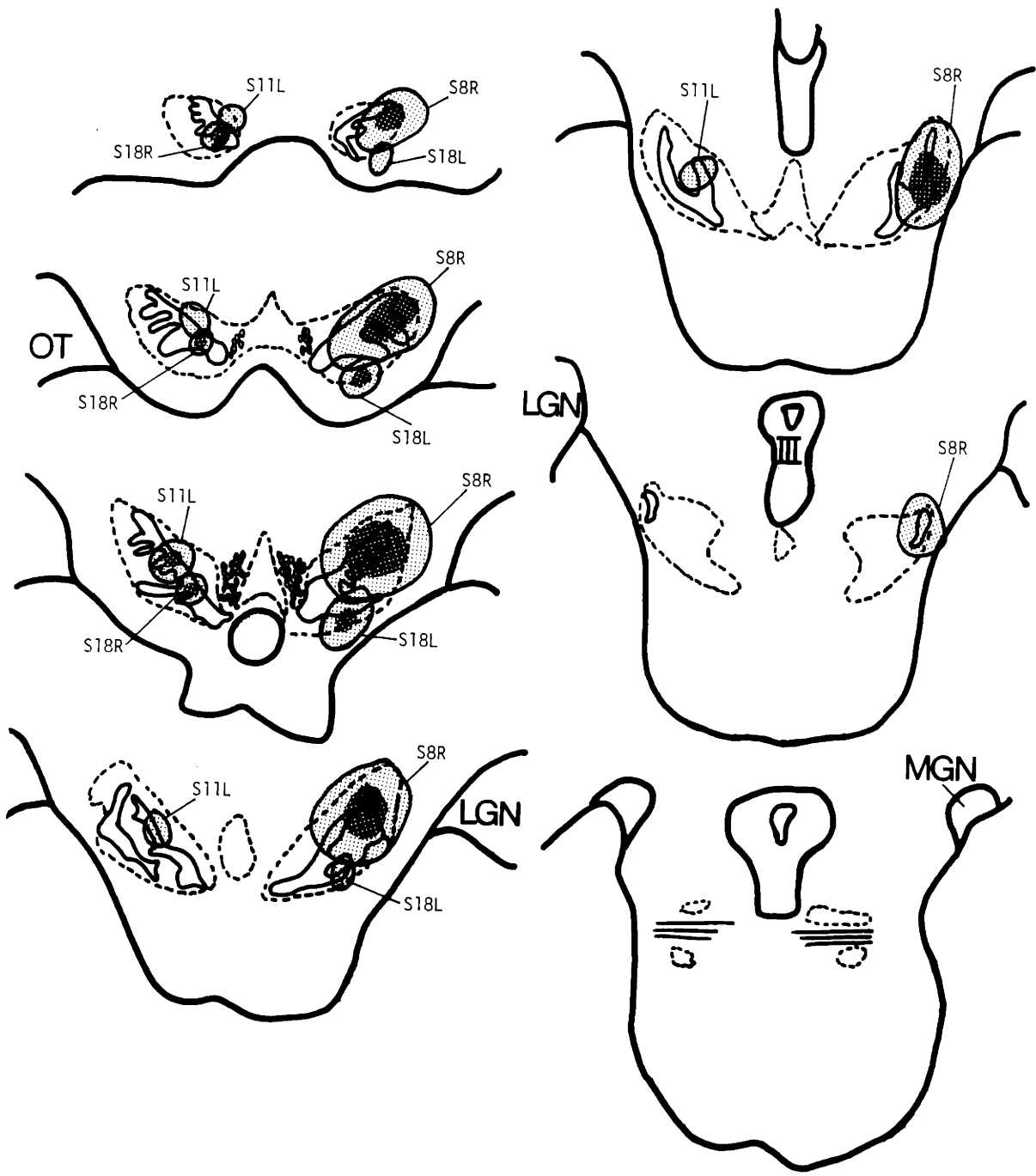


**Figure 2-5:** Injection sites eliciting labeling in the nucleus accumbens.

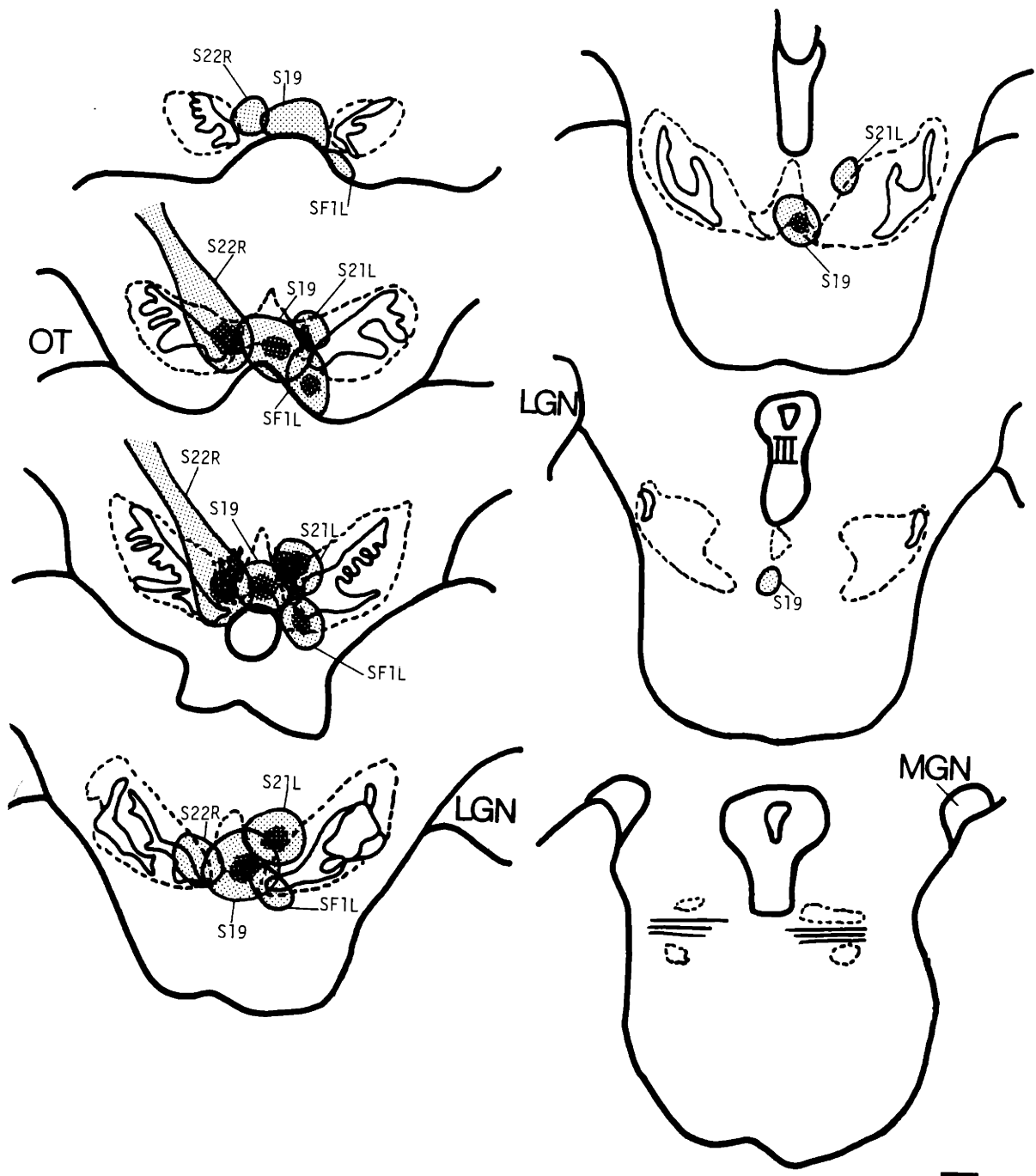
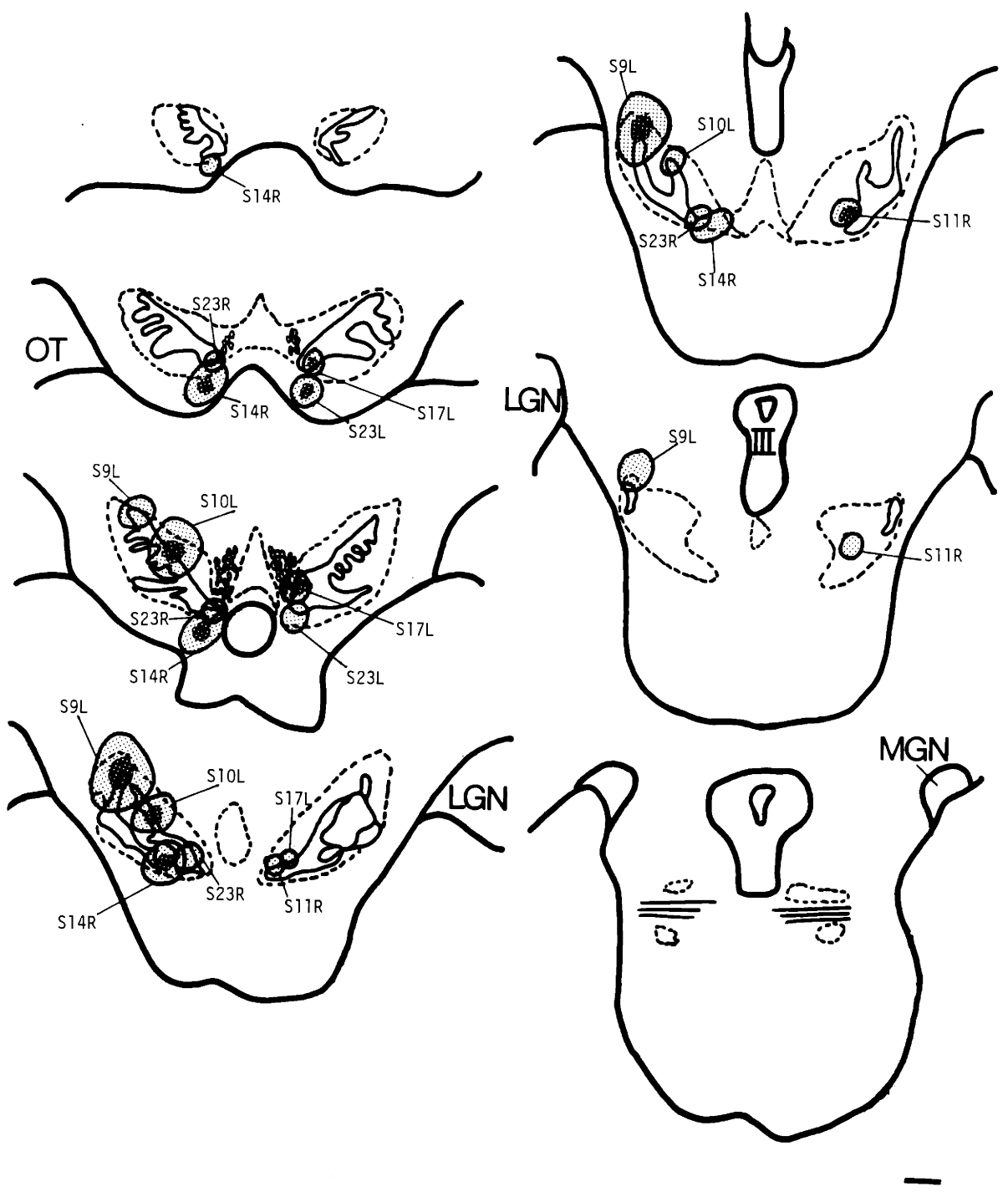




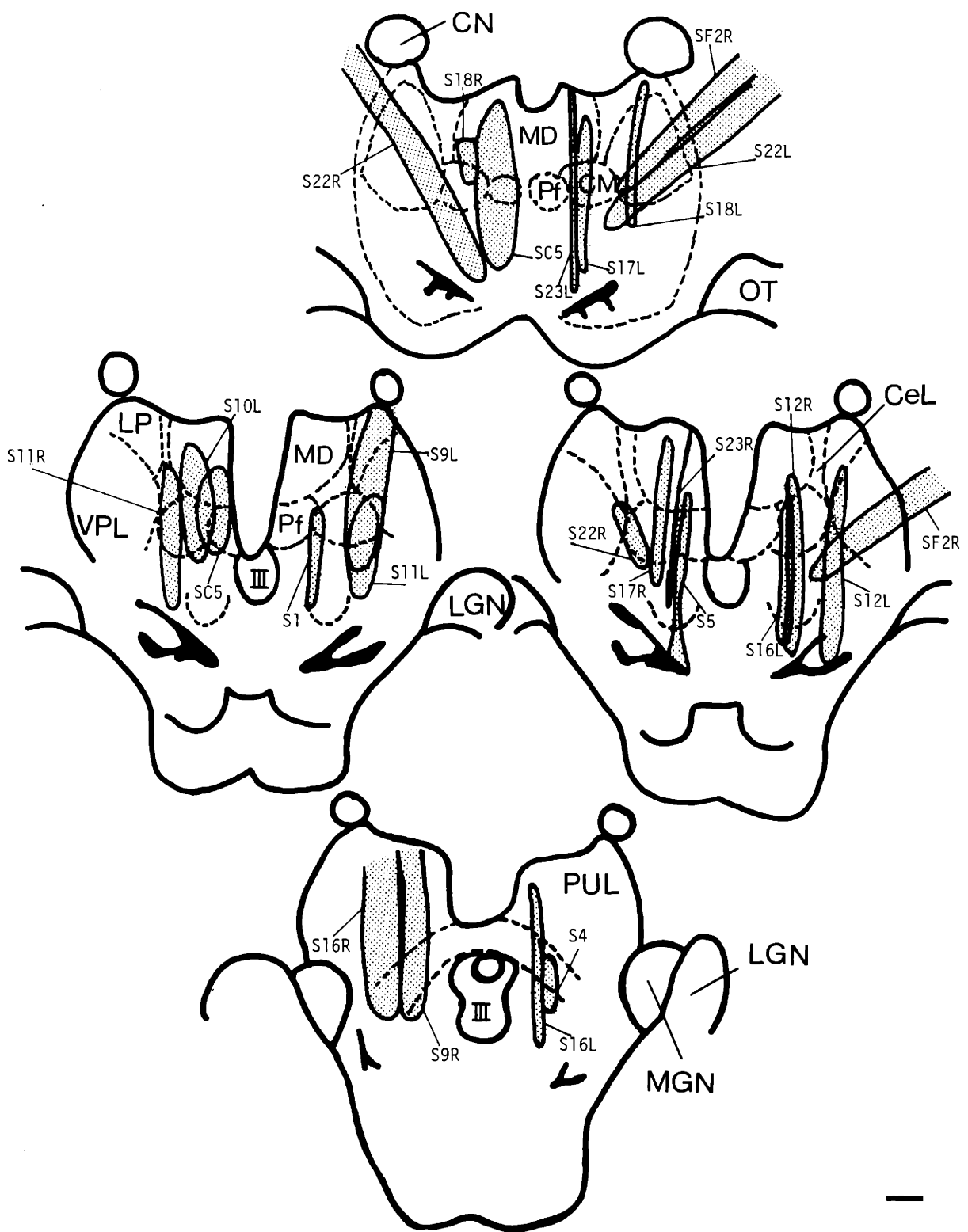
**Figure 2-6:** Injection sites resulting in mixed and homogeneous patterns of labeling.



they were too small to produce effective labeling. These injection sites are illustrated in Fig. 1. In each of these cases, very little, if any, perceptible striatal labeling was observed even after extremely long autoradiographic exposure times (e.g. up to 5 months). However, many of these injections served as useful controls for the possible contamination of thalamic afferents to the striatum. The other injections of this series (n=28), located within the A8-A9-A10 cell complex, produced very distinct patterns of striatal labeling. The relationship between different nigral cell groups and compartmentalized labeling within the striatum is described in detail below.

Many injections were associated with at least some autoradiographic labeling along the pipette track. All pipette tracks with detectable autoradiographic labeling are illustrated in Fig. 7. Most often, these tracks were small and were evident only after relatively long (compared to the exposure times necessary for detecting the injection site) autoradiographic exposure times (e.g. minimally three weeks compared to a few days). In these cases (S1, S5, S11R, S12R, S16L, S17L, S17R, S18R, S18L, S23R and S23L), weak autoradiographic labeling was observed along the pipette track and it was restricted to the antero-posterior level containing the pipette lesion. In some cases, however, the autoradiographic labeling along the pipette track was substantial, spanning a medio-lateral and antero-posterior distance of at least 1 millimeter (cases S4, SC5, S9R, S9L, S10L, S11L, S12L, S16R, S22R, SF2R); the intensity of autoradiographic labeling along the pipette track in these cases appeared to be comparable to the intensity of labeling at the injection site. Autoradiographic labeling along the pipette track was not often observed along the full vertical extent of the track, but appeared to be most dense in the middle regions of the track thereby contaminating parts of the thalamus as shown in Fig. 7.

**Figure 2-7:** Chartings of autoradiographic labeling observed along pipette tracks. The size and locations of autoradiographic labeling along the pipette tracks in all cases in which such labeling was detectable after a four week exposure time are represented schematically in transverse sections. Three anteroposterior levels are drawn: A -6.5 (top drawing), A -5.0 (middle drawings, shown twice), and A -3.5 (bottom drawing) (Emmers and Akert, 1963). The outlines of thalamic nuclei determined from Nissl-stained sections are shown by dotted lines. The substantia nigra, pars compacta is represented in solid black. The size and location of labeling observed along the pipette tracks are shown outlined in black with stippled interiors. Each case is identified by its case number. Thalamic nuclei: MD, medial dorsal nucleus; Pf, parafascicular nucleus; CM, central medial nucleus; LP, lateral posterior nucleus; VPL, ventral posterior lateral nucleus; MD, medial dorsal nucleus; CeL, central lateral nucleus; PUL, pulvinar; LGN, lateral geniculate nucleus; MGN, medial geniculate nucleus. Other abbreviations: OT, optic track; CN, caudate nucleus; III, Oculomotor nucleus. Scale bar = 1 mm.



It is very difficult to determine accurately whether or not thalamic contamination along the pipette track contributed significantly to fiber labeling within the striatum. However, based on cases with substantially labeled pipette tracks and no detectable striatal labeling, and based on topographical information from thalamostriatal investigations in the cat and monkey (Parent et. al., 1983b; Ragsdale and Graybiel, 1989b), the relative contribution of labeling along these pipette tracks to observable striatal fiber labeling can be inferred. For example, injections directed towards the caudal part of cell group A8 are likely to contaminate a central region of the pulvinar and the superior colliculus as shown in Fig. 7 (cases S9R, S16R, S16L and S4). However, only in case S4 was any detectable labeling within the striatum observed. It is likely, therefore, that any non-nigral autoradiographic contamination associated with the injection in case S4 did not contribute to striatal labeling. Similarly, injections directed towards rostral and lateral nigral regions are likely to infiltrate the central lateral nucleus, central medial nucleus, the ventral posterior nuclei and/or the lateral posterior nucleus. Cases with autoradiographic labeling along the pipette track involving these thalamic nuclei are S22R, S22L, S18L, S11R, S9L, SF2R, S12L and S11L. Controls for thalamic contamination in these nuclei are those cases with no detectable striatal labeling. Those cases with no visible striatal labeling are: S22L (dense track labeling in the ventral posterior nuclei from an oblique approach) and SF2R and S12L (dense track labeling of the lateral posterior, ventral lateral, and central medial nuclei, by oblique and vertical approaches, respectively).

Injections directed towards medial nigral regions are likely to infiltrate the lateral part of the medial dorsal nucleus, the central lateral, the parafascicular and the central medial nuclei. Autoradiographic labeling of pipette tracks involving these nuclei were found in cases S18R, SC5, S23L, S17L, S5, S12R, S10L, S17R, S1

and S16L as shown in Fig. 7. However, there was only one case with no perceptible striatal labeling, case S16L, and two cases with very weak striatal labeling, S23L and S17L (observable only after very long exposures), but the labeling of the pipette tracks in these cases was not particularly substantial, unlike the other control cases. In addition, the majority of thalamostriatal afferents originate from this particular vertical band of thalamic nuclei [see (Parent et. al., 1983b)]. It is quite possible, therefore, that fiber labeling within the striatum in those cases with substantial labeling along the pipette track (e.g. cases SC5, S10L) may be contributed to by the thalamostriatal innervation. It is important to note, however, that the pattern and topography of striatal labeling observed in all of the cases listed above was similar to the striatal labeling seen in cases which had injection sites centered in the same nigral regions but which otherwise showed no labeling along the pipette track. Each case is described below in relation to the pattern of striatal innervation observed.

### **Cell group A8 and the pars mixta**

Large fields of diffuse anterograde labeling in the striatum with embedded pockets of sharply diminished labeling were observed in all cases in which the injection sites primarily involved the tegmental regions dorsal and caudal to the main densely cellular part of the substantia nigra pars compacta (Jimenez-Castellanos and Graybiel, 1987b; Jimenez-Castellanos and Graybiel, 1989a) as illustrated in Fig. 2. In three hemispheres (cases S3, S4 and S12R), the centers of the deposits were situated in parts of cell group A8 (the retrorubral nucleus) at levels caudal to the main body of the substantia nigra pars compacta. In four cases (S1, S5, SC5 and S17R), the injection sites were centered at more anterior levels where they variably involved the rostral extension of cell group A8 and the medial part of the pars mixta and adjoining parts of the ventral tegmental area (VTA, cell group A10).

As described previously, the majority of these injections were also associated with some autoradiographic labeling along the pipette track (see Fig. 7; S1, S5, SC5, S17R, S12R and S4). The tracks of caudally-placed injections in cell group A8 are not likely to have infiltrated any particular striatopetal projection neurons judging from controls (see above) and from case S3, which showed no labeling along the pipette track. It is more difficult to assess the thalamostriatal contribution in those cases directed towards the more rostral nigral sites. However, the differences between cases in terms of the density and topography of striatal innervation appears to be most related to the size and location of the injection site, not the density of labeling along the pipette track. For example, the injection sites in cases SC5 and S1 were located in almost the exact same nigral region, although the injection site in SC5 was larger; the striatal labeling in S1 was much weaker than in case SC5, and even though the labeling of the pipette track was quite substantial in SC5, the topography of striatal labeling in these cases was the same. Similarly, the injection site size and locations of SC5 and S5 were very similar and the apparent density and topography of striatal labeling was also very similar, even though the labeling of the pipette track in SC5 was quite substantial. These examples would suggest that labeling along the pipette track cannot account for the distinct matrical labeling observed.

Studies in the cat suggest that substantial injections of anterograde tracer into the thalamic regions most heavily infiltrated in the above cases would produce striatal labeling in the matrix compartment, principally in the dorsal part of the striatum and often with discontinuous patches or fibrous labeling within the matrix (Ragsdale and Graybiel, 1989b). In most of the cases reported here striatal labeling appeared uniformly distributed within the matrix compartment in both the caudate nucleus and putamen. In two cases, S5 and S12R, labeling was enhanced



in the ventral half of the striatum, but in these cases the dorsal placement of the injection site in S12R and the involvement of the medial pars compacta and ventral tegmental neurons in S5 likely account for the enhanced ventral labeling. There was some evidence for heterogeneous labeling within the matrix compartment in two cases (cases S3 and S4, injections in caudal A8), but in these cases, either no labeling along the pipette track was observed (case S3) or the labeling along the pipette track (case S4) was too caudal to have infiltrated a major field of thalamostriatal projection neurons (corroborated by large control injections). In the majority of the cases, however, there was no evidence of non-uniform labeling of the matrix. These observations suggest that although the thalamostriatal innervation may have contributed to matrix labeling in some cases, it is unlikely to account for all of the the matrix labeling observed.

In every case, at least some of the pockets of sparse labeling could be shown to correspond to striosomes. Figs. 8 and 10 illustrate the predominant labeling of the extrastriosomal matrix in cases S3, in which the injection site was centered in A8 (Fig. 12) and S5, in which the midbrain deposit was situated more rostrally and infiltrated the pars mixta (Fig. 13). In these and other cases of the series, striosomes were identified in sections stained for butyrylcholinesterase; they appeared as zones of slightly to markedly dense activity and sometimes as zones with BuChE-rich perimeters. The fields of striatal labeling in S3 extended throughout the rostrocaudal extent of both the caudate nucleus and putamen; however, labeling in the caudate nucleus was restricted to the dorsal and lateral parts of the head and body. It is notoriously difficult to identify striosomes in much of the putamen, but as illustrated in Fig. 8, they were often clearly enough delineated to make unequivocal identification of the sparsely labeled zones as striosomes. As noted above, the labeling of the matrix compartment was not uniform.

The anterograde labeling in case S5 appeared throughout the rostrocaudal extent of both the caudate nucleus (head, body and tail) and putamen. Striosomal figures were especially clear in the caudate nucleus and again the BuChE-delineated striosomes were in correspondence with the grain-poor zones visible in adjoining autoradiograms except ventrally, where both striosomes and matrix were labeled. In each of the cases, regions where striosomes could be readily distinguished, we did not observe instances in which grain-poor zones failed to be aligned with histochemically distinct zones, except in cases S3 and S4 where some matrix heterogeneity and regionally dense labeling was observed. There were several instances in the case material, however, in which the histochemistry was inadequate to score the compartmental affiliation of the sparsely labeled zones. Outside of the striosomes, the anterograde labeling was most often quite diffusely distributed.

It is important to emphasize that when enhanced labeling within the matrix compartment was observed, it was associated with variable labeling of regions corresponding to striosomes. As shown in Figs. 8 and 10 [which correspond to the illustrations in Figs. 9 and 11 showing the zones sampled for densitometry], both cases S3 and S5 showed predominant labeling of the matrix compartment; however, in case S5, there appeared to be slightly more labeling of the striosomal compartment so that the contrast between the two compartments was not as strong as in case S3. This relationship is also indicated by densitometry measurements (see Table I) of the striosomal and matrical regions illustrated in Figs. 8 and 10. Even though there is a significant difference between the gray level densitometry measurement for striosomes and matrix in case S3 and in case S5, this difference, if evaluated in terms of the level of significance, is greater in case S3, minimally  $p < .01$ , than in case S5,  $p < .05$  (see Table I). In addition, the

**Figure 2-8:** Striatal labeling of the matrix in case S3. Adjacent sections through the striatum (CN, caudate nucleus; P, putamen) in case S3 illustrate the pattern of autoradiographic labeling elicited by an injection of  $^{35}\text{S}$ -methionine in cell group A8 (A) in relation to the disposition of striosomes (examples at asterisks) in the striatum detected with BuChE histochemistry (B). Photograph A is a dark-field image: autoradiographic labeling appears white. Most of the mesostriatal label is in the extrastriosomal matrix, leaving striosomes in the caudate nucleus and putamen as dark images in A. The injection site in this case is illustrated in Fig. 12. IC, internal capsule; NA, nucleus accumbens. Scale bar = 1 mm.

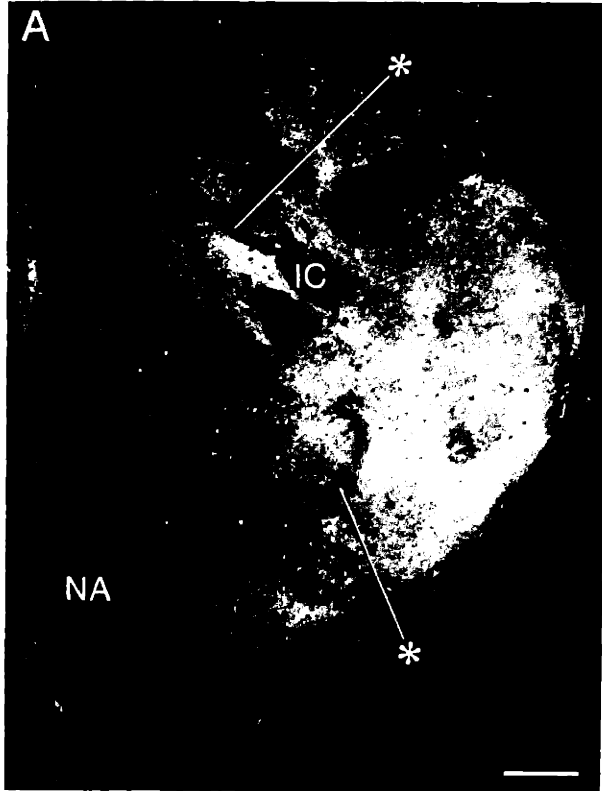


**Figure 2-9:** Drawing delineating zones for densitometry: case S3. The region of autoradiographic labeling in case S3, shown in Fig. 8A, is drawn schematically with black horizontal lines and those regions which were evaluated by densitometry are outlined: zones corresponding to striosomes (S) and other zones, arbitrarily chosen sample regions within the matrix compartment (M). The gray level intensity was measured (see Methods) in each of the zones outlined. The mean gray level density measurement and corresponding standard deviation for striosomal (S) and matrical (M) regions are shown in Table I. To aid orientation, the asterisks from Fig. 8A are also included in the drawing.

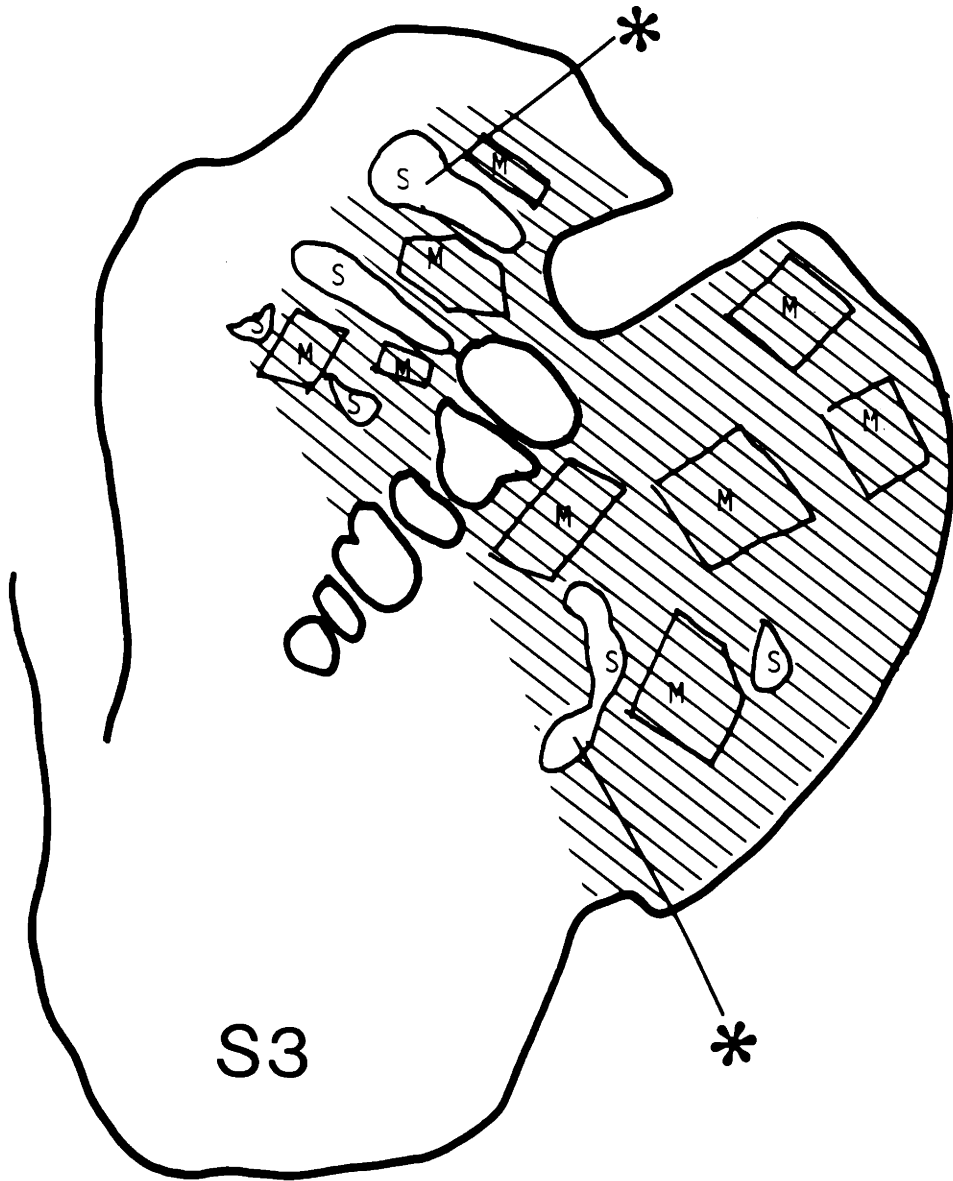


**Figure 2-10:** Striatal labeling of the matrix in case S5. Transverse sections through the striatum in case S5 illustrate enhanced anterograde labeling of the extrastriosomal matrix following an injection of  $^{35}\text{S}$ -methionine involving the pars mixta, the rostral extension of cell group A8 and adjoining parts of the ventral tegmental area (A). Striosomal figures are especially clear in the caudate nucleus. The BuChE-delineated striosomes in the serially adjacent BuChE-stained section (B) are in spatial correspondence with the grain-poor zones in the autoradiogram (example at asterisk) except ventrally, where both striosomes and matrix are labeled. The injection site in this case is shown in Fig. 13. IC, internal capsule. Scale bar = 1 mm.

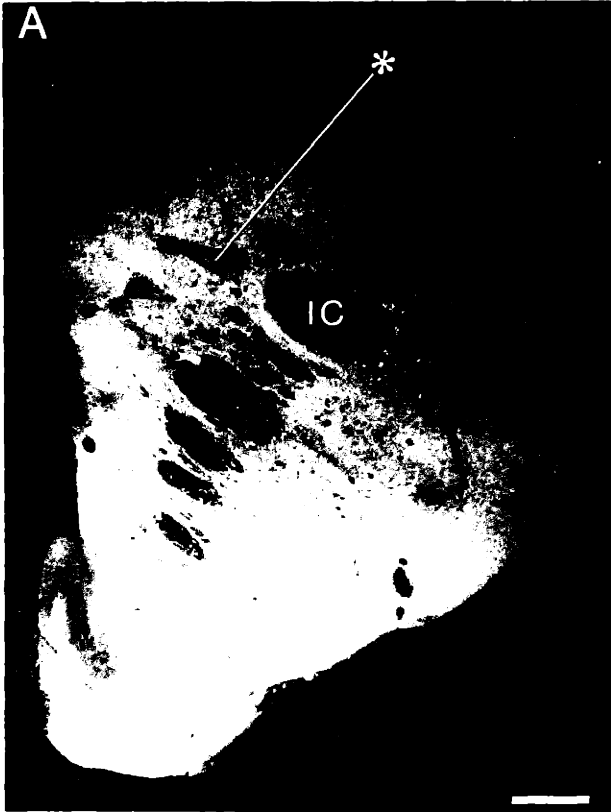




**Figure 2-11:** Drawing delineating zones for densitometry: case S5. Autoradiographic labeling in case S5, as shown in Fig. 10A, is drawn schematically. To aid orientation, the asterisk shown in Fig. 10A is also illustrated. Black horizontal and vertical lines indicate regions of enhanced labeling in the dorsal and ventral parts of the striatum, respectively. Zones corresponding to striosomes (S) and zones within the matrix (M) which were evaluated by densitometry are outlined. The gray level intensity was measured (see Methods) in each of the zones outlined. The mean gray level density measurements and corresponding standard deviations for striosomal (S) and matrical (M) regions are indicated in Table I. Comparisons between (M) and (S) regions within the dorsal part of the caudate nucleus, the dorsal part of the putamen and the ventral part of the striatum are shown separately. Some of the striosomal figures in the ventral part of the striatum which were not clearly visible in the autoradiogram were outlined with respect to BuChE-delineated striosomes in the serially adjacent section (see Fig. 10B).

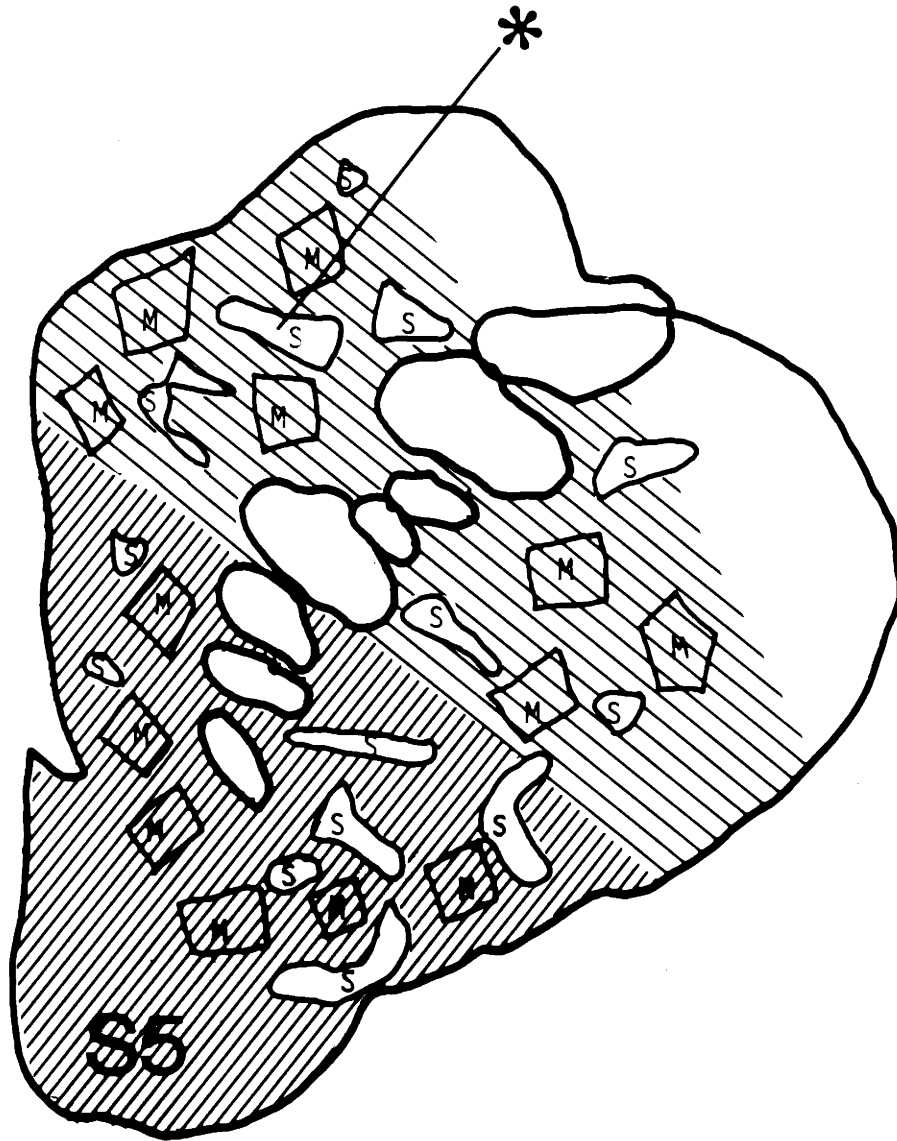


**Figure 2-12:** Injection site: case S3. Serial sections stained (A) for Nissl substance following autoradiographic processing and (B) for TH-like immunoreactivity illustrate the center of the  $^{35}\text{S}$ -methionine injection site in case S3. The anterograde labeling in the striatum in this case is illustrated in Fig. 8. The injection site is centered in cell group A8. BC, brachium conjunctivum; CGS, central gray substance; PN, pontine nuclei. Scale bar = 1 mm.

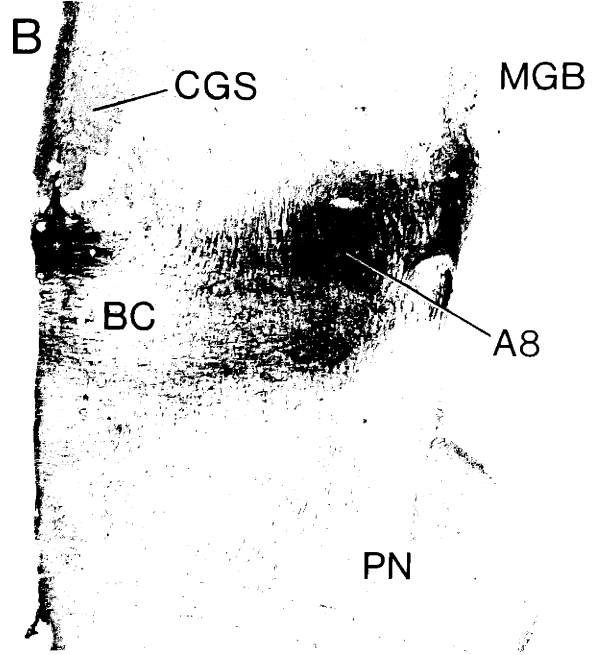


**Figure 2-13:** Injection site: case S5. Serial sections illustrating the injection site in case S5 in a Nissl-counterstained autoradiogram (A) in relation to the distribution of TH-positive staining in the nigral complex (B) are shown. The injection site is centered in the medial part of the nigral complex, involving the substantia nigra pars mixta (SNpm), the rostral extension of cell group A8 and adjoining parts of the ventral tegmental area. Striatal labeling in this case is shown in Fig. 10. SNpc, substantia nigra, pars compacta. Scale bar = 1 mm.

A

B

SNpc

SNpm

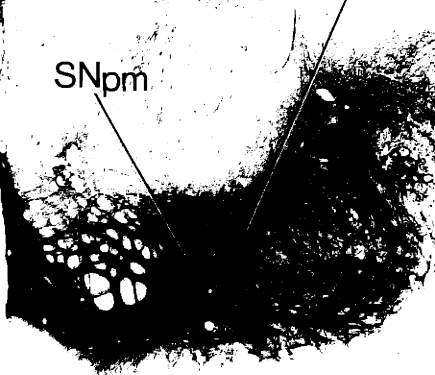


**Table I:**  
**Densitometry Measurements**

<b>Case</b>	<b>Striosomes</b>	<b>Matrix</b>	<b>Control</b>
S3 (all)	127.0 [5.4] <sup>#</sup>	141.2 [8.5] <sup>*</sup>	120.0 [1.2]
S5 (dCN)	136.0 [4.8] <sup>*&amp;+</sup>	156.5 [13.2] <sup>*&amp;</sup>	120.5 [1.9]
S5 (dP)	145.7 [14.5] <sup>*&amp;</sup>	161.0 [19.0] <sup>*&amp;</sup>	120.5 [1.9]
S5 (vCN,P)	199.6 [32.8] <sup>*+</sup>	235.0 [18.9] <sup>*</sup>	120.5 [1.9]
S11L (dCN)	205.2 [27.1] <sup>*#</sup>	168.5 [19.9] <sup>*&amp;</sup>	119.0 [1.6]
S11L (P)	213.1 [22.6] <sup>*#</sup>	173.9 [24.1] <sup>*&amp;</sup>	119.0 [1.6]
S11L (vCN)	NA	214.0 [12.7] <sup>*</sup>	119.0 [1.6]
S10R (all)	166.8 [15.2] <sup>*#</sup>	132.2 [8.0] <sup>*</sup>	119.0 [1.6]
S10R (dCN)	173.9 [12.9] <sup>*#</sup>	137.4 [6.5] <sup>*</sup>	119.0 [1.6]

**Table I:** Mean gray level density measurements and corresponding standard deviations (with standard deviations [s.d.] in brackets) of specific regions within the striatum in four cases (S3, S5, S11L and S10R). The individual zones analyzed by densitometry are outlined and described in Figs. 9, 11, 15 and 23. The data are organized in four columns: the first column identifies the the name of each case and the region evaluated; the second and third columns show the means and s.d. for striosomes and zones within the matrix, respectively, in the region evaluated; the fourth column displays the mean and s.d. of control regions (see Methods) determined for each case. \* =significantly different from control,  $p < .01$ ; #,+ =significantly different from the mean gray level intensity of the matrix in the same region  $p < .01$ ,  $p < .05$ , respectively; & =significantly different from the mean gray level intensity of the ventral region evaluated in that column,  $p < .01$ ; Regions evaluated: all, all zones drawn (see Figs. 9 and 15) were included in the mean; dCN, the dorsal part of the caudate nucleus (as indicated in Figs. 11, 15 and 23); dP, the dorsal part of the putamen (as shown in Fig. 11); vCN,P, the ventral half of the striatum (see Fig. 11); P, the entire putamen (as indicated in Fig. 23); vCN, the ventral part of the caudate nucleus (as shown in Fig. 23); NA, not applicable.

density measurement of the striosomal compartment in S3 is not significantly different from the density measurement obtained from unlabeled control regions indicating that there is virtually no labeling of the striosomal compartment in case S3. In S5, however, some labeling within the striosomal compartment was observed, and was further corroborated by a significantly higher densitometry measurement in striosomes than in unlabeled control regions. The origin of the weak striosomal labeling is unclear and will be discussed in a following section. In case S5, densitometry measurements also revealed that labeling in the dorsal part of the caudate nucleus or putamen (either striosomes or matrix) was significantly less dense than labeling in the ventral half of the striatum (both striosomes and matrix).

### **Substantia nigra, pars compacta**

A complementary pattern of intense labeling of striosomes with more modest labeling of the matrix was observed in parts of the striatum in nine hemispheres following injections centered in the main body of the substantia nigra pars compacta (see Figs. 3 and 4). Fig. 14 illustrates the pattern of striatal labeling in one of these cases, case S10R, in which the  $^{35}\text{S}$ -methionine deposit was placed just lateral to the middle of the pars compacta (Fig. 16). The deposit was ventral enough to infiltrate the ventrally extending fingers of the main horizontal band of the pars compacta (Jimenez-Castellanos and Graybiel, 1987b; Jimenez-Castellanos and Graybiel, 1989a) and also ventral enough to avoid major involvement of the overlying pars mixta. In addition, there was no detectable autoradiographic labeling along the pipette track.

Another illustration of heightened labeling of striosomes, but with moderate labeling of the matrix, comes from case S18L (Figs. 17, 18). In this case, the pattern of labeling was restricted to the very dorsal part of the head and body of



the caudate nucleus and the most rostral and dorsal part of the putamen. The enhanced striosomal labeling was apparent throughout the entire rostrocaudal extent of the dorsal head and body of the caudate nucleus. There was little or no labeling in the putamen at caudal levels. The injection site in this case (Figs. 19 and 4) was very small in cross section, located slightly caudal to that in S10R (Fig. 16). It infiltrated only the most ventral part of the pars compacta. Some weak labeling along the pipette track was observed. However, judging from cases with substantially labeled pipette tracks in similar regions of the thalamus (cases SF2R and S22L) but with no apparent striatal labeling, it is unlikely that the weak labeling observed along the pipette track in S18L contributed to the striatal labeling observed. It is important to point out that in the majority of the cases with enhanced striosomal labeling, there was very weak (cases S18L and S18R) and often no labeling (cases S10R, S20R, S20L, S21R, SF2L, S8R, S11L) along the pipette track (Fig. 7). The differences in the density and topography of striatal labeling observed in these cases appears to be directly related to the size and location of the injection site; weak labeling of thalamic regions along the pipette track does not appear to have contributed to the striatal labeling observed.

In six hemispheres, the centers of the deposits (see Figs. 3 and 4) were located both rostral and medial to the injection site shown in Fig. 16. In these six cases, the injection sites may have infiltrated the overlying pars mixta. Intensely labeled clusters of afferent fibers were observed in alignment with histochemically identified striosomes, but unlike the labeling in case S10R, moderate to dense labeling within the matrix compartment was also observed. The matrix labeling appeared much less dense than the labeling of the striosomal compartment. An example of enhanced striosomal labeling with moderate labeling in the matrix compartment is shown in case S20L (Fig. 20). In this case, rostral parts of both the

**Figure 2-14:** Enhanced labeling of striosomes: case S10R. Adjacent sections illustrate (A) anterograde labeling evoked in the striatum in case S10R by an injection of  $^{35}\text{S}$ -methionine in the substantia nigra pars compacta, and (B) the pattern of ENK immunostaining showing striosomes as zones containing few ENK-positive cell bodies (examples at asterisks). The densest fiber labeling is in striosomes of the caudate nucleus, and there is moderate labeling of the extrastriosomal matrix in the caudate nucleus. There is also slightly heightened labeling of striosomes in the putamen relative to the surrounding matrix. The injection site in this case is illustrated in Fig. 16. IC, internal capsule; OlfT, olfactory tubercle. Scale bar = 1 mm.

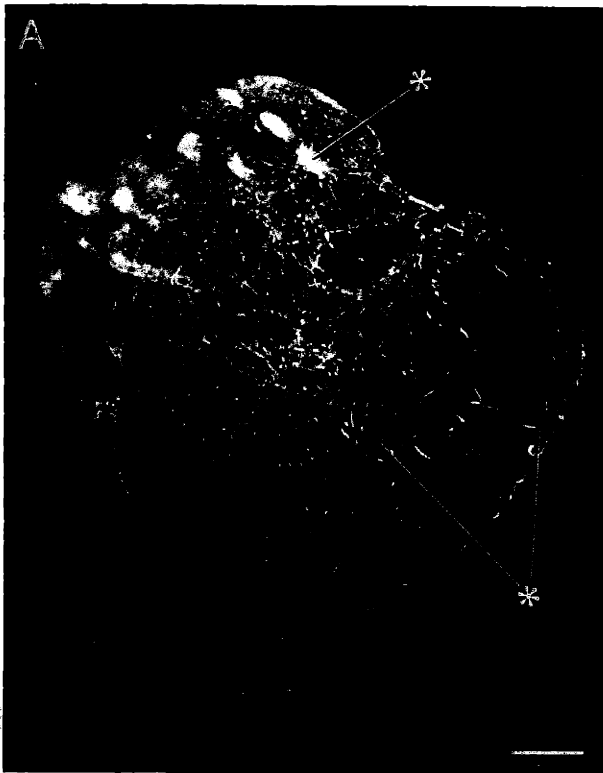


**Figure 2-15:** Drawing delineating zones for densitometry: case S10R. Enhanced labeling of striosomes (S) in case S10R, as shown in Fig. 14A, and other regions (M) arbitrarily chosen within the matrix, are outlined to indicate those zones which were evaluated by densitometry. The gray level intensity was measured (see Methods) in each of the zones outlined. The mean gray level measurement and corresponding standard deviation for striosomal (S) and matrical (M) regions are shown in Table I. A separate comparison between M and S regions only in the dorsal part of the caudate nucleus (the region with particularly enhanced labeling) is also shown; in this comparison the zones in the putamen were excluded as well as the two most ventral striosomal zones (S) and the two most ventral matrical (M) zones shown in the caudate nucleus. To aid orientation, an example of a striosome is shown with an asterisk as illustrated in Fig. 14A.

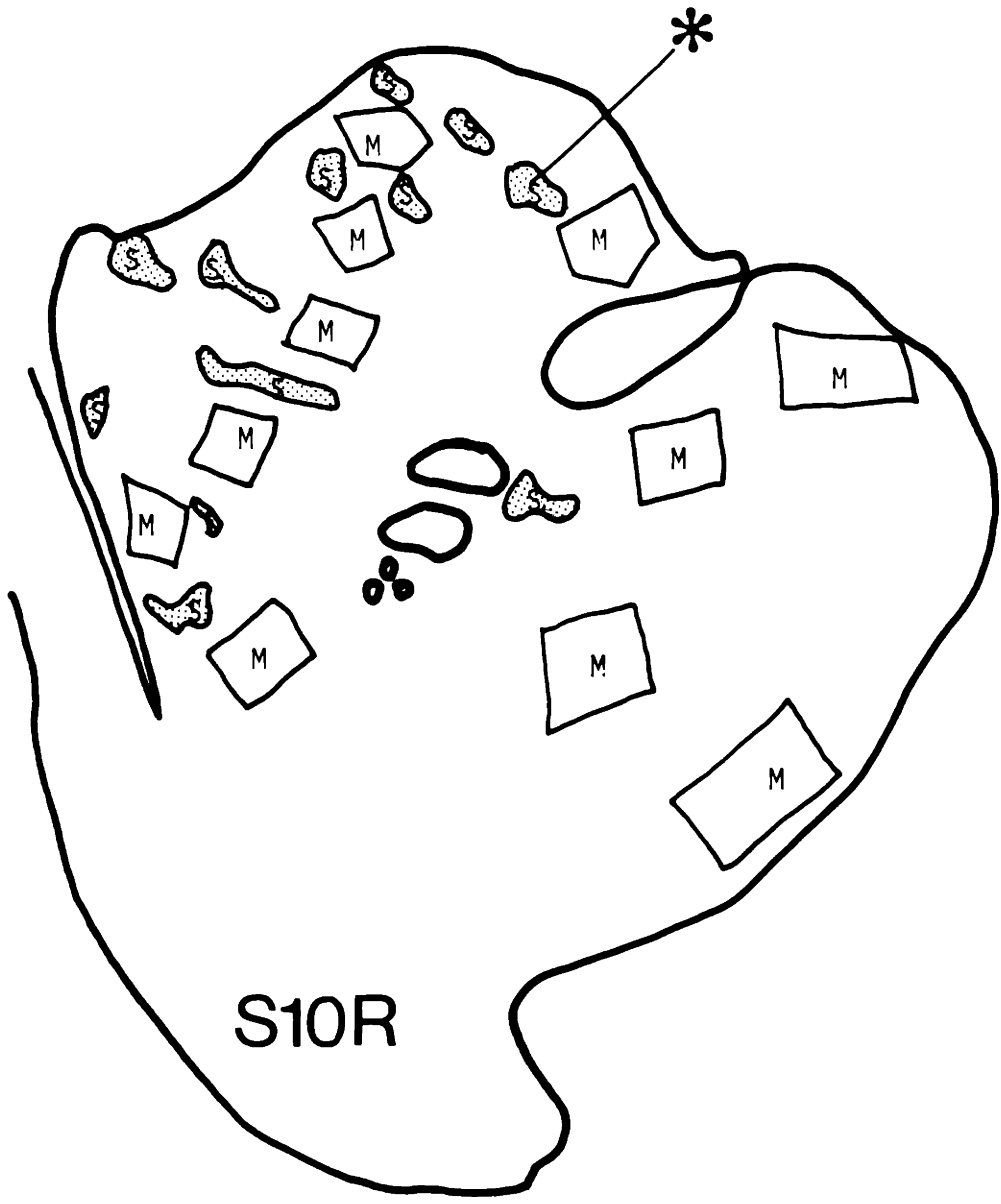


**Figure 2-16:** Injection site: case S10R. Serial sections illustrating the center of the injection site in case S10R in a Nissl-counterstained autoradiogram (A) in relation to the distribution of TH-positive staining in the nigral complex (B) are shown. The injection site is centered in the ventral part of the substantia nigra pars compacta (SNpc), and heavily infiltrates the ventrally extending fingers (f) of TH-immunoreactive neurons and neuropil. Striatal labeling in this case is shown in Fig. 14. SNpm, substantia nigra, pars mixta; Sth, subthalamic nucleus; III, third nerve; CP, cerebral peduncle. Scale bar = 1 mm.

A

Sth

B

SNpm

SNpc

f

f

CP

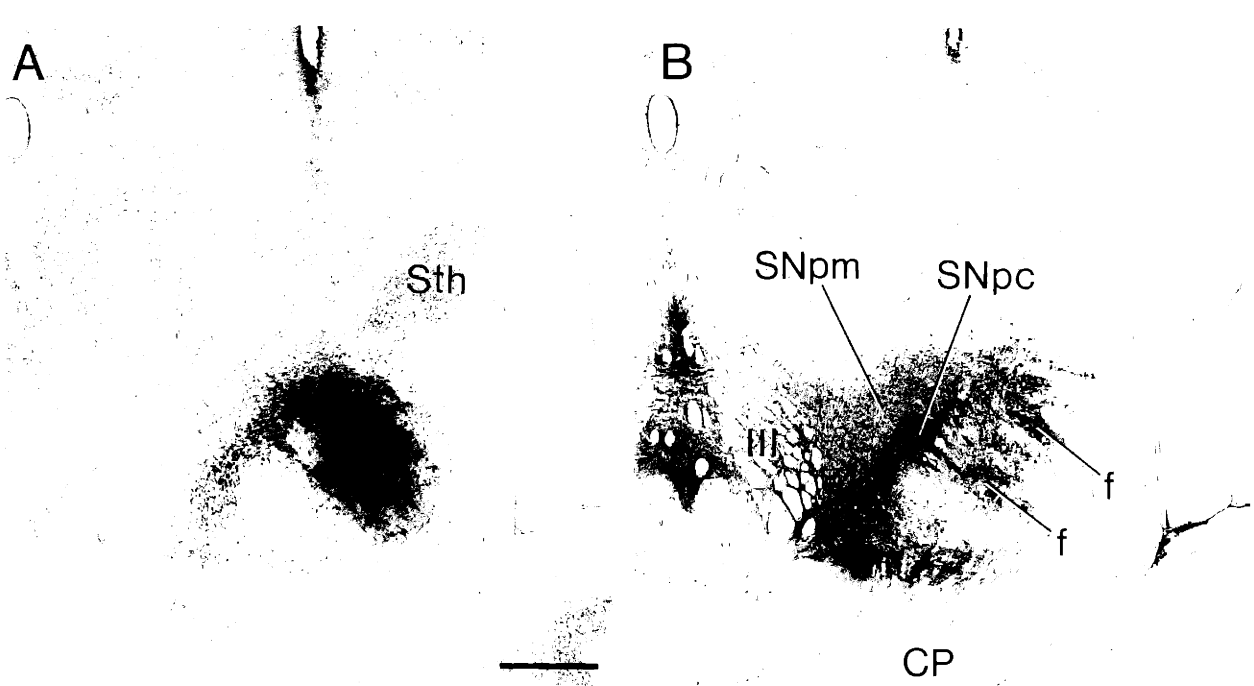


**Figure 2-17:** Enhanced labeling of striosomes: case S18L. Adjacent sections illustrating (A) anterograde labeling (shown in dark-field) evoked in the dorsal part of the striatum in case S18L by an injection of  $^{35}\text{S}$ -methionine in the substantia nigra pars compacta, and (B) the pattern of ENK immunostaining showing striosomes as zones containing few ENK-positive cell bodies (example at asterisk) are shown. The densest fiber labeling is in striosomes in the very dorsal part of the caudate nucleus and putamen, although there is moderate labeling of the extrastriosomal matrix in these same regions. The injection site in this case is shown in Fig. 19. CN, caudate nucleus; P, putamen. Scale bar = 1 mm.



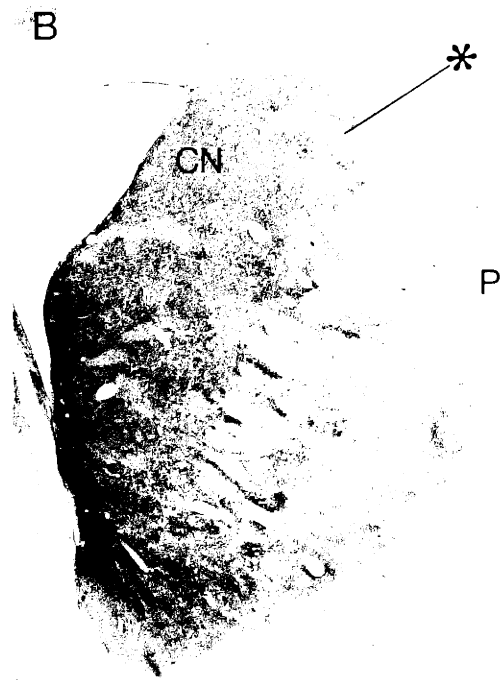


**Figure 2-18:** Enhanced labeling of striosomes: case S18L [light-field]. A higher power view (compared to Fig. 17) of the dorsal part of the striatum in case S18L is shown. Here the pattern of autoradiographic labeling in the Nissl-counterstained section is photographed as a light-field image. CN, caudate nucleus; P, putamen. Scale bar = 1 mm.

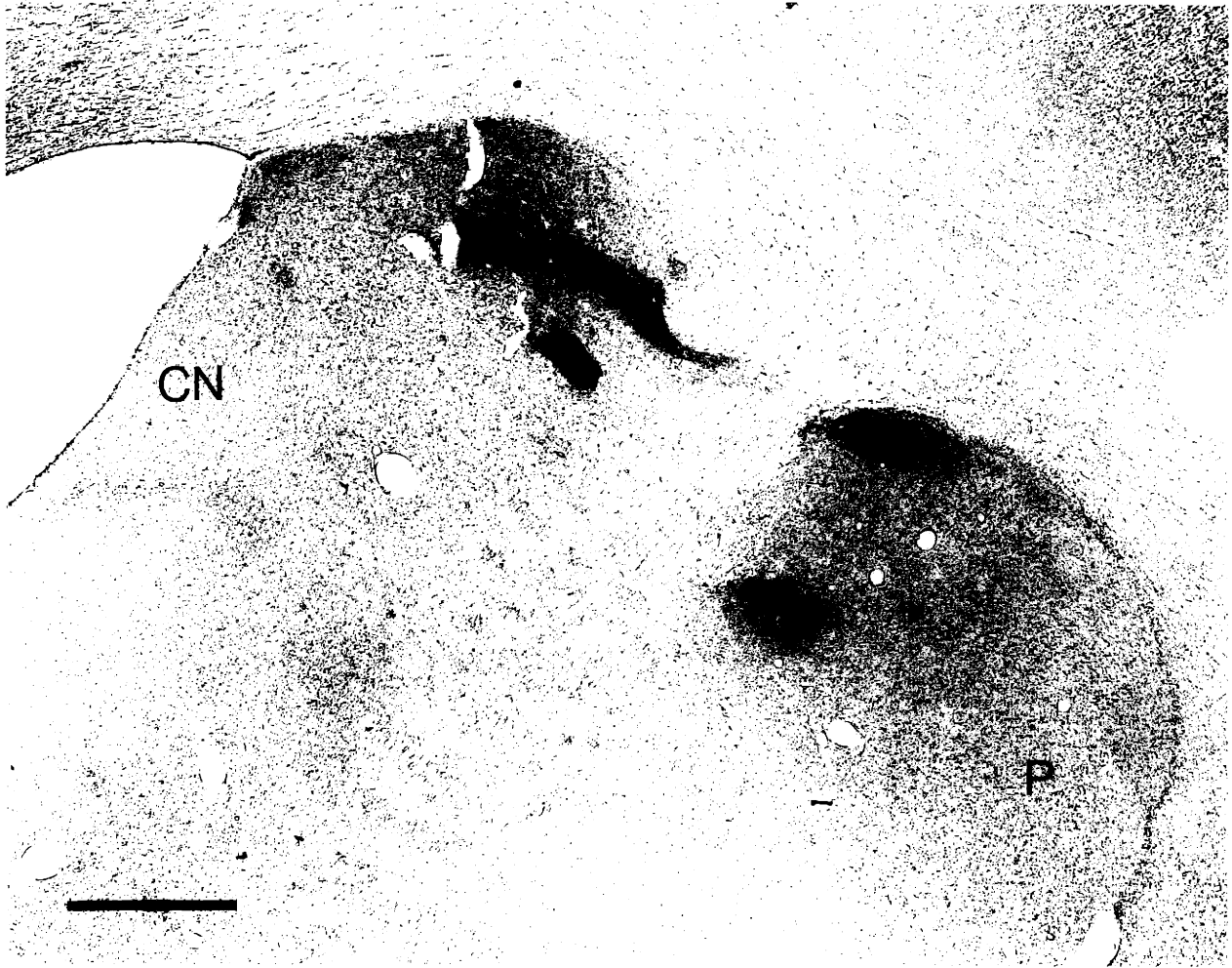
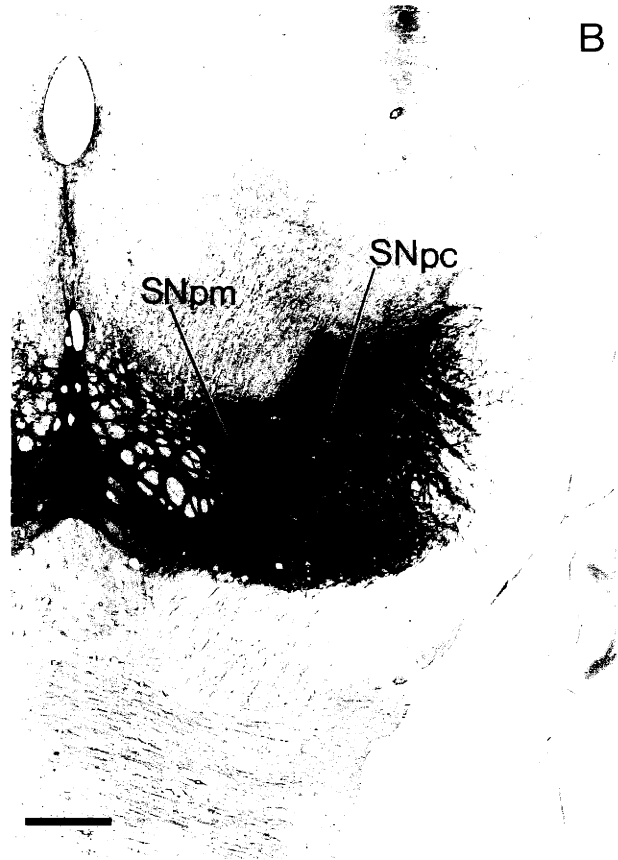


**Figure 2-19:** Injection site: case S18L. Serial transverse sections through the nigral complex in case S18L illustrate the location of the injection site in a Nissl-counterstained autoradiogram (A) in relation to the distribution of neurons detected by TH-immunostaining (B). The injection site is centered in a ventral part of the substantia nigra pars compacta (SNpc), predominantly infiltrating the dense band of cells observed in the ventral part of the substantia nigra pars compacta at middle to caudal levels. An example of the striatal labeling observed in this case is shown in Figs. 17 and 18. SNpm, substantia nigra, pars mixta. Scale bar = 1 mm.



pars compacta and the pars mixta were infiltrated with the tracer as shown in Fig. 21.

In all of these cases, identification of the intensely labeled zones as striosomes was possible in the caudate nucleus for nearly all labeled afferent fiber clusters. As shown in Fig. 14 (case S10R), the striosomes were clearest in sections stained for ENK-like immunoreactivity; they appeared as zones in which ENK-positive cell bodies were sparse. In every case in which there was heightened labeling of striosomes, this pattern appeared throughout the field of intrastriatal labeling. This field extended through the rostrocaudal extent of the head and body of the caudate nucleus, though in many cases it did not extend through the full dorso-ventral extent of the nucleus. Labeling was weak in the putamen in these cases.

In the putamen, we also observed intense autoradiographic labeling of striosomes. In parts of the caudoventral putamen striosomes were difficult or impossible to identify histochemically. Where striosomes could be positively identified in adjoining sections, the patches of anterograde label were in spatial correspondence with them, and seemed of about the same size. An example of enhanced striosomal labeling within the putamen is illustrated in Fig. 22 (case S11L). Many of the discrete zones of intense autoradiographic labeling in the putamen clearly lie in register with striosomes identified as zones with reduced populations of ENK-positive neurons. Anterograde labeling in the putaminal matrix was relatively weak. In the caudate nucleus, in this case, the labeling in the matrix was stronger than in the putamen but many striosomal forms could be identified. The injection site in this case (Fig. 24) was located caudal and slightly medial to the injection site in S10R, but also involved the lateral part of the main horizontal band at its most caudal extent; there was no labeling observed along the pipette track.

**Figure 2-20:** Enhanced labeling of striosomes: case S20L. Transverse sections through the striatum in case S20L illustrate (A) the pattern of autoradiographic labeling elicited by an injection into the substantia nigra involving both the pars compacta and the overlying pars mixta in relation to the disposition of striosomes (examples at asterisks) in the striatum detected with ENK immunostaining (B). The densest fiber labeling is in striosomes of the caudate nucleus, but there is dense labeling of the extrastriosomal matrix as well. There is also slightly heightened labeling of striosomes in the putamen relative to the surrounding matrix. The injection site in this case is illustrated in Fig. 21. IC, internal capsule. Scale bar = 1 mm.

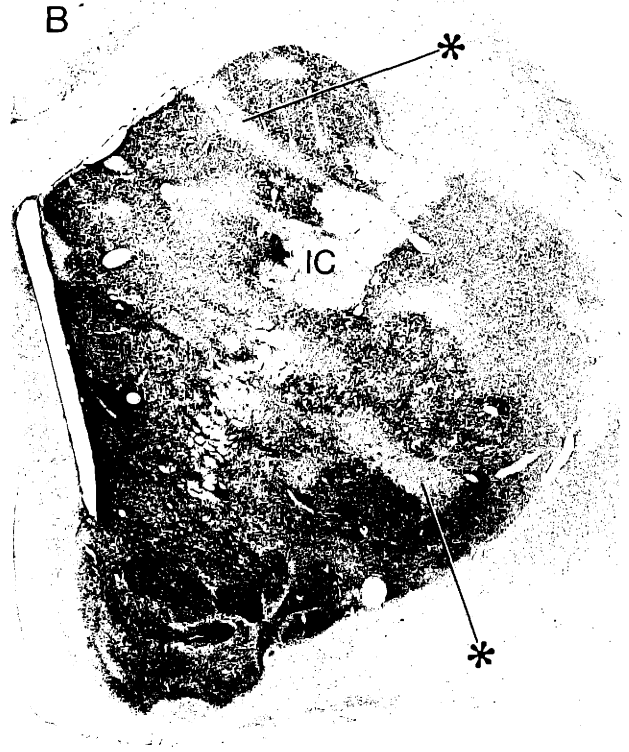
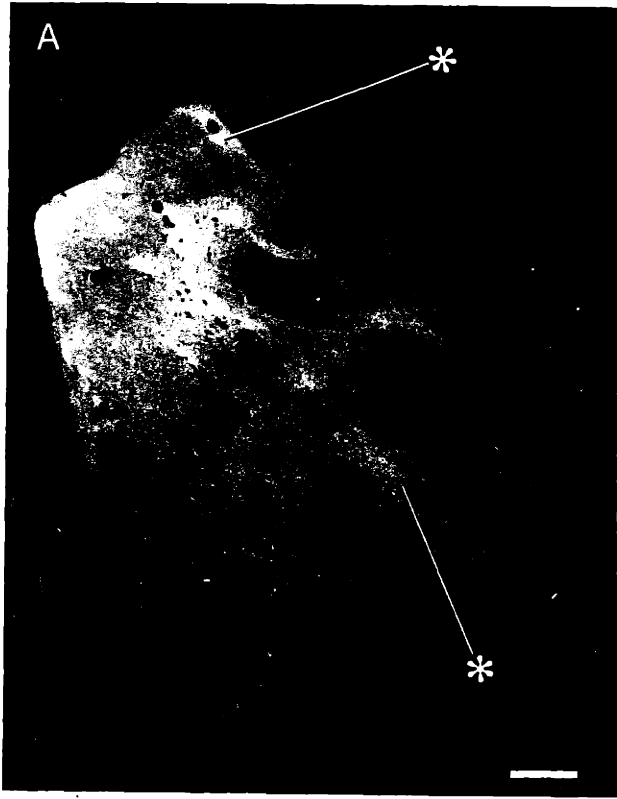
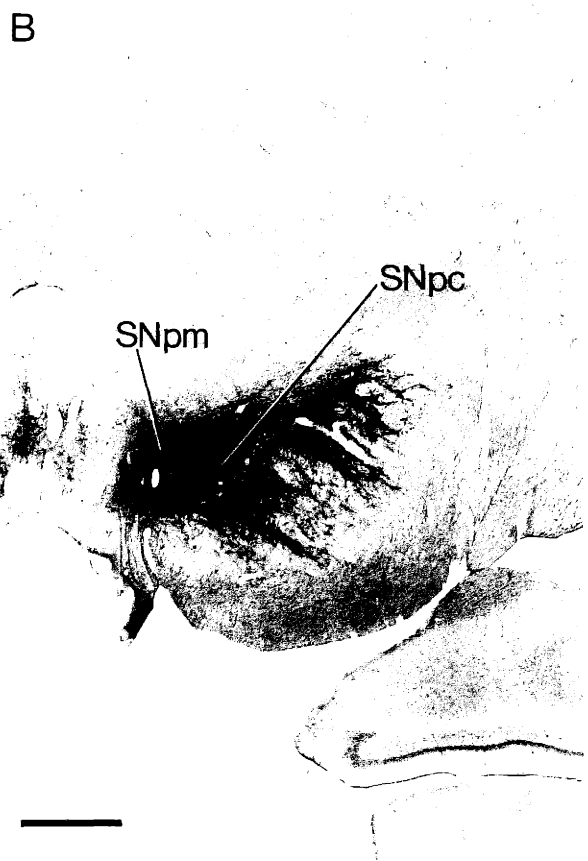




**Figure 2-21:** Injection site: case S20L. Serial transverse sections show the location of the injection site in case S20L in an autoradiogram counterstained for Nissl substance (A) in relation to the distribution of TH-positive neurons and neuropil in the nigral complex (B). The injection site is centered in the rostral part of the substantia nigra pars compacta (SNpc) also heavily infiltrating the overlying pars mixta (SNpm). Striatal labeling in this case is shown in Fig. 20. Scale bar = 1 mm.



To obtain quantitative estimates of the degree of preferential labeling of striosomes, we determined the relative gray level intensities of striosomes and matrix in case S10R (the case with strongly labeled striosomes which also appeared to have the least background matrix labeling) and in case S11L (the case with intensely labeled striosomes in the putamen which also had both striosomes and matrix labeled in the ventral caudate nucleus) [see Table I]. The sections evaluated in these cases are illustrated in Figs. 14 and 22, respectively; illustrations of the zones measured for densitometry are shown in Figs. 15 and 23.

In both cases, striosomes were significantly more intensely labeled than the matrix compartment. In addition, both the striosomal and matrix compartments were significantly more densely labeled than control regions (unlabeled cortical tissue and regions of clear glass slide). These measurements demonstrate that some background matrix labeling exists (compared to control regions) even in the case with the least observable labeling in the matrix (S10L). In case S11, the densitometry measurements also reveal significant labeling of the matrix. In addition, it is interesting that the density of labeling measured in the ventral caudate nucleus, where dense homogeneous labeling was observed (see Fig. 22), was comparable in density to the labeling of observable striosomes, suggesting that within the region where the tracer was injected (see Fig. 4 and 24), there exists a strong projection to both striosomes and matrix.

### **Cell group A10**

In one brain (S19), two injections (cases S19R and S19L, from right and left oblique approaches) were centered at the midline at two rostrocaudal levels infiltrating only the midline dopamine-containing cells of the ventral tegmental area. One of the two injections also labeled cells slightly lateral to the midline but still medial to the oculomotor fibers. These injection sites are shown in Figs. 5, 25

**Figure 2-22:** Enhanced labeling of striosomes in the putamen: case S11L. Autoradiographic labeling of striosomes observed in case S11L with an injection site involving the lateral part of the main horizontal band at its most caudal extent (A), and (B), the pattern of ENK immunostaining showing striosomes as zones containing few ENK-positive cell bodies (example at asterisk) in the caudate nucleus (CN) and putamen (P) are illustrated. The densest fiber labeling is in striosomes in the putamen and in the matrix in the ventral part of the caudate nucleus. There is also heightened labeling of striosomes in the dorsal part of the caudate nucleus relative to the surrounding matrix. The injection site in this case is illustrated in Fig. 24. IC, internal capsule. Scale bar = 1 mm.

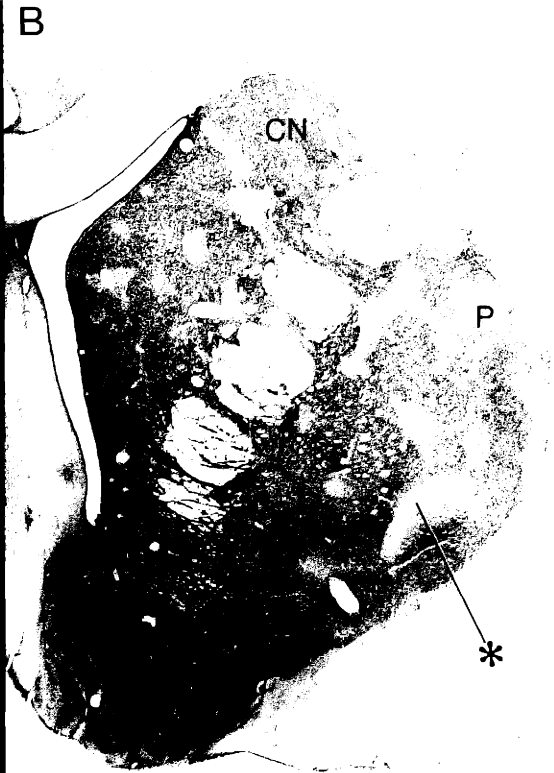
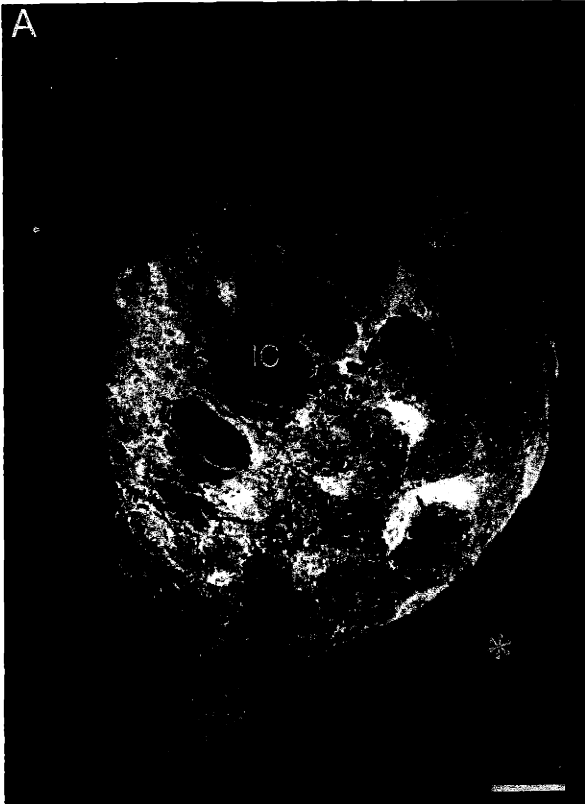
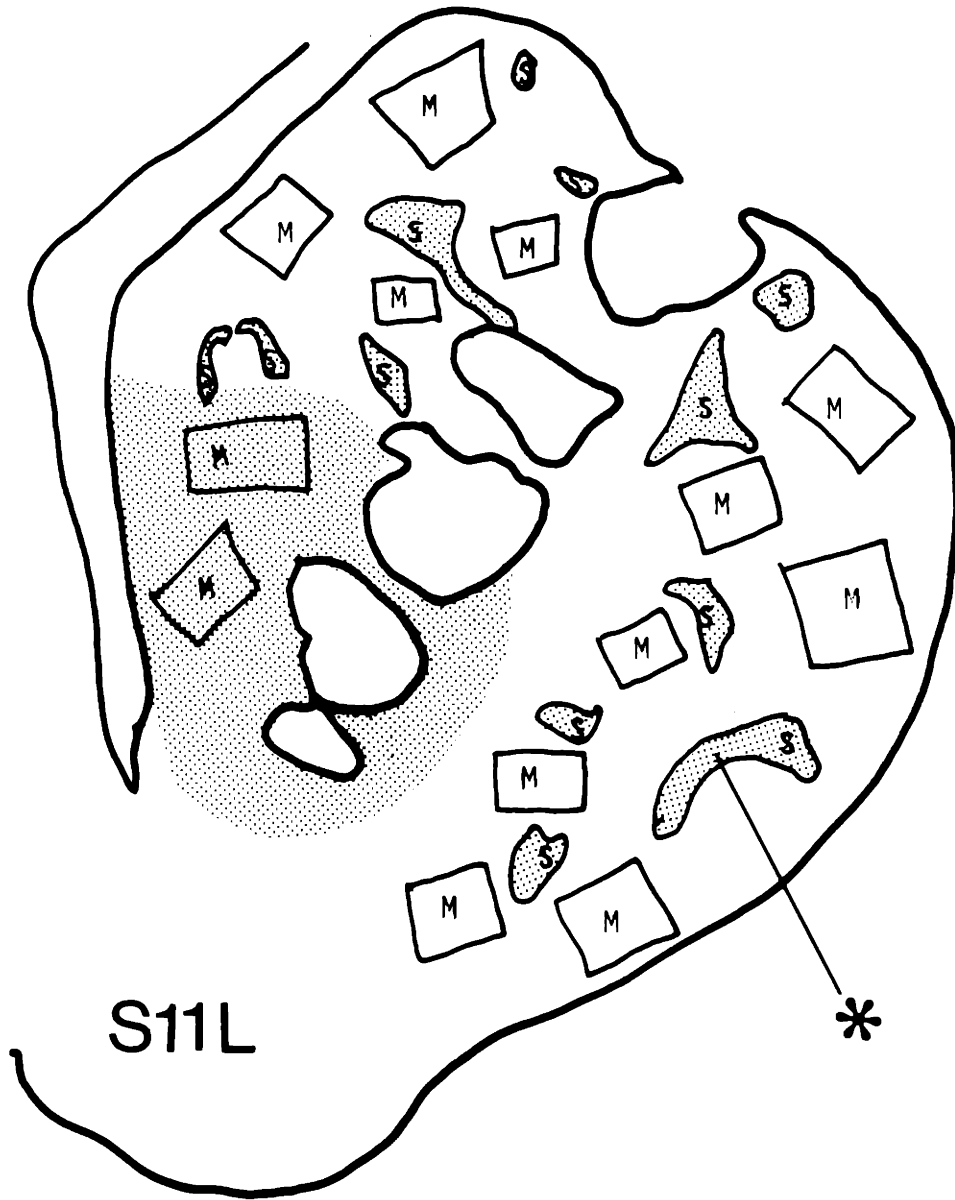


**Figure 2-23:** Drawing delineating zones for densitometry: case S11L. Autoradiographic labeling in case S11L, as shown in Fig. 22A, is drawn schematically. Striosomes (S) and regions within the matrix (M) are outlined to indicate those zones which were evaluated by densitometry. The gray level intensity was measured (see Methods) in each of the zones outlined. The mean gray level measurement and corresponding standard deviation for S and M regions are shown in Table I. Separate comparisons between M and S regions in the putamen only and in the dorsal part of the caudate nucleus only (excluding the homogeneously labeled region in the ventral part of the caudate nucleus) are also indicated in Table I. To aid orientation, an example of a striosome is shown with an asterisk as illustrated in Fig. 22.



S11L

**Figure 2-24:** Injection site: case S11L. Serial transverse sections through the nigral complex in case S11L show the location of the injection site in a Nissl counterstained autoradiogram (A) in relation to the distribution of TH-positive neurons and neuropil (B). The injection site is centered in the substantia nigra pars compacta (SNpc), heavily infiltrating neurons of the main horizontal band without strong involvement of the overlying pars mixta (SNpm). Striatal labeling in this case is shown in Fig. 22. Scale bar = 1 mm.



A

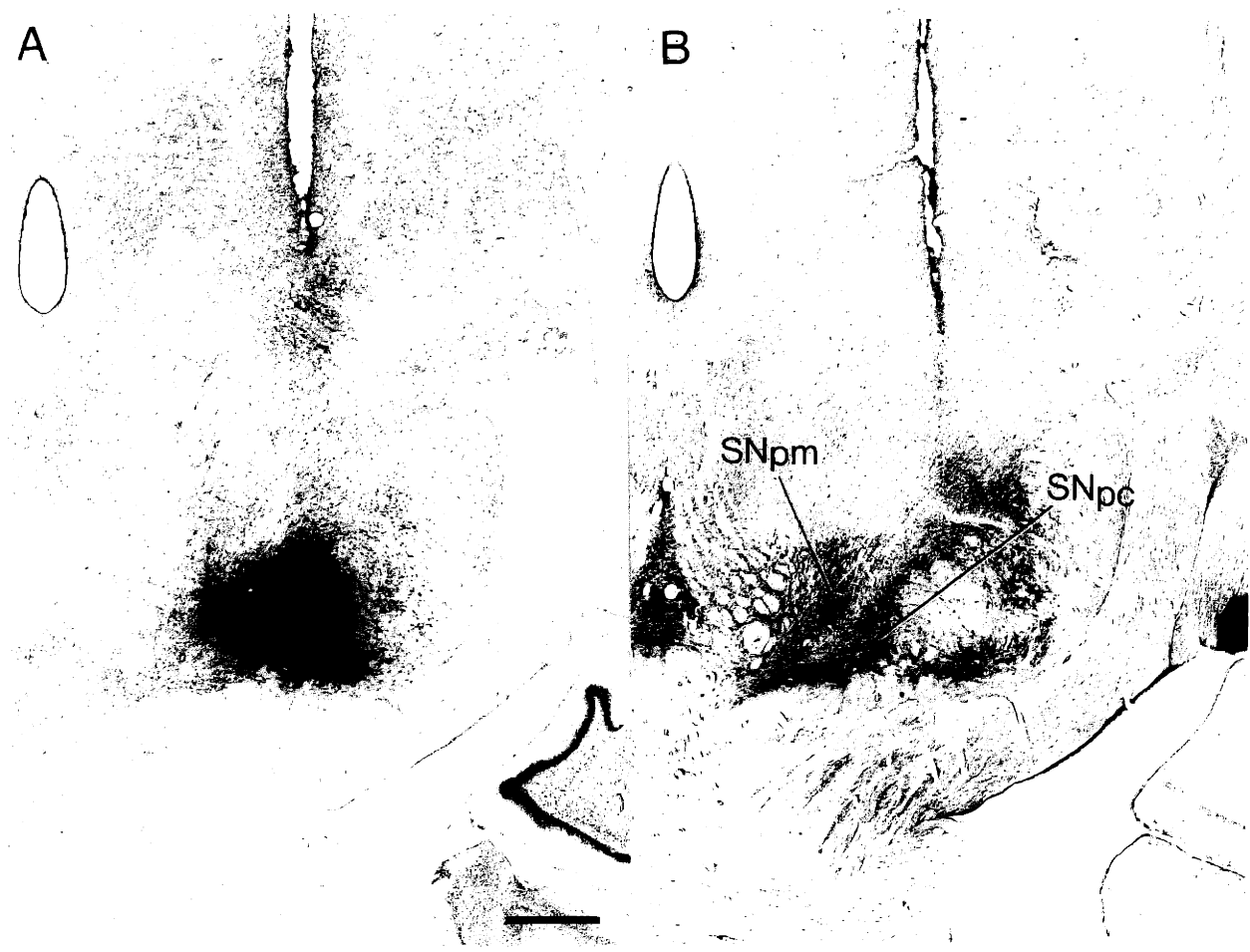


B



SNpm

SNpc

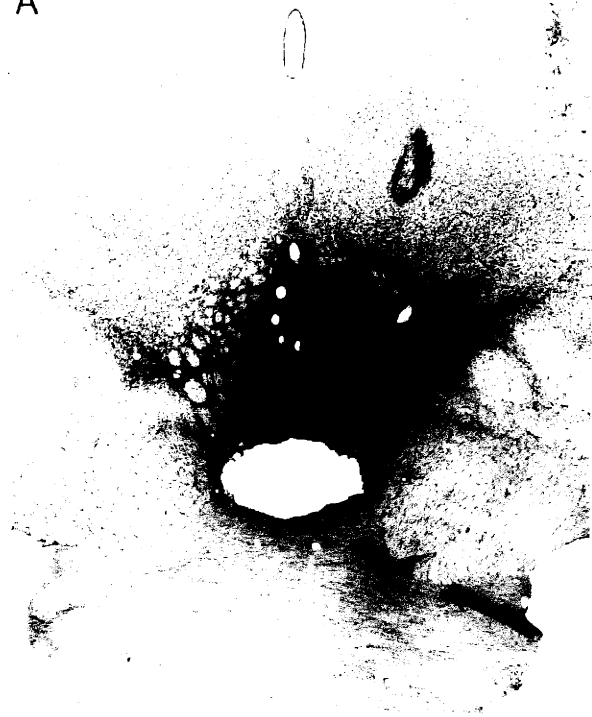


and 26. There was no observable labeling along the pipette tracks. The striatal labeling resulting from these circumscribed injections was completely restricted to the most ventral part of the striatum, ventral to the junction between the caudate nucleus and putamen and including the nucleus accumbens and the olfactory tubercle. Ipsilateral to the paramedian injection, very weak labeling was also observed in the most ventral part of the putamen. This weak labeling was distinctly heterogeneous and appeared to correspond in size and pattern to matrical labeling, but very few striosomal "avoids" were detectable histochemically (see Fig. 27). On the other side of the brain (Fig. 28), ipsilateral to the restricted midline injection, labeling within the caudate nucleus and putamen was barely visible even after being exposed for up to 4 months. These were the only cases for which striatal labeling could not be identified along the entire rostrocaudal extent of the striatum.

Anterograde labeling throughout the ventral part of the striatum was also observed in other cases of this series (SF1L, S22R, S21L, S5; see Fig. 5); in one case, case S5 (Fig. 10), the anterograde labeling in the ventral half of the striatum was particularly dense. In all of these cases, injection sites predominantly infiltrated the medial part of the pars compacta, the medial pars mixta and those neurons of the ventral tegmental area known to be interspersed between the oculomotor fibers. It was not possible to identify histochemically matrical labeling within the most ventral part of the caudate nucleus and putamen, due to the complicated histochemical patterning normally observed in this region; however, some heterogeneity was detected in cases S21L and SF1L, in the ventral putamen, and in case S22R, in the ventral part of the caudate nucleus.

**Figure 2-25:** Injection site [VTA]: case S19, rostral. Serial sections stained (A) for Nissl substance following autoradiographic processing and (B) for TH-like immunoreactivity illustrate the injection site in case S19. The anterograde labeling in the striatum in this case is illustrated in Figs. 27 and 28. The injection site is centered in cell group A10, the ventral tegmental area (VTA). A second injection was similarly placed just caudal to this injection, as shown in Fig. 26. Scale bar = 1 mm.

A



B



**Figure 2-26:** Injection site [VTA]: case S19, caudal. Serial sections illustrate the injection site in case S19 in a Nissl-counterstained autoradiogram (A) in relation to the distribution of TH-positive staining in the nigral complex (B). The injection site is centered in cell group A10, the ventral tegmental area (VTA). A similarly placed injection (just rostral to this injection) was also made in this case, as shown in Fig. 25. The anterograde labeling in the striatum in this case is illustrated in Figs. 27 and 28. Scale bar = 1 mm.

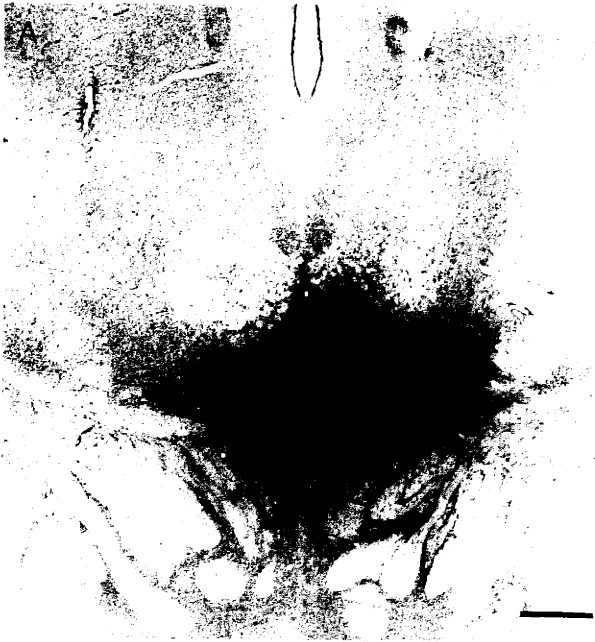


**Figure 2-27:** Striatal labeling: case S19L. Adjacent sections through the striatum (CN, caudate nucleus; P, putamen) in case S19L illustrate (A) the pattern of autoradiographic labeling elicited by an injection in cell group A10 in relation to the location of striosomes in the striatum detected with ENK immunostaining (B). Most of the mesostriatal label is in the nucleus accumbens, although some very weak labeling in the extrastriosomal matrix is visible in the ventral part of the putamen (examples at asterisk). The labeling within the striatum on the other side of the brain (case S19R) is shown in Fig. 28. Scale bar = 1 mm.

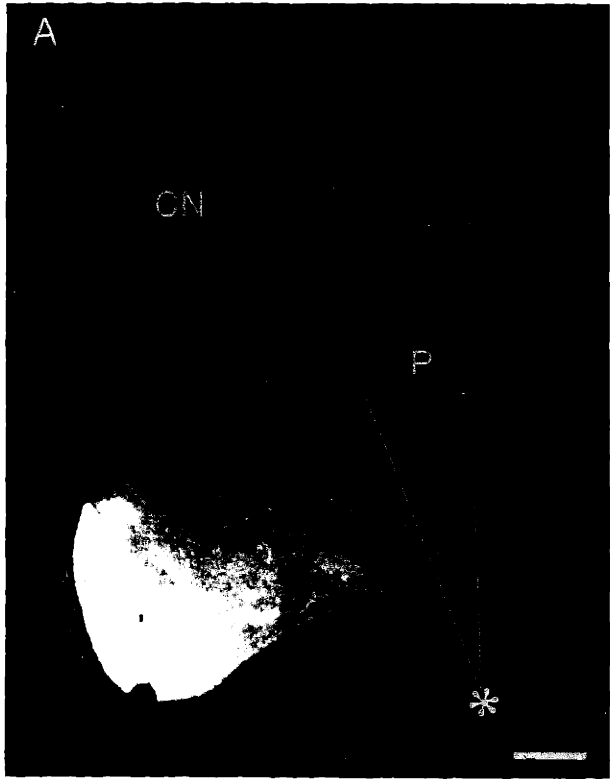
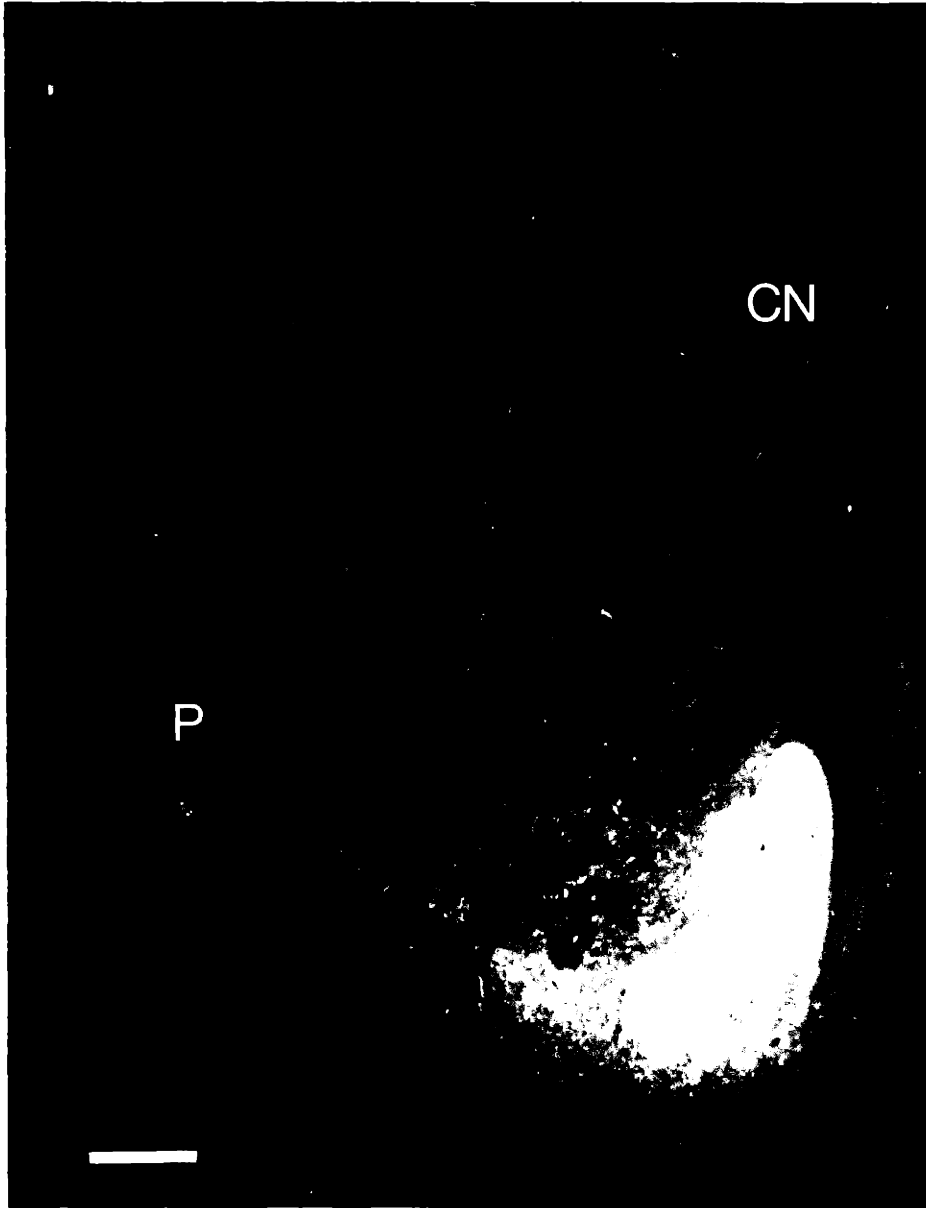




**Figure 2-28:** Striatal labeling: case S19R. A transverse section through the striatum in case S19R illustrates anterograde labeling within the nucleus accumbens evoked by an injection in cell group A10. The injection site in this case is shown in Figs. 25 and 26. The labeling within the striatum observed on the other side of the brain (case S19L) is shown in Fig. 27. CN, caudate nucleus; P, putamen. Scale bar = 1 mm.



## "Mixed" Injections

In several of the cases of this series, the injection sites were large and the tracer appeared to have infiltrated much of the medial part of the pars compacta as well as parts of cell group A8, the pars mixta and to variable extents, cell group A10. In these cases, striking patterns of partial labeling, homogeneous labeling and/or regionally selective compartmentalized labeling was observed.

An example of regionally specific labeling is illustrated in S11L (Fig. 22). Patchy labeling was present in the putamen though at the same level diffuse labeling was present in the ventral part of the caudate nucleus. It was also possible to observe slightly enhanced striosomal labeling at one rostrocaudal level and evidence for matrical labeling at another level (cases S14R and S23R). In these cases, the injection sites were centered in the medial part of the nigral complex and therefore likely infiltrated neurons of the main horizontal band as well as the rostral part of A8 (see Fig. 6). This suggestion is further corroborated by case S17L with an injection site slightly rostral to those of S14R and S23R; in this case, labeling was predominantly homogeneous, although some weak, but enhanced striosomal labeling could be observed in small, restricted regions of the caudate nucleus. In two cases (S10L and S9L), labeling was predominantly homogeneous throughout the striatum except for some slightly enhanced striosomal labeling in some parts of the putamen. In one case (S11R) evidence for some slightly enhanced matrical labeling within the caudate nucleus and putamen was detected at some levels although predominantly homogeneous labeling was observed at most levels. Only in one case, in which labeling was extremely weak (barely visible even after a 3 month exposure), was striatal labeling observed with no apparent compartmentalized labeling detected (S23L). The injection sites for these cases are shown in Fig. 6. Labeling along the pipette track is illustrated in Fig. 7.

We could not always determine whether patches of dense labeling "filled" striosomes and whether the lacunae represented striosomal "avoids", or whether the failure of patterning in the immunohistochemistry accurately reflected a paucity of striosomes (e.g. in the central-caudal putamen). The general patterning (patchy, lacunar) of labeling in such sections was similar, however, to that in other sections in which matches with striosomes could be made. We did not evaluate the exact size of strongly labeled or weakly labeled zones corresponding to striosomes in relation to the size of striosome markers in adjoining sections, although the sizes of the two sets of patches were roughly similar. We cannot, however, say whether the labeling patterns showed any specializations or striosomal borders such as found in primates with immunoreactivities for SP-like and ENK-like antigens and ligand binding for neurotensin binding sites (Graybiel, 1986b; Faull et. al., 1989)

It was also difficult to assess the contribution of a thalamostriatal innervation because in the majority of these cases injections were accompanied by some labeling along the pipette track. However, case S14R (with predominantly homogeneous labeling and some evidence for both enhanced striosomes and enhanced matrix in certain regions) showed no labeling along the pipette track. In addition, there was little evidence for homogeneous labeling within the striatum in cats with injections in various parts of the thalamus (Ragsdale and Graybiel, 1989b). Judging from findings with restricted deposits, the differential involvement of part of A8, the pars mixta and part of the main body of the substantia nigra pars compacta most likely accounts for these different homogeneous and mixed patterns of intrastriatal labeling.

### **Mesostriatal Topography**

In many cases, both for the predominant striosomal (patchy) labeling and for the predominant matrical (lacunar) labeling, there were systematic shifts in the

dorsoventral location of the main fields innervated by labeled fibers. For example, dorsally placed injections within the main horizontal band of the pars compacta and within the pars mixta resulted in labeling of more ventrally situated striatal regions than did ventrally placed injections (within the pars compacta and the ventrally-extending finger-like regions and within the ventral part of the pars mixta) which produced labeling in restricted dorsal parts of the caudate nucleus and putamen. This type of inverted dorsoventral nigrostriatal topography is similar to that described previously in the rat (Beckstead, 1987a; Fallon and Moore, 1978; Faull and Mehler, 1978; Nauta et. al., 1978), cat (Royce, 1978; Royce and Laine, 1984; Szabo, 1980a; Jimenez-Castellanos and Graybiel, 1987a) and monkey (Carpenter and Peter, 1972; Szabo, 1980b).

In almost every case of this series at least some labeling was apparent through the entire rostrocaudal extent of the striatum (the putamen and the head, body and tail of the caudate nucleus). For cases with preferential labeling of striosomes, striosomes in the caudate nucleus were predominantly labeled by tracer injections into anterior and lateral parts of the pars compacta whereas striosomes within the putamen (where they could be identified as such) were labeled by injections involving slightly more medial and caudal parts of the pars compacta. There was also a partly shifted but otherwise apparently parallel organization of the midbrain projections to the matrix. In several cases we observed that the caudal parts of cell group A8 project mainly to the putamenal matrix (where it could be identified histochemically), whereas with more anterior injections in A8, invariably involving the pars mixta, it was matrical parts of the caudate nucleus (and dorsal, rostral putamen, as well) that were most strongly labeled. No examples of matrical labeling restricted entirely to the caudate nucleus were observed.

Although striatal labeling was apparent at all rostrocaudal levels (even if occasionally weak or diffuse), in many cases, particular anteroposterior levels appeared more densely innervated than others. Therefore, it appears that there is some topographic enhancement of a given projection from certain nigral regions to distinct anteroposterior levels, including some differentiation of the caudate nucleus and putamen. It should be noted, however, that it was very difficult to interpret accurately the evidence for striatal labeling at all anteroposterior levels. As shown in Figs. 1-6, the majority of the cases with perceptible striatal labeling also show some labeling within the nigral complex throughout the rostrocaudal extent of the the nigral complex (20 out of 29 cases), even though the "centers" of the injections may have been more restricted. In a few cases, injections were either smaller or centered in the extreme rostral or caudal parts and were therefore restricted to the rostral half (n=6) or the caudal half (n=3) of the A8-A9-A10 cell complex. Even in these cases, however, some striatal labeling (even if very weak) was observed at all rostrocaudal levels. It is possible that some of the fairly dense labeling in the substantia nigra, especially that contributing to the anteroposterior elongation of the injection site, was labeling of fibers running through the substantia nigra on their way to the striatum, or even partly of fibers of interneuronal origin. It was difficult to determine what elements were labeled in the zones of weak labeling observed at the periphery of nigral injections.

From several cases in which very large injections were made, we have strong evidence suggesting that mesostriatal projections are exclusively ipsilateral. Judging from cases in which very large unilateral injections were made and from some cases in which large injections were made on one side and on the other side injections were made which did not infiltrate the nigral complex, there was no evidence for striatal labeling contralateral to the large injections within the nigral

complex. At most, contralateral to these large injections, it was sometimes possible to observe very weak labeling within the medial forebrain bundle, just above the nigral complex.

## Discussion

The findings in these experiments suggest that in the primate, spatially separate parts of the dopamine-containing cell complex of the midbrain project, respectively, to striosomes and to the extrastriosomal matrix of the striatum. The A8 cell group and at least part of the pars mixta were implicated as sources of a strikingly selective innervation of the extrastriosomal matrix, where extrastriosomal matrix could be identified as such. At least the lateral part of the main horizontal band of the pars compacta of the substantia nigra with its ventrally descending finger-like extensions was identified as projecting strongly to striosomes. The differential striatal projections of the medial part of the main horizontal band and of the overlying pars mixta was more difficult to determine because most injection sites in the medial part of the nigral complex apparently infiltrated neurons of the medial part of the pars compacta as well as at least the rostral part of cell group A8.

*Subdivisions within cell groups A8 and A9.* Given the complex topography of the A8-A9-A10 cell complex, identifying the borders of the regions giving rise to differential projections to striosomes and to the matrix is likely to require work with tracers that can be more sharply confined to the tissue immediately around the injection pipette than the amino acid solutions that we employed. Nevertheless, the findings clearly suggest that at least part of the pars compacta of the substantia nigra has preferential projections to striosomes while at least part of cell group A8 targets the matrix. These findings are in good accord with previous studies in the rat (Deutch et. al., 1984; Gerfen, 1985; Moon-Edley and Herkenham,

1983) and cat (Jimenez-Castellanos and Graybiel, 1985; Jimenez-Castellanos and Graybiel, 1986; Jimenez-Castellanos and Graybiel, 1987a). In both species cell group A8 has been identified as the source of a projection to the matrix compartment of the striatum. The experiments we report here leave open the possibility that some part of this continuum, either within the main body of cell group A8 or more anteriorly in its zone of fusion with the pars mixta, projects to striosomes. Nevertheless, the experiments demonstrate unequivocally that a principal target of cell group A8 and at least the caudal part of the pars mixta is the extrastriosomal matrix.

In both rat and cat, it is the more ventrally situated cells of the substantia nigra's pars compacta that have been suggested to project preferentially to striosomes. In the rat, the pars compacta can be divided into dorsal and ventral tiers (Fallon and Moore, 1978; Fallon et. al., 1978; Fallon and Loughlin, 1982; Gerfen et. al., 1987a), the more ventral tier apparently projecting to striosomes. In the cat, there is a ventromedially situated hypercellular zone within the pars compacta (the densocellular zone) which appears, along with its rostral extensions, to be the main (but not only) striosome-projecting part of the compacta. Caudal striosomes are also labeled by injection sites centered in the pars lateralis of the substantia nigra (Jimenez-Castellanos and Graybiel, 1987a). The topography of the nigral complex is different in the primate, rat and cat. However, if the main part of the pars compacta with its ventrally-extending fingers is considered as a ventral tier of A9 and the pars mixta as a dorsal tier of the same cell group, the situation might be quite similar to that in cat and rat: the dorsally situated pars mixta of the monkey (at least in part) appears to project to the matrix as the dorsal pars compacta (rat) and diffuse part of the pars compacta (cat) are reported to; and the ventrally situated more densocellular part of the pars compacta with



ventral extensions into the pars reticulata projects (at least in part) to the striosomal system as the corresponding ventral tier in the rat and the densocellular zone in the cat are reported to do.

A number of factors contribute to the overall complexity of the primate substantia nigra which make the job of dissecting specific subdivisions within the nigral complex very difficult. The topographical location of the different cell groups changes dramatically from one anteroposterior level to another (see Figs. 1 and 2 of chapter one). The dopamine-containing neurons of the pars mixta and cell group A8 form a continuous band of cells from rostral to caudal levels, but the predominant position of these neurons shifts from dorsal to the main horizontal band of the pars compacta to a position medial and caudal to the densely packed neurons of the pars compacta. Similarly, at rostral levels, there is a discrete band of neurons making up the main horizontal band of the pars compacta and the ventrally descending finger-like regions are easily recognizable, but at progressively more caudal levels, there are prominent dorsal and ventral bands of neurons that intersect medially; in the most caudal regions, this double band of cells becomes displaced laterally. This complex configuration of neurons makes it technically difficult to confine injections to a particular cell group. In addition, identifying borders between the pars mixta, the pars compacta and cell group A8 is often impossible. In sections immunostained for tyrosine-hydroxylase, the neurons and neuropil of the main horizontal band generally appear more densely stained than the more loosely organized neurons of either the overlying pars mixta or cell group A8. However, in the middle region of the nigral complex, for example, where there is a dorsal and ventral dense band of cells, often there is no distinguishable border between the overlying pars mixta and the dorsal band of neurons within the pars compacta.

The fact that the pars compacta, the pars mixta and cell group A8 are arranged in a somewhat intertwined configuration at many levels could account for why the most clear example of striosomal labeling (case S10R) was observed in the case with an injection site most completely confined to the lateral part of the main horizontal band, where the pars mixta is less prominent and there is no contamination with cell group A8, and why the best example of matrinal labeling (case S3), with no detectable labeling in regions corresponding to striosomes, was observed following an injection into the caudal part of cell group A8, thereby not contaminating any part of the main horizontal band. Even with very small injections in other parts of the nigral complex enhanced labeling of one compartment was normally accompanied by some labeling, even if very weak, of the other compartment; therefore, even if there are fully selective subgroups of striosome- and matrix-projecting neurons, it would be difficult, if not impossible, to inject them exclusively because 1) technically, injections cannot be made into a distinct region without contaminating other parts of the nigral complex, 2) groups of neurons with compartmentally distinct projections could be arranged in interdigitating clusters, for example, and would therefore be too small to be infiltrated separately except perhaps in certain parts of the nigral complex, or 3) there also exist groups of neurons throughout the nigral complex that project to both striatal compartments.

Some labeling of the matrix appeared along with heightened labeling of striosomes in all cases of predominant striosomal labeling, and some grain was evident in regions corresponding to striosomes in cases of predominant labeling of the matrix. These findings were also confirmed by the densitometry measurements in cases S5, S10R and S11L. It is possible in all such cases that the injection sites infiltrated both striosome-projecting and matrix-projecting subdivisions of the

mesencephalon, but in doing so strongly favored one or the other. Alternatively, all parts of the midbrain injected may contain groups of neurons or single neurons projecting both to striosomes and to the adjoining matrix. The differential density of labeling in striosomes and in matrix in most of the cases described here suggests that compartmental selectivity is characteristic of the mesostriatal projections of a large part of the A8-A9 cell groups even if some mixed-compartment targeting occurs.

Evidence for the clustering of distinct populations of neurons comes from the work of Parent and colleagues (Parent et. al., 1983b; Parent et. al., 1983a) and others (Jimenez-Castellanos and Graybiel, 1989a). These authors showed that injections of retrograde tracers into the caudate nucleus and putamen revealed clusters of interdigitating nigrocaudate and nigroputaminal neurons throughout the entire extent of the substantia nigra, although nigrocaudate neurons were found to be more predominant dorsorostrally compared to nigroputaminal neurons, which appeared to be most prominent ventrocaudally (Parent et. al., 1983b; Parent et. al., 1983a). If a similar organization of striosome- and matrix-projecting cell groups exists it would be virtually impossible to inject single clusters of neurons. Similarly, if there are also groups of neurons which project to both compartments it may be technically impossible to dissect these subdivisions unless they are confined to fairly large, spatially distinct regions of the nigral complex.

It is hoped that the heterogeneous organization of certain neurotransmitter-related compounds will help to dissect these important subdivisions within the nigral complex. For example, in the rodent substantia nigra, it appears that neurons containing calcium binding protein (CaBP) project exclusively to the matrix compartment (Gerfen et. al., 1985; Gerfen et. al., 1987b); it is not yet clear whether CaBP characterizes matrix-projecting cells of the nigral complex in the

primate, although many neurons containing CaBP may be found in the region of cell group A8 (Langer and Graybiel, unpublished observations). In the cat, the densocellular zone which projects predominantly to striosomes (Jimenez-Castellanos and Graybiel, 1987a) is also characterized by heightened labeling of sigma binding sites and particularly reduced labeling of dopamine, D1, binding sites (Besson et. al., 1988; Graybiel et. al., 1989a). A heterogeneous distribution of D1 and sigma binding sites has also recently been observed in the primate nigral complex (Graybiel, personal communication). It will be interesting to compare experimentally identified zones in the monkey with those zones visible by other techniques which have revealed a heterogeneous organization of different neurotransmitter-related substances. If there are similarities across species, it may be possible to extend the findings to the substantia nigra of the human brain, where histochemical differences, differences in packing density, different degrees of melanization, and differential susceptibility to damage have been reported (Hirsch et. al., 1988; Deutch et. al., 1986; German et. al., 1988; Gibb et. al., 1988).

### **Patterns of anterograde labeling in the striatum**

One of the most difficult problems that arises from the findings reported here is trying to determine the kind (or kinds) of labeled fibers and terminals that account for the different types of striatal labeling observed. For example, perhaps there are different kinds of fibers with different terminal arbors innervating either striosomal or matrix regions. Another possibility is that the same fiber innervates both regions but has specialized terminal endings or additional bouton structures in striosomal regions. Alternatively, neurons projecting to either striosomes or matrical regions (or to both) are the same kind of fiber but the total number of fibers (or branches) or the total amount of label transported determines the density of fiber labeling; in this case, three possible systems are possible: there exist

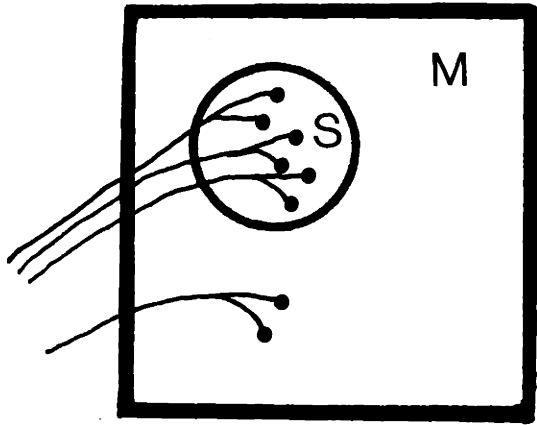
neurons projecting to striosomes, to matrix, and/or to both. These possibilities are represented schematically in Fig. 29.

It was not possible to analyze separately probable bouton structures and fibers. In fact, many of the afferent fibers in the striatum make en passant synapses (Fox et. al., 1971) and this is true of dopamine-containing afferents as well as others according to observations carried out at the ultrastructural level (Pickel et. al., 1981; Freund et. al., 1984; Descarries et. al., 1980). In the rat it has been suggested that cortical fibers innervating the caudoputamen are of two different types, one with tufted terminal ramifications and the other with poorly branched, widely spaced terminals (Wilson and Xu, 1988). Looking in the rodent striatum, Olson and colleagues (Olson et. al., 1972) suggested that two types of dopamine nerve terminals exist; they observed that dopamine-containing terminals (labeled by catecholamine fluorescence) of both the limbic forebrain in the adult and the dopamine islands in the neonate had a "dotted" appearance whereas the majority of the striatum had a "diffuse" appearance. The exact types of fibers and types of terminal distribution which account for the appearance of these different fluorescent patterns is not clear, although a somewhat similar pattern was reported by Gerfen and colleagues (Gerfen et. al., 1987a) after injecting certain regions of the adult rodent substantia nigra with *Phaseolus vulgaris*-leucoagglutinin; fibers confined to patches had more numerous boutons and a more "crinkled" appearance than fibers labeled in matrix regions.

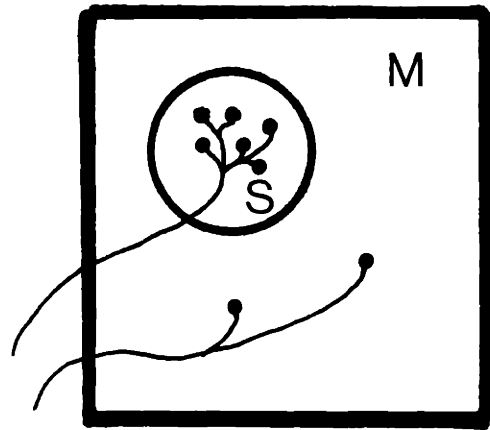
We could not detect such patterning in the present material; <sup>35</sup>S-methionine labeling does not provide enough resolution to determine the morphology of labeled fibers and terminals. Studies with other tracers could be helpful in resolving this particular technical difficulty (see chapter three). It is important to note, however, that in some cases there were regions in which striatal labeling was close to uniform

**Figure 2-29:** Schematic representations of possible modes of termination. Four different modes of termination are illustrated; see text for details. M, matrix; S, striosomes.

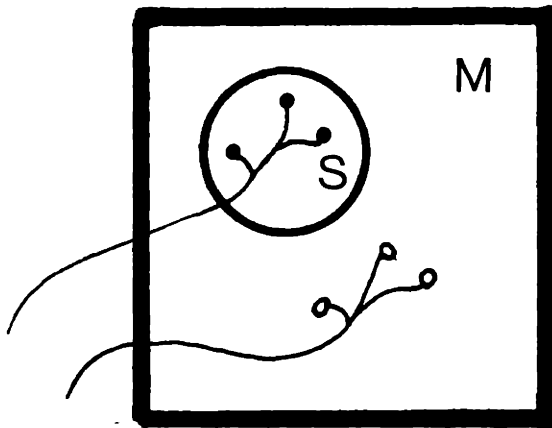
# POSSIBLE MODES OF MESOSTRIATAL TERMINATION



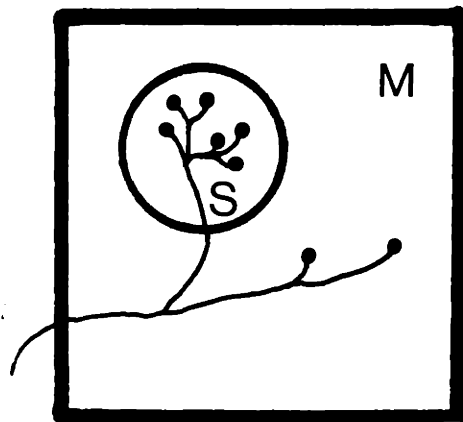
THE NUMBER OF  
FIBERS DETERMINES  
THE DENSITY OF  
LABELING



THERE ARE  
DIFFERENT  
KINDS OF  
FIBERS



THERE ARE  
DIFFERENT RATES  
OF TRANSPORT



SOME FIBERS  
HAVE SPECIALIZED  
ENDINGS IN ONE OF  
THE COMPARTMENTS

across striosomal and matrical divisions. The comparison of the density of labeling by densitometry in case S11L of the homogeneous region in the ventral caudate nucleus and striosomes in other parts of the striatum suggests that labeling within regions which appear homogeneous may be as dense as labeling within heightened striosomes. Thus the respective innervations of striosomes and matrix by some midbrain regions must be equivalently dense in at least some parts of the striatum. Accordingly, it seems unlikely that the patchy appearance of the striosomal patterning we saw exclusively reflected a particularly dense mode of termination in striosomes as opposed to a spatial predilection of some fibers for striosomes.

Another possibility is that certain neurons or groups of neurons or even certain branches (e.g. externally regulated) have different transport or metabolic characteristics which account for differential densities of terminal labeling. Support for this suggestion comes from several different observations. First, Olson and colleagues (Olson et. al., 1972) showed that after administering a tyrosine hydroxylase inhibitor (H44/68) to adult rats, fluorescent islands were observed within the striatum, which normally appears homogeneously fluorescent with catecholamine fluorescence techniques; they suggested that the dopamine turnover in the nerve terminals in the fluorescent islands was lower than dopamine turnover in the surrounding striatal regions. Second, immunostaining for tyrosine hydroxylase appears heterogeneous in the striatum of cats, monkeys and humans; it has been suggested that the reduced immunostaining observed in striosomal regions may reflect metabolic differences between the dopamine-containing fibers innervating striosomal and matrical regions (Graybiel et. al., 1987). Third, in the present study, comparisons between cases with similar size injections but with different survival times indicate clearly that longer survival times will increase the overall intensity of striatal labeling observed suggesting that more label is being



transported with longer survival times. This particular observation lends support to the hypothesis that if two (or more) neuronal systems could be shown to have different rates of amino acid transport it could be reflected by the density of terminal labeling elicited by these different neuronal systems.

*Topography of the mesostriatal projection.* Carpenter and colleagues (Carpenter and Peter, 1972; Carpenter et. al., 1976) have claimed that the caudal two-thirds of the primate substantia nigra projects predominantly to the putamen and parts of the body and tail of the caudate nucleus whereas neurons from the rostral third of the substantia nigra mainly innervate the head of the caudate nucleus. Szabo (Szabo, 1980b), however, reported that neurons of the rostral two-thirds of the substantia nigra project to the head of the caudate nucleus whereas the nigroputaminal neurons are located in the caudal third of the substantia nigra. Parent and colleagues (Parent et. al., 1983b; Parent et. al., 1983a) found that neurons projecting to either the caudate nucleus or the putamen could be observed at all rostrocaudal levels, although they did observe some predominance of neurons projecting to the caudate nucleus in dorsorostral regions compared to some predominance of nigroputaminal neurons in ventrocaudal regions of the substantia nigra. In the present study, some labeling within the striatum was observed at every rostrocaudal level after almost every nigral injection. Because the majority of injections could be shown to be span almost the entire rostrocaudal extent of the nigral complex, even though labeling may have appeared weak in the extreme periphery, it is very difficult to evaluate the anteroposterior topography; however, in those cases with injections which were restricted to either the rostral or caudal half of the nigral complex, there appeared to be an extended projection domain: labeling was observed at all striatal levels, but labeling appeared somewhat enhanced in the rostral (more caudate nucleus) or caudal (more putamen) half of

the striatum, respectively. The evidence on the topography of mesostriatal connections does favor some anteroposterior ordering for the striosomal as well as the matrical parts of the mesostriatal system. For example, rostral (and lateral) injections predominantly labeled striosomes in the caudate nucleus whereas caudal injections in A8 elicited labeling in the matrix compartment, predominantly in the putamen.

We did not detect any mediolateral topography in the cases described here. The only medio-lateral distinctions observed were those resulting from lateral nigral injections (which tended to restrict the injection field to the main horizontal band of the pars compacta), which resulted in enhanced striosomal labeling whereas medial injections (which also definitively involved caudal levels and therefore infiltrated neurons of cell group A8) elicited enhanced labeling in the matrix compartment. A mediolateral topographical relationship was described in the primate by Szabo (Szabo, 1980b), although Parent and colleagues (Parent et al., 1983b; Parent et al., 1983a), using the same tracer, horseradish peroxidase, did not find any evidence to support a mediolateral topographical relationship.

The evidence for the existence of inverted dorsoventral topography, also previously described in the rat (Beckstead et al., 1979; Fallon and Moore, 1978; Faull and Mehler, 1978; Nauta et al., 1978; Swanson, 1982), cat (Royce, 1978; Royce and Laine, 1984; Szabo, 1979; Szabo, 1980a; Ususnoff et al., 1976; Jimenez-Castellanos and Graybiel, 1987a) and monkey (Carpenter and Peter, 1972; Szabo, 1979; Szabo, 1980b), could be found in many of the cases reported here. In particular, as described for case S18L, a small, ventral injection within the pars compacta labeled only the most dorsal part of the striatum. Conversely, in all cases where labeling was fairly restricted to the ventral half of the caudate nucleus and/or putamen, the injection site appeared to be restricted to a dorsal part of the

A8-A9 cell complex and/or at least partly infiltrated the medial neurons of the ventral tegmental area.

The ventral part of the striatum appeared to be densely innervated in those cases with injections sites infiltrating neurons of the medial part of the nigral complex, particularly within the region between the lateralmost oculomotor fibers and the midline. Similarly, Hemphill and colleagues (Hemphill et. al., 1981) found that injections of the retrograde tracer, horseradish peroxidase, into the nucleus accumbens<sup>1</sup> labeled cells in the ventral tegmental area as well as some cells in the medial edge of the pars compacta. Injections confined to those neurons located at the midline (and just lateral to them), cases S19R and S19L, resulted in striatal labeling restricted to the ventralmost part of the caudate nucleus and putamen, extending down to the ventral region at the base of the brain. This region corresponds to the nucleus accumbens, according to White's description (White, 1981) of the nucleus accumbens in the human brain, which includes the ventralmost part of the caudate nucleus, even in very rostral sections, and the antero-medial border of the putamen rostral to the level of the anterior commissure.

The present findings of a projection from ventral tegmental neurons to a restricted zone within the ventral part of the striatum suggests that the striatal projection zone of cell group A10 makes up a substantially smaller proportion of the striatum than was observed in either the rat or cat (Swanson, 1982; Jimenez-Castellanos and Graybiel, 1987a). This particular species difference is not

---

<sup>1</sup>The nucleus accumbens in this study was considered to be: "the more ventral striatal area extending down to the base of the brain ... including striatal parts of the region called the anterior perforated substance ... excluding the lateral area near the olfactory tract." The exact nomenclature and regions which are included in descriptions of the ventral striatum vary greatly among studies and among species.

surprising, because the proportional number of ventral tegmental neurons and the proportional size of the ventral tegmental area are also substantially smaller in the primate brain than in either the cat or the rat (Poirier et. al., 1983) [see chapter one]. This species difference does suggest, however, that there is a less pronounced limbic input from the ventral tegmental area to the ventral part of the striatum than in the rat and cat (and less in cat than in the rat) indicating either a diminished need for limbic-related striatal input or a different organizational schema for limbic-related trans-striatal channeling. Although there is clearly a proportionally diminished projection from the A10 cell group in the primate brain, recent evidence on the local compartmentalization and regional dissociation (e.g. differences in afferent input to caudate nucleus and putamen) of both limbic-related and sensorimotor input to the primate striatum would support the hypothesis that an organizational schema different from that observed in the rat and cat (corresponding to distinguishable ventral and dorsal striatal zones) exists in the primate brain (Alexander et. al., 1988; Donoghue and Herkenham, 1986; Kunzle, 1975; Goldman and Nauta, 1977; Graybiel, 1989; Graybiel, 1984a; Graybiel and Ragsdale, 1979; Parent et. al., 1983b; Parent et. al., 1983a; Ragsdale and Graybiel, 1981; Ragsdale and Graybiel, 1988a; Ragsdale and Graybiel, 1989a).

In some cases with injection sites infiltrating neurons lateral to the midline, labeling within the ventralmost part of the caudate nucleus and putamen appeared heterogeneous, but striosomal and matrical regions were not often identifiable histochemically. However, the histochemical compartmentalization of ventral striatal regions is not equivalent to that observed in more dorsal striatal regions; the histochemical and immunohistochemical localization of many of the numerous substances which have been shown to reveal striosomal patterns of labeling in more dorsal regions of the striatum may appear heterogeneously distributed in the

ventral part of the striatum, but with a greater degree of complexity (Voorn et. al., 1988b; Graybiel, 1984b; Graybiel et. al., 1981). In addition, the compartments observed there may not be equivalent to striosomes. In the cat, for example, the complex, ventral striatal compartments observed are not characterized by either reduced acetylcholinesterase staining or  $^3\text{H}$ -thymidine autoradiography (marking the early born cell groups) (Graybiel, 1984b; Graybiel et. al., 1981; Ragsdale and Graybiel, 1981; Ragsdale and Graybiel, 1987), important features of striosomes in more dorsal regions.

### **Technical Considerations**

*Histochemical identification of striosomes.* Striosomes could not be identified histochemically at all levels of the striatum in every case. The greatest difficulty was at levels through the mid-caudal putamen, where striosomes were rarely clear, but at other levels within the putamen or caudate nucleus striosomal compartmentalization was also not always possible to detect. However, even when the histochemistry was not informative with regard to whether compartmental divisions were present, the anterograde labeling in such districts was often patchy or lacunar. In fact, no sharp difference was observed in the patchiness or lacunar organization of the midbrain innervation of these regions whether the patches and lacunae could be scored as striosomal or not.

Afferent-fiber clusters organized in striosome-like patches have been observed in the tissue identified histochemically as extrastriosomal matrix in anterograde transport studies of thalamic, amygdalar and cortical afferents to the striatum (Alexander et. al., 1988; Flaherty et. al., 1989; Graybiel et. al., 1989b; Malach and Graybiel, 1986; Ragsdale and Graybiel, 1988a; Ragsdale and Graybiel, 1988b; Ragsdale and Graybiel, 1989a) and, in experiments with mixed anterograde-retrograde tracers, in the connections linking striatum and substantia nigra (Kemel

et. al., 1989). Accordingly, it is possible that some of the heterogeneity in mesostriatal innervation patterns observed here in the monkey reflected a comparable mosaicism of the matrix rather than striosomal ordering. In every case, however, many or most of the patches of enhanced or weak labeling visible in the autoradiograms could be matched to striosomes visible in adjoining sections stained for met-enkephalin-like immunoreactivity or butyrylcholinesterase activity. Moreover, in the regions in which striosomal staining patterns were clear, few if any patches of enhanced or reduced labeling lay in the extrastriosomal matrix. There were a few instances where labeling within the extrastriosomal matrix was non-uniform (e.g. case S3, Fig. 8) which suggests that a heterogeneous projection to the matrix compartment from at least the caudal part of cell group A8 may indeed exist. In the majority of the cases in this series, however, it seems that the heterogeneity in the mesostriatal projection was striosomal.

*Chemospecificity of the connections.* Each deposit eliciting labeling in the striatum infiltrated regions containing many TH-positive neurons. For technical reasons, we were unable to determine whether the mesostriatal projections labeled in these cases were specific to such immunohistochemically identified neurons. However, in the rat, it has been estimated that at most only about 5% of all mesostriatal projection neurons do not contain dopamine (Van der Kooy et. al., 1981). Immunohistochemical identification of dopamine-containing (TH-immunoreactive) fibers has also been combined with anterograde labeling of mesostriatal fibers in the rat (Gerfen et. al., 1987a), and evidence from these studies suggests that the non-dopaminergic contingent of mesostriatal fibers mainly innervates the striatal matrix in this species. If these estimates for the rat hold also for the monkey, it would imply that most of the matrical and all of the striosomal afferents we observed were, in fact, dopamine-containing fibers.

*Autoradiographic labeling along the pipette track.* The extent of thalamic contamination in each case with visible autoradiographic labeling along the pipette track was described in detail previously. In cases with predominant labeling of striosomes, very few injections were accompanied by labeling along the pipette track. Similarly, there was no evidence of any labeling along the pipette track in the case with injections centered in cell group A10. In these cases, there was apparently no significant labeling of thalamostriatal afferents. For cases with caudal injections in A8, there were control cases without any visible striatal labeling which indicated that at these levels contamination of the pipette track was insignificant with respect to striatal labeling. In those cases with prominent labeling of the matrix compartment and with injections directed towards the pars mixta and rostral extension of cell group A8, it was more difficult to determine whether the infiltration of thalamic neurons contributed significantly to labeling within the striatum. Judging from previous observations in the cat (Ragsdale and Graybiel, 1989b), if thalamostriatal afferents from the regions infiltrated with tracer had accounted for the matrical labeling observed, one would have expected to see particular patterns of matrical labeling in the matrix compartment, for example, labeling principally in the dorsal part of the striatum or discontinuous patches or particularly fibrous labeling within the matrix (Ragsdale and Graybiel, 1989b), which was not observed in the cases described here (with the exception of the caudal A8 injections which had no evidence of thalamostriatal contamination). It is possible, however, that the predominant patterns of these thalamostriatal afferents were masked by the more densely labeled mesostriatal afferents. The results of the present study strongly suggest that although it is possible that the labeling of thalamostriatal afferents contributed to some of the striatal labeling observed, the thalamostriatal labeling cannot account for the distinct local and regional patterns observed in the present cases.

## Functional Implications

Dopamine-containing terminals in the striatum are well placed to influence the efficacy of transmission from specific afferent systems to the medium spiny neurons that give rise to the outputs of the striatum (Freund et. al., 1984). A major implication of our observations is that in the primate, the activity of such dopamine-containing afferents of the striatum may be different in striosomes and matrix by virtue of different regulation of striosome-projecting and matrix-projecting parts of the A8-A9-A10 cell complex. The key finding is of spatial separation of subpopulations of midbrain neurons projecting to these two striatal compartments. This physical separation suggests, though it does not prove, that the different subgroups may come under the control of different afferent systems. It is also known that different parts of the A8-A9-A10 complex--including parts here suggested to have different compartmental targets in the striatum-- have different profiles of peptide immunoreactivities (Beckstead, 1987a; Chesselet and Graybiel, 1986; Graybiel and Ragsdale, 1983; Waters et. al., 1988) and receptor-related binding sites (Marshall et. al., 1985; Joyce et. al., 1986; Beckstead et. al., 1988; Besson et. al., 1988; Graybiel et. al., 1989a). Insofar as activity of these midbrain neurons is reflected at the terminals of their axons in the striatum (Cheramy et. al., 1987; Kemelet. al., 1989), these different distributions are likely to imply different dopaminergic modulation in the striatum and, given the present findings, distinct dopaminergic modulation of medium spiny cells in striosomes and in matrix.

This possibility is particularly interesting because the configuration of connections reported here suggests that nearby striosomal and non-striosomal parts of any given striatal region could be innervated by non-adjointing parts of the A8-A9-A10 complex. As a consequence, in any particular district of the striatum,



neural processing (for example, of inputs from the neocortex) could be under the influence of different and perhaps even independent dopaminergic systems in adjoining striosomal and nonstriosomal zones. The extensive elaboration of compartmentalization in the primate striatum would not only have the advantage of bringing into close proximity the terminal distributions of different sets of corticostriatal and other forebrain afferents (Ragsdale and Graybiel, 1989b; Ragsdale and Graybiel, 1989a), but would also permit locally specific tuning of intrastriatal processing by the actions of dopamine contained in compartmentally targeted mesostriatal systems.

## Chapter 3

# The Mesostriatal Projection II: Anterograde and Retrograde Results with Horseradish Peroxidase, Fast Blue and Phaseolus vulgaris-leucoagglutinin [PHA-L]

### Abstract

The anterograde and retrograde tracers horseradish peroxidase conjugated with wheat germ agglutinin (WGA-HRP) or fast blue (FB) were injected into distinct regions of the nigral complex in 7 squirrel monkeys (13 hemispheres). *Phaseolus vulgaris*-leucoagglutinin [PHA-L] was iontophoretically injected into the region of the substantia nigra in 5 squirrel monkeys (10 hemispheres). The locations of injection sites were plotted with respect to the cell groups visible in tyrosine hydroxylase immunostained sections. The anterograde fiber labeling and the location of retrogradely labeled cells were charted in relation to histochemically identified striosomes in serially adjacent sections stained for met-enkephalin-like immunoreactivity or butyrylcholinesterase activity.

The pattern of labeling observed following injections of WGA-HRP and FB corroborated the results described in an earlier study (chapter two) indicating the existence of compartmentally differentiated neuronal systems originating from distinct regions within the A8-A9-A10 cell complex. In addition, retrogradely labeled cells were observed within zones of enhanced striosomal anterograde labeling, suggesting the existence of a reciprocal connection between the striosome-projecting part of the pars compacta and those striatal cells within striosomes which project to the substantia nigra.

Preliminary results with PHA-L indicate that there are fibers with different morphologies and patterns of termination within striosomes and within the matrix compartment. The morphologically distinct fibers observed include 1) single, long, extended arbors with apparently few bouton swellings, 2) groups of relatively smooth fibers forming a dense plexus of neuropil with small varicosities, as well as 3) single, short fibers with a restricted "starburst" pattern of extensive branches and large, bulbous bouton-like structures. These findings also provide previously undocumented information regarding the morphological characteristics of nigrostriatal fibers terminating within the striatum of the primate.

## Introduction

The majority of the afferent and efferent connections of the striatum have been shown to be organized with respect to histochemically identifiable striosomes [see (Graybiel, 1989)]. For example, in the cat, sensory and motor cortex project predominantly to the matrix compartment (Ragsdale and Graybiel, 1981) whereas striosomes receive inputs from prefrontal and insulotemporal cortex as well as the basolateral amygdala (Ragsdale and Graybiel, 1988a; Ragsdale and Graybiel, 1981; Ragsdale and Graybiel, 1989a). In addition, distinct cell groups within the substantia nigra pars compacta can be shown to project predominantly to either striosomes or the matrix compartment (Jimenez-Castellanos and Graybiel, 1986; Jimenez-Castellanos and Graybiel, 1987a; Feigenbaum and Graybiel, 1988; Langer and Graybiel, 1989). The matrix area appears to be the principal origin of striatal outflow to the pallidum and substantia nigra pars reticulata (Graybiel et. al., 1979; Graybiel and Ragsdale, 1979; Jimenez-Castellanos and Graybiel, 1989b; Gimenez-Amaya and Graybiel, 1989); a projection from striosomes to nigral tissue in or adjacent to part of the pars compacta has been observed in the rat and cat (Jimenez-Castellanos and Graybiel, 1986; Jimenez-Castellanos and Graybiel, 1989b; Gerfen, 1985). In the primate brain, however, the efferent projections from striosomes have not yet been identified.

These observations, and those of the previous study (see chapter two), prompted an additional investigation, with different tracers, of the connections between the substantia nigra and the striatum in the primate. By injecting tracers which are transported both retrogradely and anterogradely into the nigral complex, it is possible to observe anterogradely labeled fibers as well as retrogradely labeled cells within the striatum. In addition, by injecting a tracer such as PHA-L, it is possible to observe certain morphological characteristics which are not detectable

with most other tracers. The major goals of the present study were, therefore, to corroborate earlier findings (chapter two) with additional tracers, to determine whether a connection would be observed between striatal efferent neurons in striosomes and the striosome-projecting cells of the pars compacta in the squirrel monkey brain, and to try to characterize the morphological features of mesostriatal fibers in the primate striatum.

## Materials and Methods

Unilateral or bilateral injections of the anterograde and retrograde tracers horseradish peroxidase conjugated with wheat germ agglutinin (WGA-HRP, as a 10-15% solution in saline), fast blue (FB, as a 10% solution in saline) or *Phaseolus vulgaris*-leucoagglutinin (PHA-L, Vector Laboratories, prepared as a 2.5% solution in 0.1 M phosphate-buffered saline, pH 7.4) were placed under stereotaxic guidance (Emmers and Akert, 1963; Gergen and MacLean, 1962) into sites within the A8-A9-A10 cell complex of the midbrain of 10 adult squirrel monkeys (*Saimiri Sciureus*) [20 hemispheres; 23 different injections: WGA-HRP, n=10; FB, n=3; PHA-L, n=10] tranquilized with ketamine hydrochloride (Ketaset, 40 mg/kg IM) and anesthetized with Nembutal (50 mg/kg IP). Deposits of WGA-HRP or FB were delivered by pressure injection: puffs of air applied to glass micropipettes (with tip diameters varying between 20 and 30 $\mu$ m) with a Pneumatic PicoPump (PV800, World Precision Instruments). Injected volumes varied between 5 and 20 nl. For PHA-L, micropipettes with a tip diameter between 20 and 30  $\mu$ m were filled through the tip via air vacuum. A silver wire was inserted into the micropipette and into the solution of PHA-L; the wire was connected to the positive terminal of a constant current device. The negative terminal was connected to a syringe needle placed between the skin and muscle of the skull. 7-10  $\mu$ amps of positive, pulsed (7 seconds on, 7 seconds off) current was applied for 20 minutes per injection. In four

hemispheres, three consecutive injections, one above the other at 0.2 mm intervals, were made in series with a five minute waiting period between injections.

After 2 day survivals for cases with WGA-HRP and 12-14 day survivals for cases with FB and PHA-L the animals were deeply anesthetized with Nembutal and were perfused transcardially with 500 ml of 0.9% saline followed by 1.5 liters of 4% paraformaldehyde and 5% sucrose in 0.1 M dibasic phosphate buffer and 0.9% saline (pH 7.4, PBS) and then by 1.5 liters of PBS containing 5% sucrose. Brains were blocked stereotaxically in the frontal plane and blocks were washed overnight in PBS containing 20% sucrose and cut in the frontal plane into 40 $\mu$ m sections on a freezing microtome. In cases with PHA-L, sections were collected and stored in Tris-saline 0.5 M at 4°C until they were processed for the immunohistochemical localization of PHA-L.

Adjoining sets of sections through the striatum were stained, respectively, for (a) acetylcholinesterase (Geneser-Jensen and Blackstad, 1971; Graybiel and Ragsdale, 1978), with acetylthiocholine iodide as substrate and ethopropazine hydrochloride (Parsidol, Warner-Lambert) as the pseudocholinesterase inhibitor, (b) butyrylcholinesterase [BuChE] (Graybiel and Ragsdale, 1980), with butyrylthiocholine iodide in the presence of the cholinesterase inhibitor BW284c51 (Burroughs Wellcome), and (c) met-enkephalin (ENK)-like immunoreactivity [by protocol B of Graybiel and Chesselet (Graybiel and Chesselet, 1984) with antiserum kindly provided by Dr. R. Elde, diluted 1:1000]. The single-cycle peroxidase-antiperoxidase (PAP) method (Sternberger, 1979) followed for the immunohistochemistry included the following steps: 1) Pretreatment with normal goat serum (1:30), hydrogen peroxide (3%), and Triton X-100 (0.2%); 2) primary antiserum incubation; 3) goat anti-rabbit IgG (1:50); 4) rabbit PAP (1:30); 5) diaminobenzidine (DAB, Sigma) reaction. Series of sections through the midbrain

were stained for tyrosine hydroxylase-like immunoreactivity, protocol according to Graybiel et. al. (Graybiel et. al., 1987) with Eugene Tech antiserum diluted 1:240, AChE activity and for Nissl substance with cresylecht violet.

*WGA-HRP and FB histochemistry:* Sections processed for WGA-HRP were reacted according to the tetramethylbenzidine (TMB) protocol of Mesulam (Mesulam, 1978) with concentrations of hydrogen peroxide (0.009% - 0.018%) determined by trials. Incubation solutions were changed every 5 minutes over a period of 30 minutes. Sections were rapidly mounted from 0.1M acetate buffer, air dried, defatted and coverslipped. Sections to be viewed for fast blue were mounted out of 0.1 M phosphate buffer (pH 7.4, PB) onto uncoated slides, air dried, coverslipped with a 1:1 glycerol-PB solution and stored at -20°C for later viewing.

*PHA-L immunohistochemistry:* Sections were washed briefly in Tris-buffered saline (TBS) 0.5 M for ten minutes at room temperature, followed by one hour incubation in TBS, 0.25% Triton-X100 (TX) and 2% normal rabbit serum (NRbS) and three ten-minute washes in TBS. Sections were then incubated for 36-48 hours at 4°C in the primary antiserum containing goat anti-PHA-L (Vector Laboratories) diluted 1:1000 in TBS with 2% NRbS and 0.25% TX. The following steps were carried out at room temperature. Sections were subsequently rinsed in TBS (every rinse = three ten-minute washes), incubated for one hour in biotinylated rabbit anti-goat IgG (Vector Laboratories, ABC Vectastain Kit) diluted 4.4:1000 in TBS, 2%NRbS and 0.25% TX and rinsed again. The final peroxidase incubation followed: one hour with Avidin Biotin peroxidase complex (Vectastain Kit) diluted 8.8:1000 in TBS. Sections were then rinsed in TBS, rinsed again in Tris (no saline 0.5 M), and reacted with 0.05% 3,3'diaminobenzidine (DAB, Sigma) in Tris and 0.04% hydrogen peroxide for 10 to 15 minutes. After many rinses in Tris, sections were mounted, air-dried and coverslipped.

*Analysis:* The distribution of labeling with WGA-HRP and PHA-L was analyzed in the striatum with lightfield and darkfield optics. Additionally, in cases with WGA-HRP crossed polarizers were used to enhance the visualization of the TMB reaction product (Illing and Wassle, 1979). Neuropil and cell bodies containing FB were viewed under fluorescent illumination. All anterograde fiber labeling and retrograde cell labeling was mapped, when possible, in relation to the distribution of striosomal figures visible in serially adjacent sections immunostained for met-enkephalin or stained for BuChE. Selected sections of injection sites labeled with WGA-HRP were incubated in 0.05% DAB and 0.0024% hydrogen peroxide in a 0.05 M Tris solution to help identify the centers of the deposits. The location of injection sites were charted with respect to regional landmarks in the A8-A9-A10 region identified in adjoining sections stained for TH-like immunoreactivity and for AChE activity (Arsenault et. al., 1988; Jimenez-Castellanos and Graybiel, 1987a; Jimenez-Castellanos and Graybiel, 1987b).

## Results

Anterograde labeling within the striatum was observed in all injected hemispheres, although the extent and topography of labeling varied between cases. As described previously (chapter two) the location of the injection site could be shown to be related to compartmentalized and regional characteristics of labeling within the ipsilateral striatum. Injection sites for all cases are illustrated in Figs. 1-3; the associated labeling observed along the pipette track in several of these cases is shown in Fig. 4.

*Horseradish peroxidase:* Those injection sites located within the lateral part of the main horizontal band of the substantia nigra pars compacta (see Fig. 1; n=6) produced enhanced labeling within striosomes, although moderate to dense labeling of the matrix was also observed in these cases. An example of enhanced

### **Figures 1 through 3: Chartings of Injection Sites**

In the following figures, the locations of injection sites in the nigral complex are indicated semi-schematically in drawings of seven rostrocaudally ordered transverse sections through the midbrain of the squirrel monkey. The drawings were made from seven sections spaced approximately 0.5 mm apart. The outline of the substantia nigra, shown as dotted lines, was determined by the location of neurons and neuropil observed in serially adjacent sections immunostained for TH. Within the zones marked by the dotted lines are solid outlines showing the location of densely-packed TH-positive neurons and neuropil, corresponding to the pars compacta. The second and third sections also show the location of the oculomotor fibers lateral to the midline. In the seventh section, the horizontal fibers of the decussation of the brachium conjunctivum are shown as solid lines. The injection sites have been grouped separately according to the type of tracer used: injections with WGA-HRP, FB and PHA-L are shown, respectively, in Figs. 1, 2, and 3. Each injection site is outlined with stippled interiors. OT, optic track; LGN, lateral geniculate nucleus; III, oculomotor nucleus; MGN, medial geniculate nucleus. Scale bar = 1 mm.



**Figure 3-1:** Injection sites: Cases with WGA-HRP.

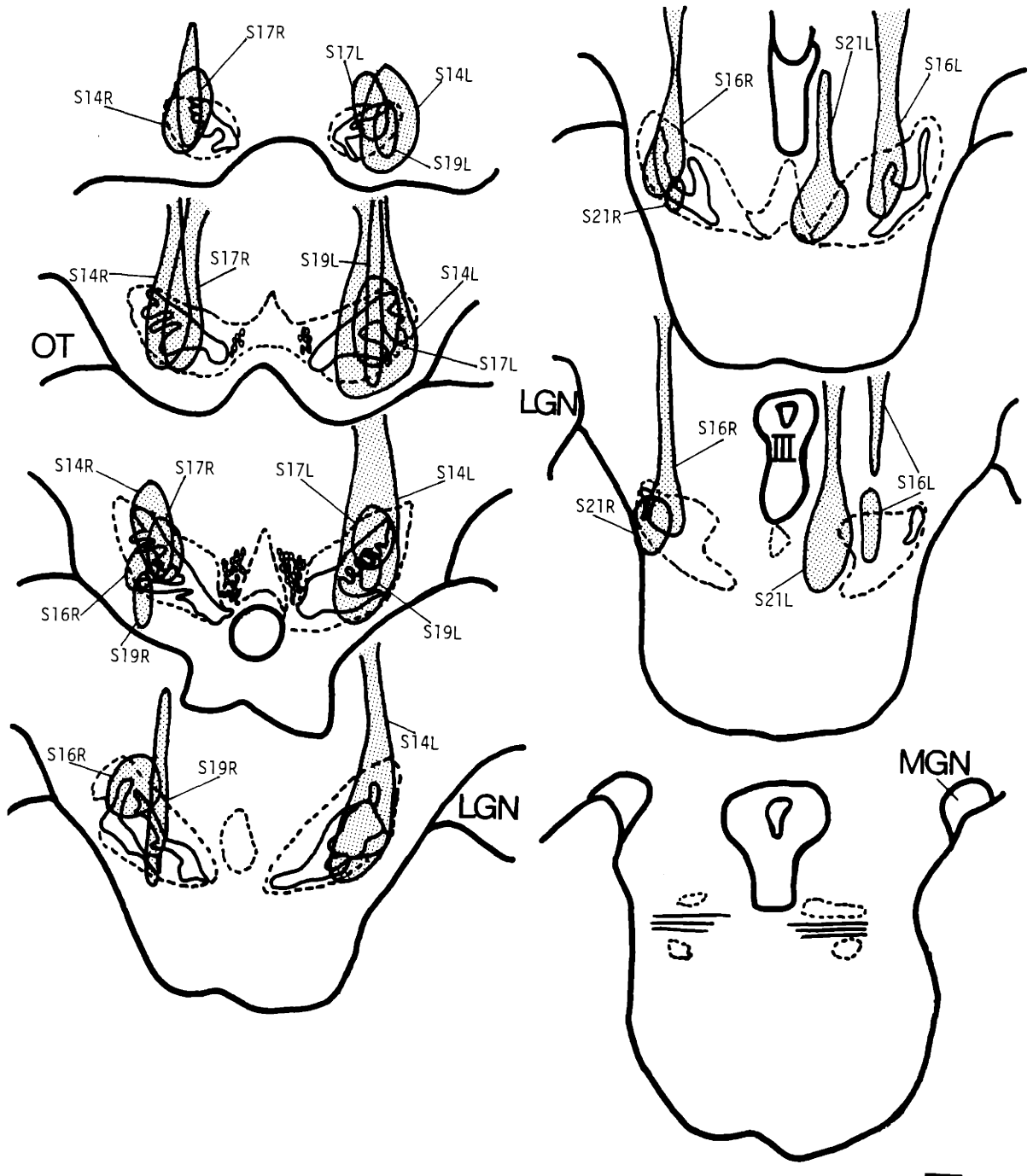


**Figure 3-2:** Injection sites: Cases with FB.

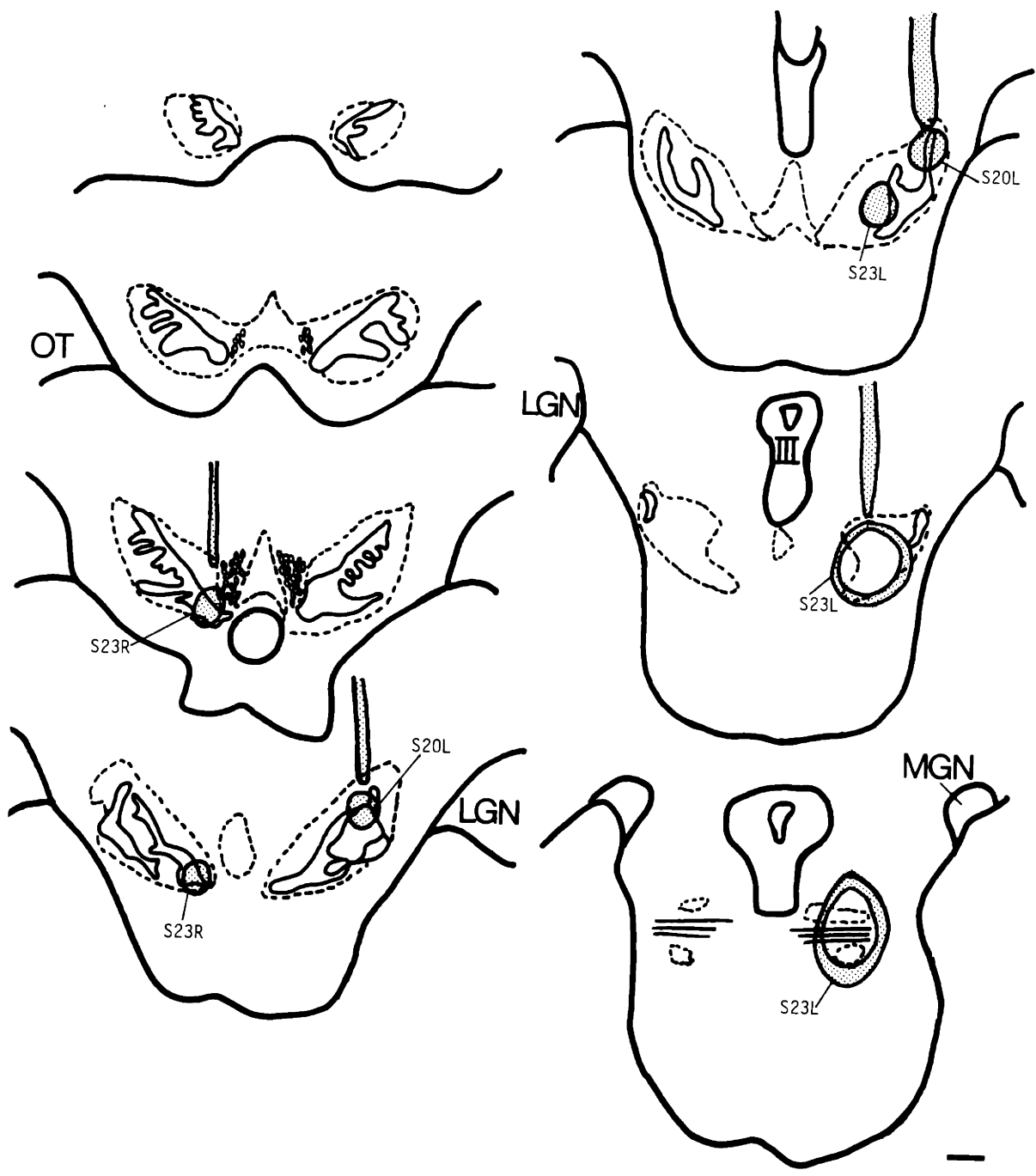


**Figure 3-3:** Injection sites: Cases with PHA-L.

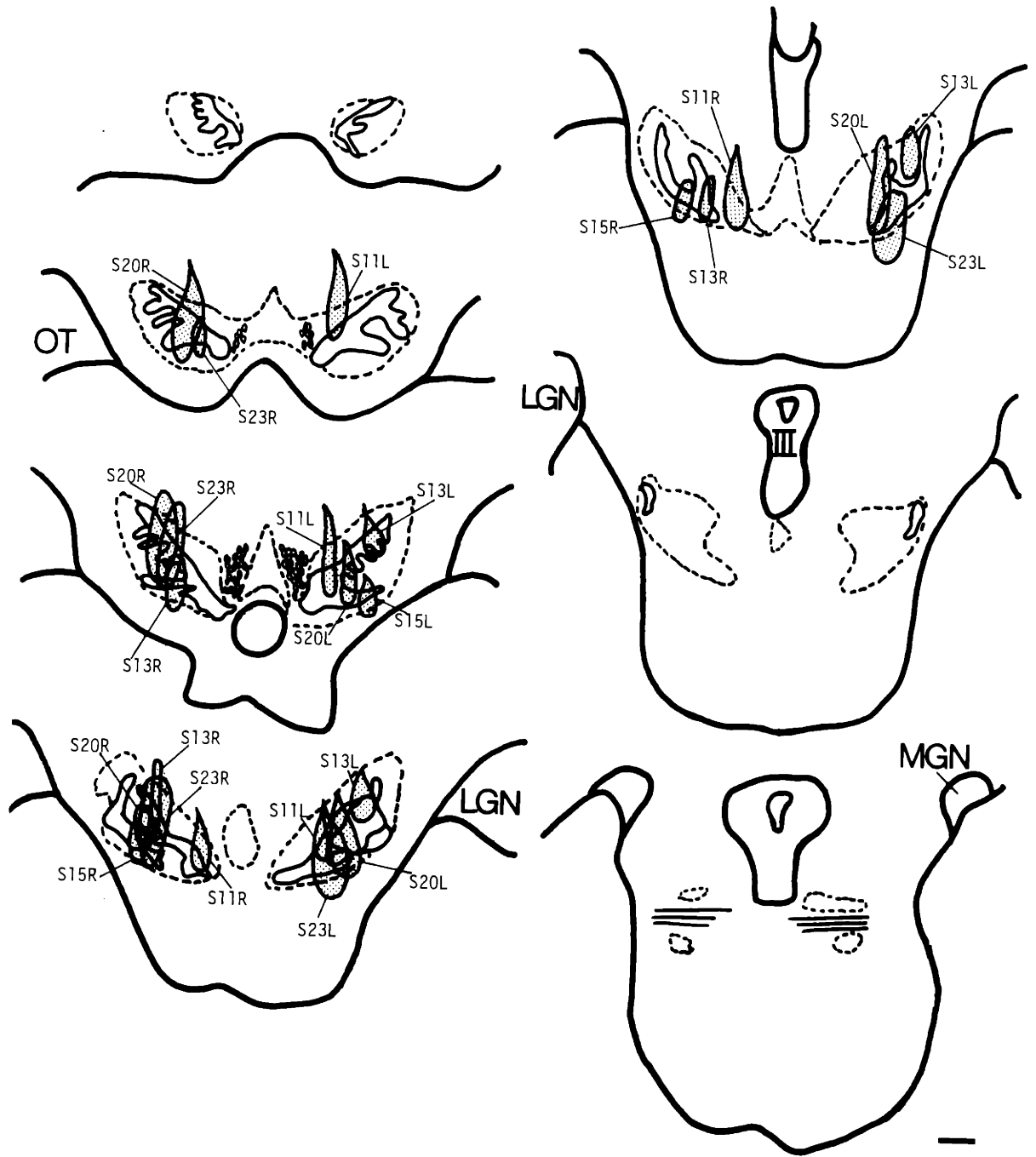


**Figure 3-4:** Chartings of labeling along the pipette tracks: WGA-HRP and FB. The size and locations of labeling along the pipette tracks were drawn for all cases in which such labeling was detectable. Three anteroposterior levels are drawn: A -6.5 (top drawing), A -5.0 (middle drawings, shown twice), and A -3.5 (bottom drawing) (Emmers and Akert, 1963). The outlines of thalamic nuclei determined from Nissl-stained sections are shown by dotted lines. The substantia nigra, pars compacta is represented in solid black. The size and location of labeling observed along the pipette tracks are shown outlined in black with stippled interiors. Each case is identified by its case number. Thalamic nuclei: MD, medial dorsal nucleus; Pf, parafascicular nucleus; CM, central medial nucleus; LP, lateral posterior nucleus; VPL, ventral posterior lateral nucleus; MD, medial dorsal nucleus; CeL, central lateral nucleus; PUL, pulvinar; LGN, lateral geniculate nucleus; MGN, medial geniculate nucleus. Other abbreviations: OT, optic track; CN, caudate nucleus; III, Oculomotor nucleus. Scale bar = 1 mm.

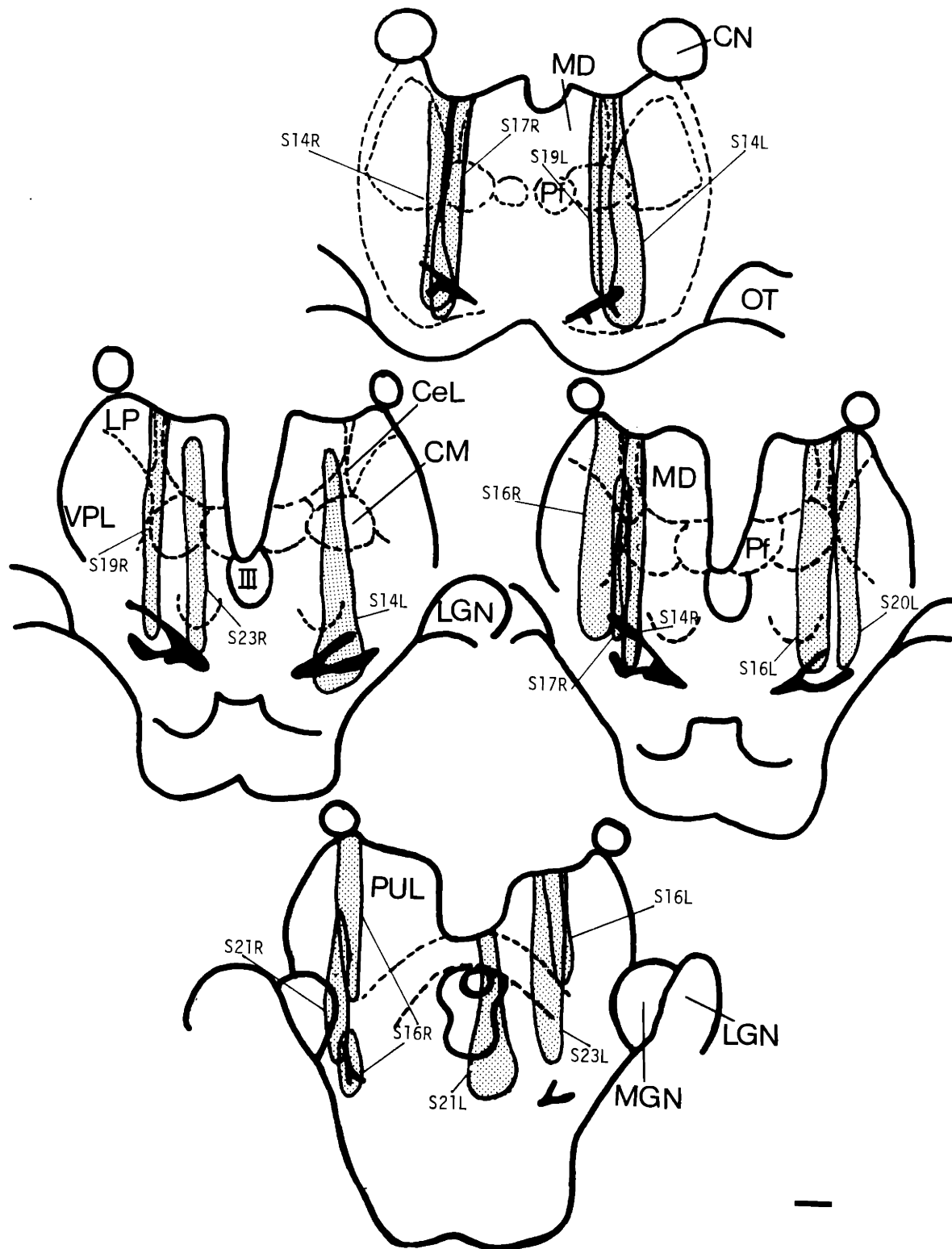




**Figure 3-5:** Striatal labeling with WGA-HRP: case S14L. Serially adjacent sections through the striatum in case S14L illustrate anterograde fiber labeling and retrograde cell labeling following injections of WGA-HRP into the lateral part of the main horizontal band (A). Enhanced anterograde labeling is visible in the caudate nucleus corresponding to the location of striosomes (examples at asterisk) detectable by ENK immunostaining (B). There are retrogradely labeled cells within striosomes as well as within some matrical regions, for example, within the ventral part of the caudate nucleus. The injection site in this case is illustrated in Fig. 1. IC, internal capsule. Scale bar = 1 mm.

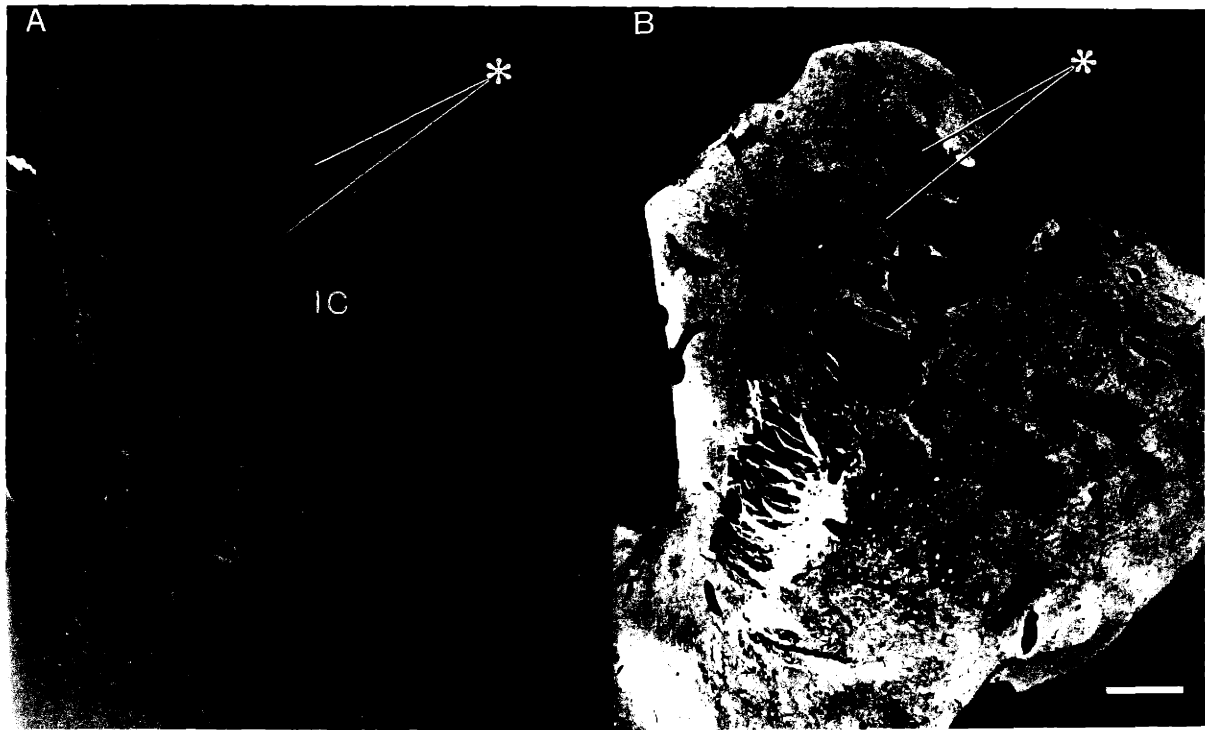
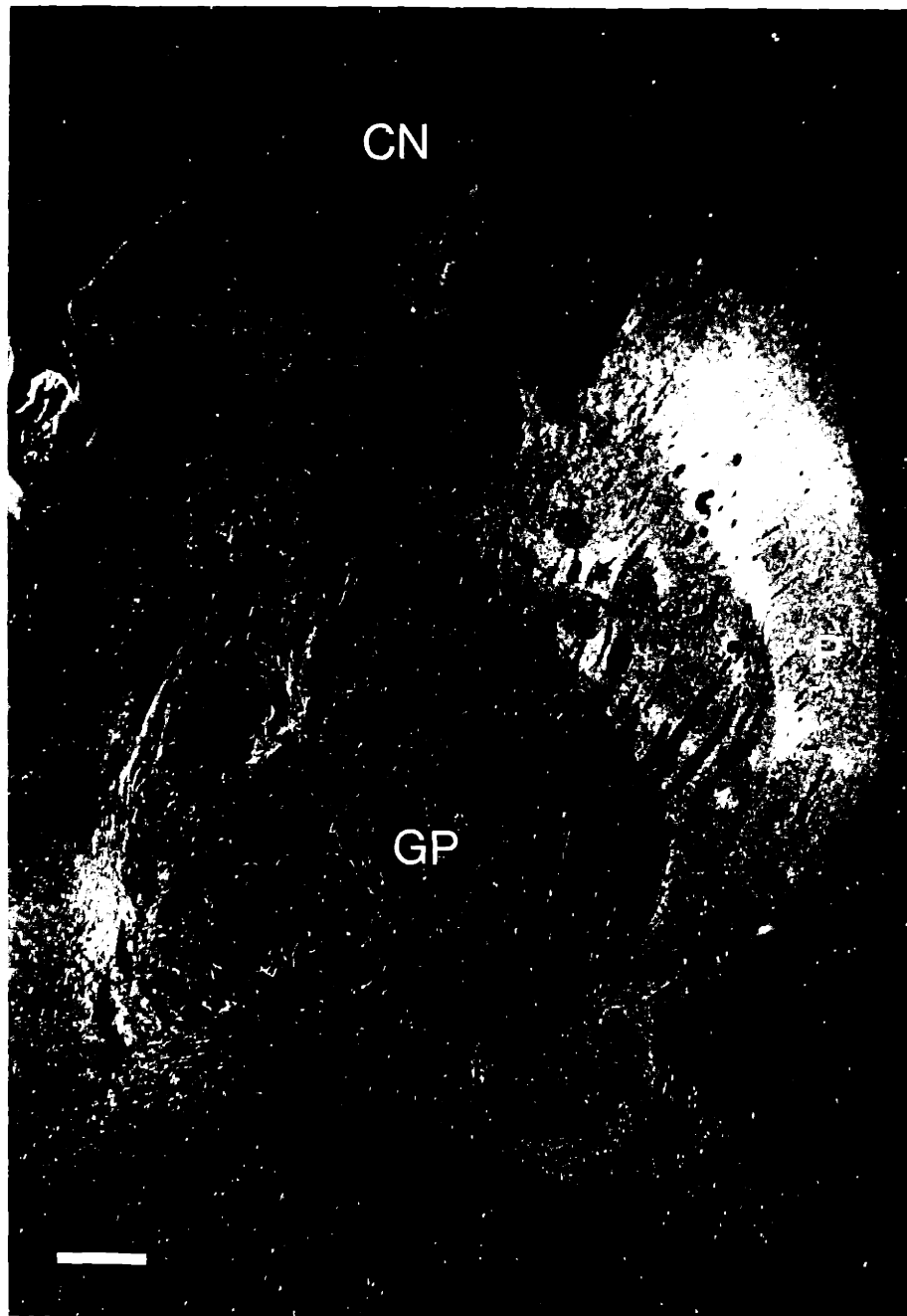


**Figure 3-6:** Striatal labeling with WGA-HRP: case S16L. A transverse section through the striatum in case S16L illustrating the anterograde fiber labeling visible following an injection of WGA-HRP into the caudal part of cell group A8. The pattern of heterogeneous labeling within the putamen appears to be restricted to the extrastriosomal matrix even though histochemically identifiable striosomes in a serially-adjointing section are not available. This section was photographed in dark-field with crossed-polarizers (Illing and Wassle, 1979). The injection site in this case is shown in Fig. 1. CN, caudate nucleus; P, putamen; GP, globus pallidus. Scale bar = 1 mm.



striosomal labeling is shown in Fig. 5 (case S14L). In cases with injection sites variably involving the pars mixta and A8 regions (see Fig. 1; n=2), there was evidence for patches of weak labeling embedded in fields of more densely labeled fibers; these patches of weak labeling corresponded to striosomes where they could be identified as such. In the caudal part of the putamen, for example, what appeared to be a pattern of striosomal "avoids" could not be identified histochemically (see Fig. 6); it is rare to be able to identify striosomes in this region with the histochemical markers currently available. In one case, S16L, as shown in Fig. 6, labeling within the putative matrix was not uniform, similar to findings in previous autoradiographic cases (chapter two) after injections into the caudal part of cell group A8.

In most hemispheres, even though compartmentalized patterns were detected in certain regions of the striatum, much of the labeling appeared diffuse and homogeneous. In some cases anterograde labeling appeared enhanced in a particular region of the striatum, for example, within the dorsal or ventral part of either the caudate nucleus or the putamen. In general, as described previously, the dorsoventral location of the injection site had an inverted relationship with the dorsoventral location of the anterogradely labeled fibers and, in addition, there was some evidence for anteroposterior topography as described previously (chapter two). Apparently more dense (or even more distinctly compartmentalized) labeling within the caudate nucleus was observed with rostral injections compared to more dense (or more distinctly compartmentalized) labeling in the putamen which was observed with injections located in the caudal part of the nigral complex.

There are two major problems of interpretation with the use of WGA-HRP as compared to <sup>35</sup>S-methionine: 1) fibers, as well as cell bodies, within the region of the injection will transport the label and 2) there is often extremely dense leakage

of the tracer along the pipette track, leading to the contamination of large regions of the thalamus (see Fig. 4). One advantage of WGA-HRP is that because it is transported both retrogradely and anterogradely one way to determine the extent of thalamic contamination is to look within the globus pallidus for retrogradely labeled cells. The projection to the thalamus from the globus pallidus is from the internal segment (Nauta and Mehler, 1966; Carpenter and Strominger, 1967; Mehler and Nauta, 1974). In the case with patterned labeling in the caudal putamen described above, retrogradely labeled cells were observed in the internal segment of the globus pallidus, indicating that some retrograde transport of the label from thalamic nuclei had occurred and implying that anterograde transport to the striatum may also have occurred. However, in most cases, only a few retrogradely labeled cells were detected within the internal segment of the globus pallidus even though massive and dense labeling along the pipette track was observed; it is, accordingly, very difficult to assess the possible contribution of anterograde thalamostriatal labeling to the striatal labeling detected.

Retrogradely labeled cells were observed in the caudate nucleus and in the putamen, more rarely, in several hemispheres ( $n=6$ ), particularly in those cases with evidence for enhanced labeling within striosomes. These retrogradely labeled cells, surprisingly few in number, were most prominent within striosomal regions in the caudate nucleus but could also be observed in zones not identified as striosomes, such as at the ventricular surface or within the most ventral part of the caudate nucleus or putamen. These cells may be detected even at low magnification as shown in Fig. 5. In those cases with injections involving the pars mixta and cell group A8 ( $n=2$ ), no retrogradely labeled cells were observed in the striatum.

*Fast blue:* In three cases fast blue was injected into the region of the nigral

complex. The injection sites are shown in Fig. 2 and the labeling observed along the pipette track is indicated in Fig. 4. As with WGA-HRP, fairly dense labeling along the pipette track was observed in all cases. The extent of thalamic contamination was unclear; however, as will be described below, very little labeling within the matrix compartment was observed in these cases which would not have been expected if the regions of the thalamus labeled along the pipette track had contributed significantly to striatal labeling (Ragsdale and Graybiel, 1989b).

One of the injections (case S23L, see Fig. 2) was extremely large because fast blue must often be injected with very high pressure to overcome clogging difficulties; in this case, the bolus injection created a lesion in the caudal part of the nigral complex. There was no detectable labeling within the striatum in this case. In the other two cases, however, anterograde and retrograde labeling was observed within the striatum. In both cases (injection sites shown in Fig. 2) the labeling was very weak but fiber labeling within zones histochemically identified as striosomes was clearly observed. In these zones, retrogradely labeled cells were also observed. Anterograde and retrograde labeling with fast blue within the caudate nucleus is illustrated in Fig. 7 (case S23R).

In case S23R, with an injection centered in the medial part of the pars compacta (see Fig. 2), striosomes were clearly distinguishable in the caudate nucleus as patches of enhanced fiber labeling with strongly labeled cells. These zones of enhanced labeling could be shown to correspond to striosomes in serially adjacent sections. Similar zones of enhanced labeling with retrogradely labeled cells within the rostradorsal putamen were observed infrequently; in general, however, retrogradely labeled cells within the putamen were rarely detected. In case S20L, with an injection site in the caudal and lateral part of the pars compacta (see Fig. 2), labeling within the striatum was more difficult to detect

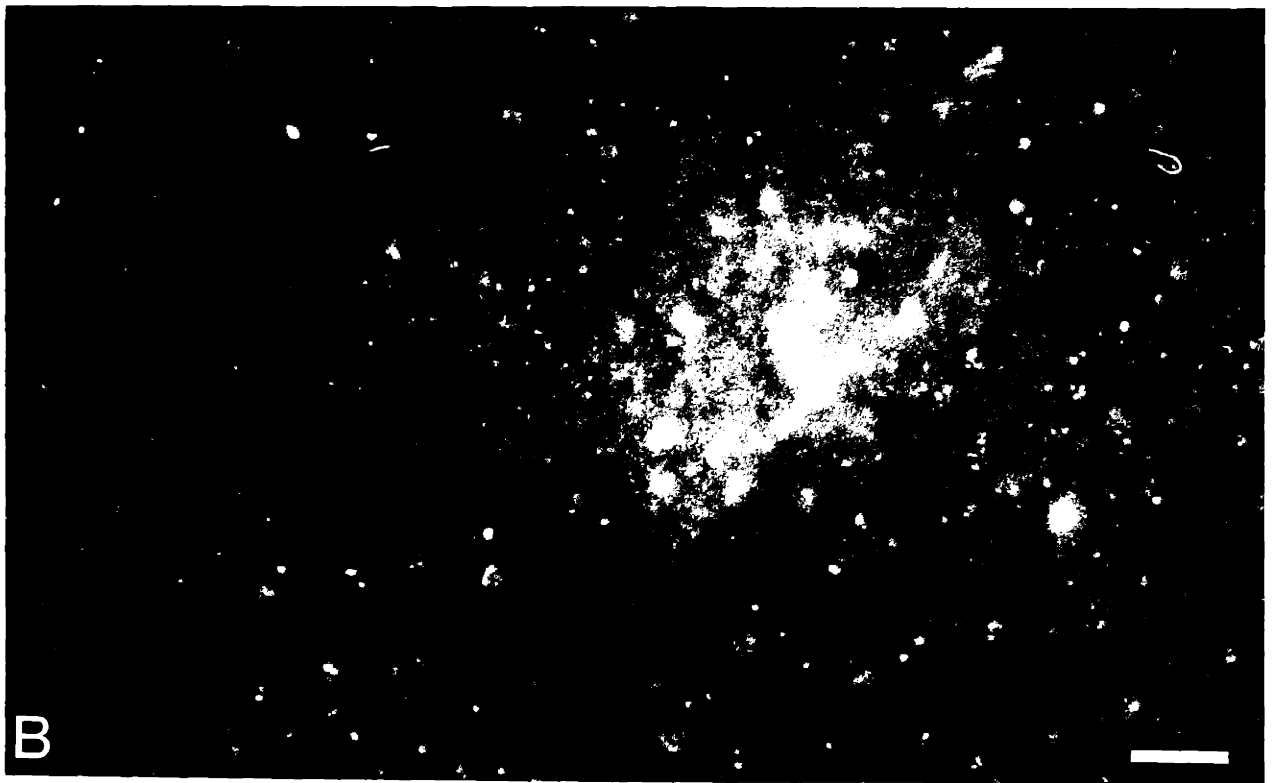
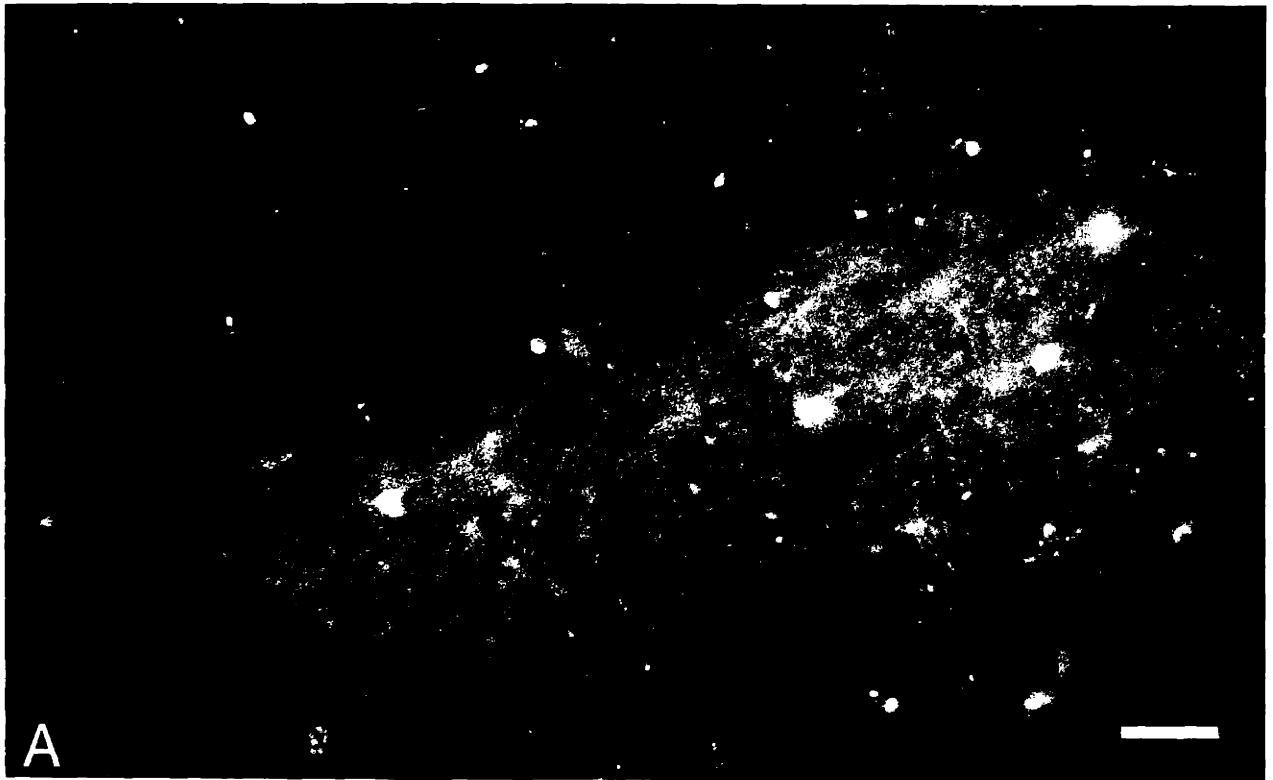
than in S23R; however, when striatal labeling was observed, it was most clearly distinguishable in the caudal part of the head and body of the caudate nucleus. Zones of enhanced labeling corresponded to histochemically identified striosomes and also contained retrogradely labeled cells. In case S23R some retrogradely labeled cells were also observed in zones not corresponding to striosomes, similar to that described for retrogradely labeled cells with WGA-HRP. For example, the retrogradely labeled cells, not located within striosomes, were observed in the ventral regions of the caudate nucleus (particularly near the ventricular surface) and the putamen (in its most ventral part) perhaps indicating that the injection infiltrated a dorsal region of the pars reticulata.

It was not possible to be sure in any of the above cases (WGA-HRP or FB) whether retrograde labeling could be accounted for by infiltrating regions of the pars reticulata; however, in one case S20L (FB), the injection site appeared to be restricted to the dorsal part of the substantia nigra and there were few retrogradely labeled cells detectable outside of regions corresponding to striosomes. Unfortunately, in this case both retrograde and anterograde labeling was generally very weak so that no strong conclusions may be drawn from this particular example. As shown in Fig. 7, there were also many examples of autofluorescent cells; these cells were much less fluorescent than those containing fast blue (apparent in Fig. 7) and under fluorescent illumination, these cells were most distinguishable by their green, rather than blue, fluorescence.

*PHA-L:* Labeled fibers within the striatum were observed in all cases after iontophoretic injections of PHA-L into the nigral complex. The injection sites in each case are illustrated in Fig. 3. There was very little evidence for labeling along the pipette track. A thin line of dense labeling was visible in every case, but the density and width of the staining along the pipette track was virtually equivalent



**Figure 3-7:** Retrogradely labeled cells in striosomes: fast blue. Two transverse sections through the caudate nucleus in case S23R following an injection of fast blue into the substantia nigra, pars compacta are shown. These sections, viewed and photographed under fluorescent illumination, illustrate the location of retrogradely labeled cells inside zones of anterogradely labeled fibers, corresponding to histochemically identified striosomes. In (A) there appears to be a large zone of anterograde fiber labeling with few retrogradely-labeled cells whereas in (B), within the dense region of anterograde labeling there are many retrogradely-labeled cells. Other less intensely fluorescent cells are also visible within the photograph, but these neurons are autofluorescent cells, appearing green instead of blue, when viewed under the optimal fluorescent filter for fast blue. The injection site in this case is shown in Fig. 2. Scale bar = 50  $\mu$ m.



in sections immunostained for PHA-L or for TH, suggesting that the thin line of dense staining observed in each case resulted from non-specific immunostaining as a result of the pipette lesion.

The relationship between injection site location and the topography of labeled striatal fibers was similar to that observed with other anterograde tracers (see chapter two). For example, dorsally placed injection sites resulted in PHA-L labeling within the ventral part of the striatum (e.g. case S11L, S13L; see Fig. 3) and with more caudally-situated injection sites, the density of fibers observed within the putamen was enhanced. The density of fiber labeling observed varied from case to case and was dependent on the current intensity and duration. For example, those cases receiving triple (vertically continuous) injections (see Methods) showed substantially more fiber labeling within the striatum than cases with single injections. Similarly, higher (10  $\mu$ amps) current intensities resulted in a greater number of fibers labeled compared to lower current intensities (7  $\mu$ amps). An example of a "triple injection site" is illustrated in Fig. 11; this injection site resulted in the labeling of fibers shown in Fig. 9.

In each of the cases, fibers or groups of fibers could be distinguished by their morphology, density of innervation and their distribution with respect to the location of striosomes. Figs. 8-10 illustrate examples of the different fibers observed; they include: 1) long, fairly smooth, single fibers with few or no branches found predominantly within the matrix compartment (Fig. 8); 2) dense plexuses of fibers with small but frequent varicosities, common within both the matrix and striosomal compartments (Figs. 9 and 10); and 3) thick fibers with many terminal branches and large, bulbous bouton-like structures, very rarely labeled and observed only within the matrix compartment (Fig. 8).

There were many instances where small or broad regions within the caudate

nucleus and/or the putamen appeared to contain a particularly dense plexus of fibers; the dense plexus was located either a) within the matrix compartment, b) within a striosome or c) within a region where both compartments could be identified histochemically. In no case did the fiber patterns seem to vary at striosomal borders. This lack of compartmental variation was particularly evident in cases S20R, S20L, S23R and S23L. In these cases, the injection site likely infiltrated parts of the pars mixta or cell group A8 as well as the horizontal band of the pars compacta. The injections in these cases were intended to be large; three consecutive vertical injections were made in each case in an attempt to label more fibers than had been observed in other previous cases with single injections (S11R, S11L, S13R, S13L, S15R, S15L). A particularly dense network of fibers, from a zone identified as matrix, is illustrated in Fig. 10 (case S20R). In cases with single injections there were very few fibers and terminals labeled and they were visible only sporadically as single fibers; groups of fibers were rarely observed.

It was very difficult to determine the effective injection site in all of the above cases; some clearly labeled cells were observed at the injection site and slightly peripheral to it, but at the center of the injection site (for example, see Fig. 11) it was not possible to determine which cells were infiltrated with the tracer. It is possible, therefore, that if the tracer deposit had been clearly restricted to the main horizontal band of the substantia nigra, for example, that we might have observed fiber labeling more restricted to zones identified as striosomes. The evidence does indicate, however, that with the injection sites shown in Fig. 3, labeled fibers observed in zones corresponding to striosomes and in regions identified histochemically as matrix were not clearly distinguishable morphologically (see Fig. 9), the exception being that the single, long fibers (Fig. 8B) and the short, thick fibers with bulbous endings (Fig. 8A) were generally only observed in regions corresponding to the matrix compartment.

**Figure 3-8:** PHA-L-labeled striatal fibers: single fibers in the matrix. Two types of fibers labeled with a PHA-L injection into the nigral complex in case S20L are illustrated. The regions in which these fibers were observed were identified histochemically in serially adjoining sections as extrastriosomal matrix. In (A) a thick fiber with large, bulbous endings is shown. This type of fiber was rarely observed in the striatum and, when detected, appeared only within the matrix compartment. In (B) a single, thin branching fiber is shown with slight swellings along the fiber; long, single fibers were rarely observed in the striosomal compartment. Scale bar = 50  $\mu$ m.

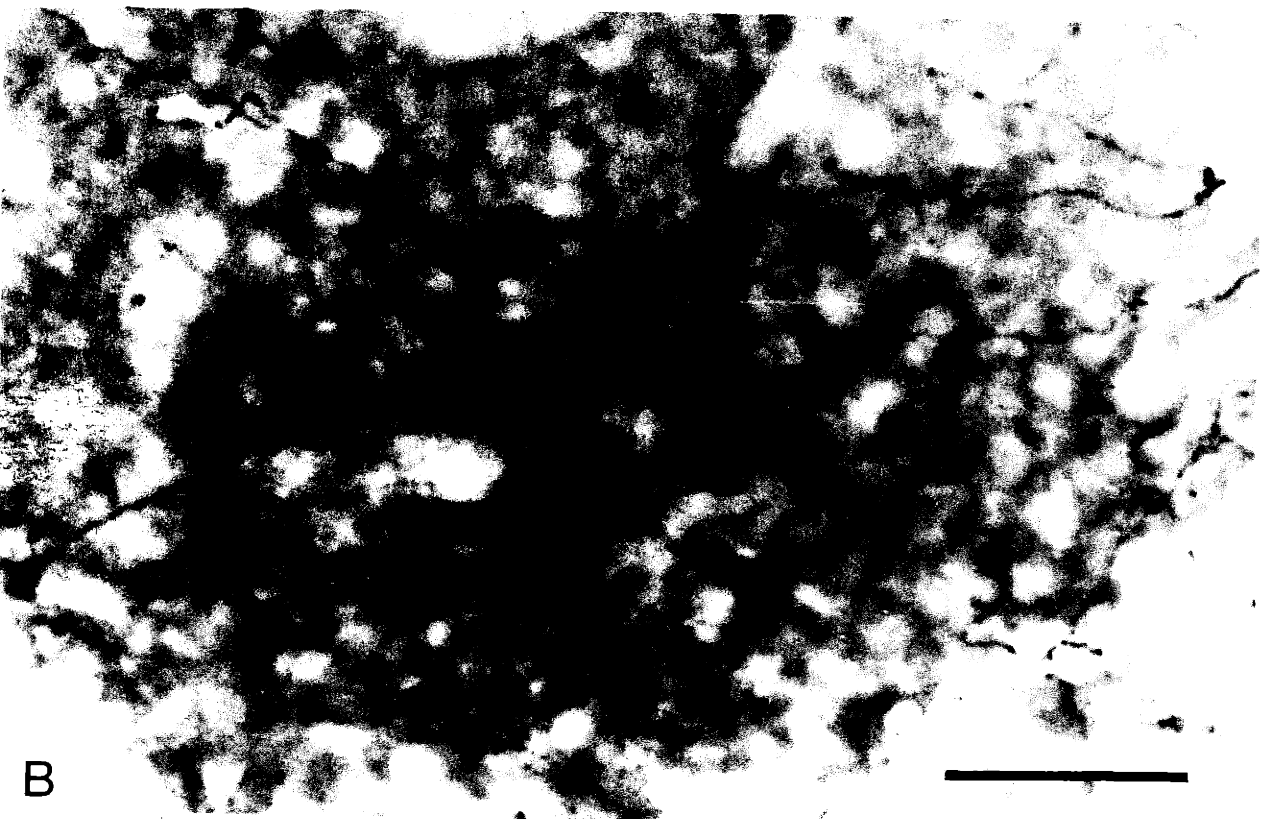
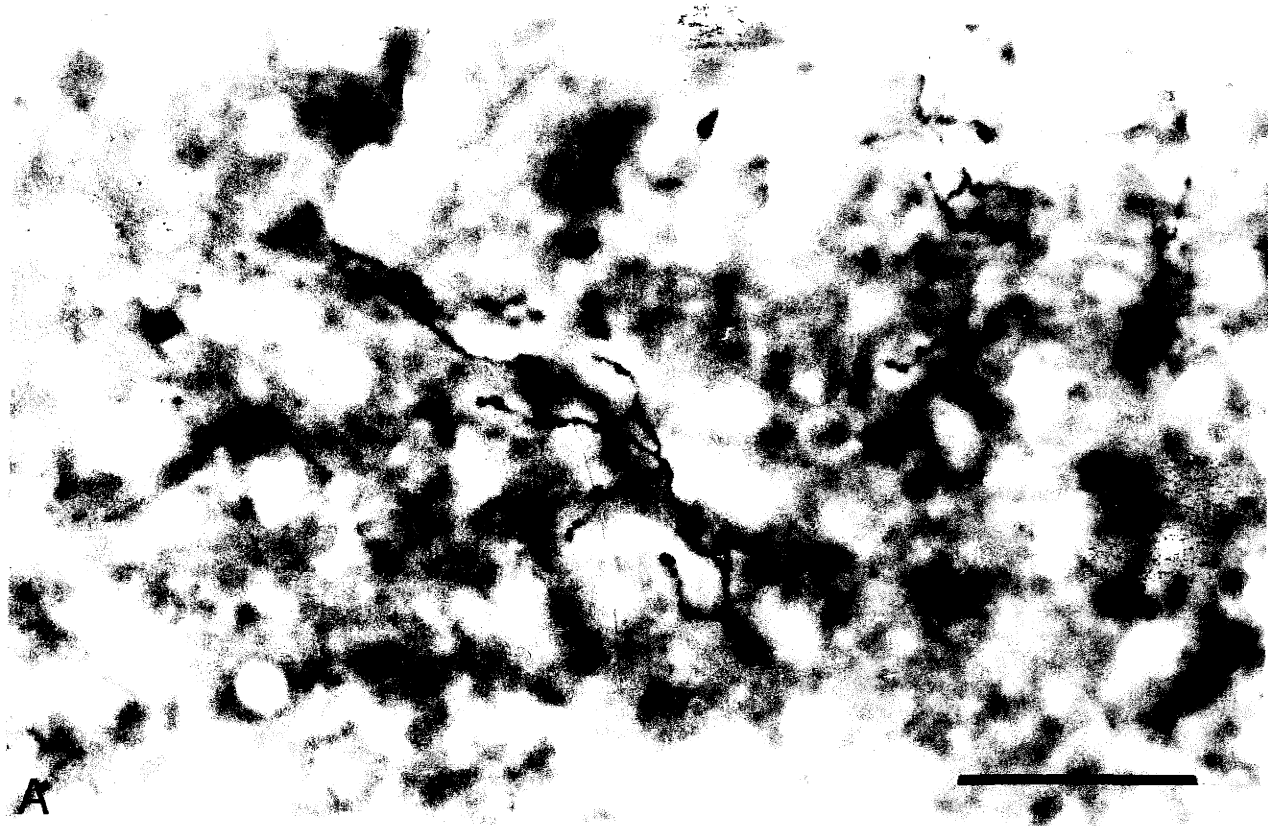


**Figure 3-9:** PHA-L-labeled striatal fibers: in and out of striosomes. A dense plexus of fibers labeled within regions identified histochemically as (A) a striosome or (B) as extrastriosomal matrix following an injection of PHA-L into the nigral complex of case S23R is shown. In both of these regions the types of fibers appear very similar. The injection site in this case is illustrated in Fig. 3. bv, blood vessel. Scale bar = 50  $\mu$ m.

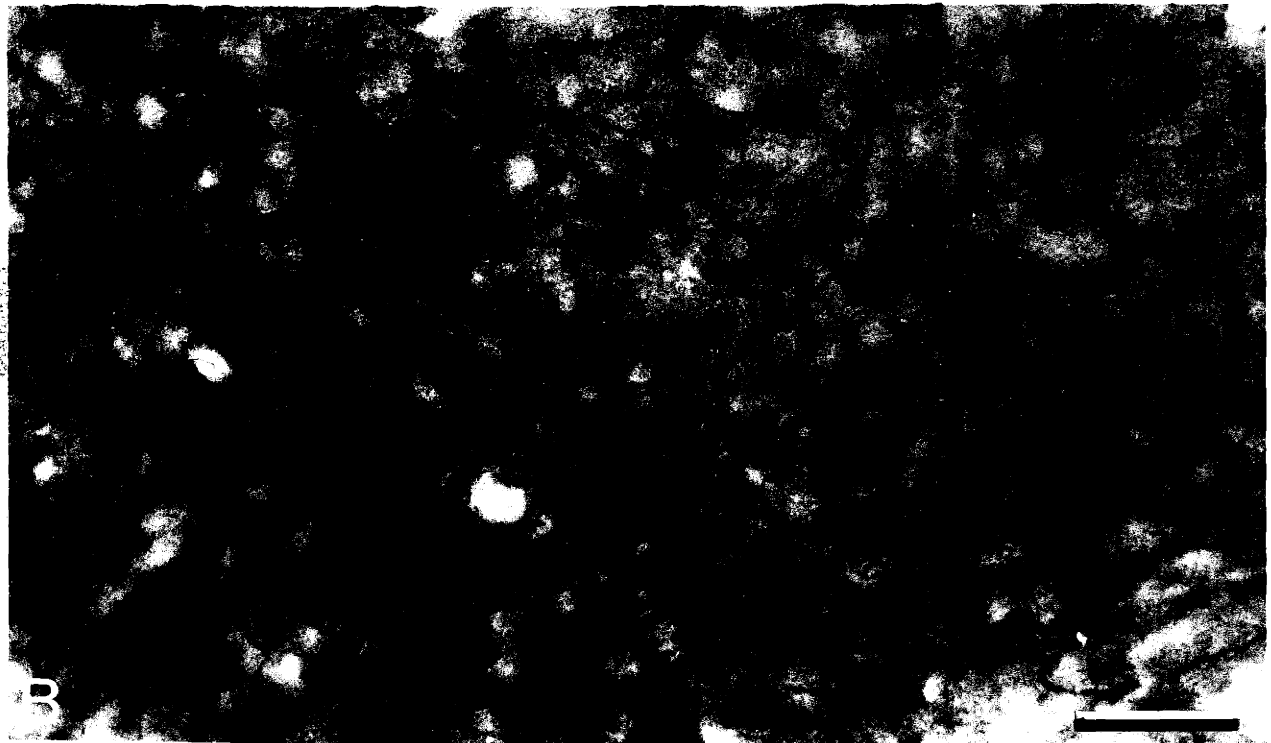




**Figure 3-10:** PHA-L-labeled striatal fibers: a dense plexus in the matrix. A very dense network of fibers labeled by an injection of PHA-L into the nigral complex in case S20R is shown. The entire region is within histochemically identifiable matrix. The injection site in this case is illustrated in Fig. 3. Scale bar = 50  $\mu$ m.

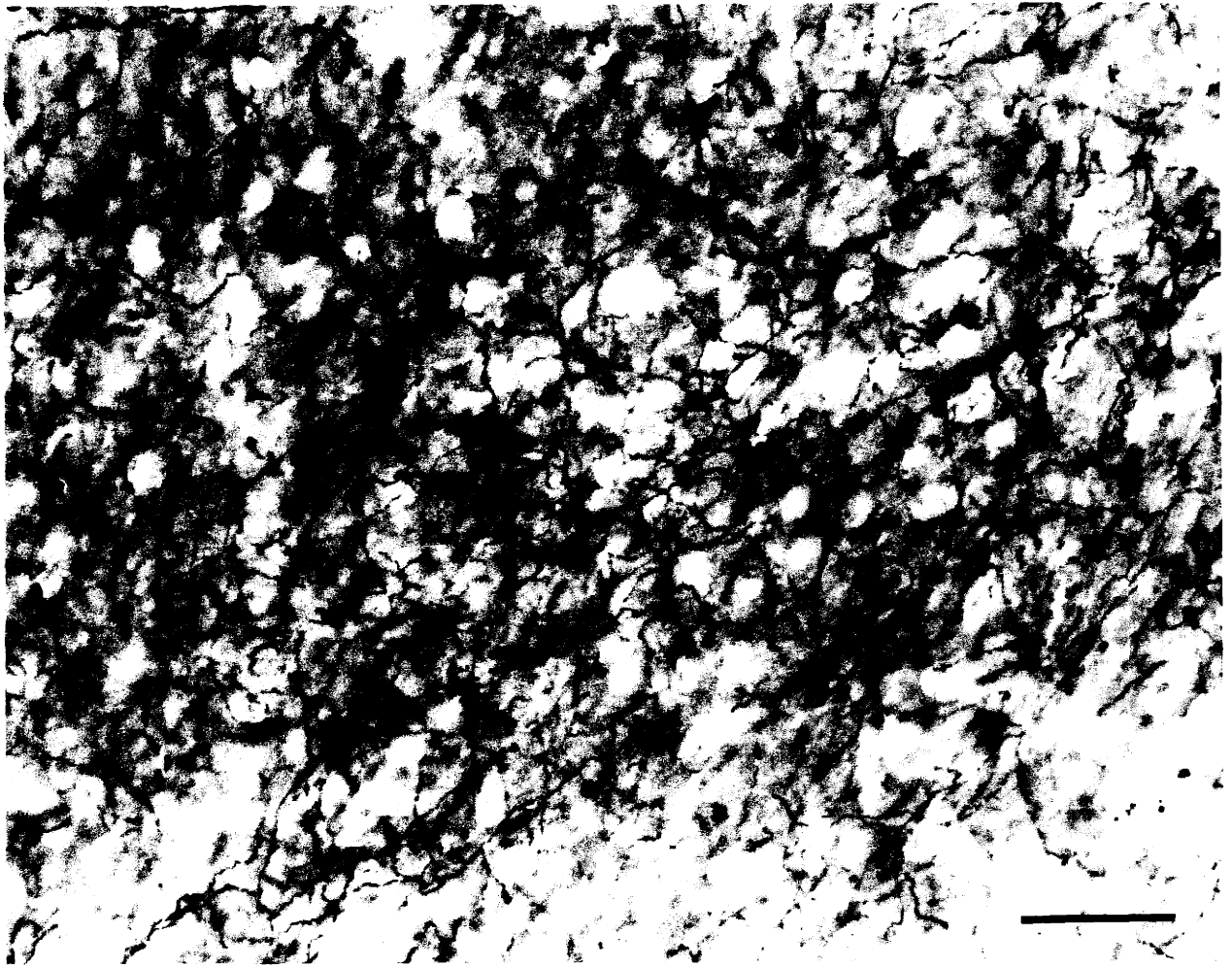


**Figure 3-11:** PHA-L injection site photograph: case S23R. An example of a triple injection site (three consecutive iontophoretic injections spaced by 0.2 mm in the vertical axis) from case S23R is shown. Within the center of the injection site the particular neurons labeled are difficult to identify. The location of the injection site in this case relative to other peripheral structures is illustrated in Fig. 3. Scale bar = 500  $\mu\text{m}$ .



## Discussion

With the anterograde and retrograde tracers WGA-HRP and FB it was possible to demonstrate compartmentally differentiated mesostriatal systems originating from distinct regions within the A8-A9-A10 cell complex, as had been previously observed with injections of  $^{35}\text{S}$ -methionine (see chapter two). These tracers were also useful in identifying a potential reciprocal relationship between the region within the nigral complex observed to contain striosome-projecting neurons and those striatonigral projection neurons within striosomes. This latter finding is in keeping with recent work in the cat (Jimenez-Castellanos and Graybiel, 1989b) indicating a similar anatomical relationship. The findings reported here with the anterograde tracer PHA-L have also helped to further characterize mesostriatal connectivity; some morphological features of mesostriatal fibers originating from certain regions of the nigral complex were identified.

**WGA-HRP and FB in mesostriatal pathways:** With injections of  $^{35}\text{S}$ -methionine in 40 cases (chapter two), distinct regions within the nigral complex were identified which appeared to differentially project to the striosomal and matrix compartments of the striatum. In the present experiments many of the original observations made in the previous autoradiographic study with respect to mesostriatal topography were corroborated; for example, enhanced labeling of striosomes or matrix was observed in those cases with injection sites centered in the main horizontal band and in A8, respectively. However, in comparison, WGA-HRP and FB were not as informative with respect to delineating striatal compartments because the labeling within the striatum often appeared diffuse, and, at least with WGA-HRP, it was very difficult to determine accurately the size and location of effective injection sites. In addition, with both WGA-HRP and FB the size and intensity of the labeling along the pipette track was substantial, leading to

potentially significant contamination of thalamostriatal projection neurons. The relative contribution to striatal labeling from thalamostriatal afferents is difficult to interpret, although in most cases there were rarely more than a few retrogradely labeled cells observed within the internal segment of the globus pallidus [the projection to the thalamus from the globus pallidus is largely from the internal segment (Nauta and Mehler, 1966; Carpenter and Strominger, 1967; Mehler and Nauta, 1974)].

It was hoped that these tracers might also provide additional information on the type of fibers contributing to the different patterns of striatal labeling. As with  $^{35}\text{S}$ -methionine, however, the labeling observed within the striatum was not identifiable within particular types of fibers, although the difference between fiber labeling and retrograde cell labeling was clearly distinguishable. PHA-L (see below) was much more informative with regard to the morphological characteristics of mesostriatal fibers.

**WGA-HRP and FB in striatonigral pathways:** Labeling of projection neurons predominantly within striosomes of the caudate nucleus was observed in several cases with injections centered in the main horizontal band of the pars compacta; some labeled neurons were also found in the extrastriosomal matrix of the ventromedial caudate nucleus and the ventrolateral putamen in most of these cases. No retrogradely labeled cells were observed in those cases with injections largely infiltrating neurons of the pars mixta and cell group A8. These findings are in accord with previous studies in the rat (Gerfen, 1985; Gerfen et. al., 1987a) and cat (Jimenez-Castellanos and Graybiel, 1985; Jimenez-Castellanos and Graybiel, 1989b). In these species there appear to be reciprocally linked projections between the neurons of the striosome-projecting zone of the pars compacta and striatonigral neurons within striosomes. According to Jimenez-Castellanos and Graybiel

(Jimenez-Castellanos and Graybiel, 1989b; Jimenez-Castellanos and Graybiel, 1985), the projections from cell group A8 to the striatum in the cat appeared only weakly reciprocated, if at all, although other studies in the rat (Nauta et. al., 1978) and cat (Groenewegen and Russchen, 1984) have shown that there is a substantial projection from ventral regions of the striatum to parts of cell group A8 and cell group A10. The striatal projection neurons of the extrastriosomal matrix, in particular, have been shown to project predominantly to the pars reticulata and the globus pallidus (Graybiel et. al., 1979; Gerfen, 1985; Jimenez-Castellanos and Graybiel, 1989b). Similarly, the cell-labeling observed in the extrastriosomal matrix in the present study is very likely to have originated from terminals within the pars reticulata; the effective injection sites in these cases were difficult to delineate and it was not possible to determine whether injections into the pars compacta also substantially infiltrated regions of the pars reticulata.

In the present study the majority of the labeled striatal neurons were observed in the caudate nucleus. This finding is consistent with previous studies in the squirrel monkey (Parent et. al., 1984; Smith and Parent, 1986) indicating that putaminofugal neurons project predominantly to the globus pallidus whereas caudatofugal neurons terminate largely within the substantia nigra. In these studies some striatonigral fibers were reported to terminate within the pars compacta as described previously in the rat and cat. In fact, caudatonigral and putaminonigral (much fewer putaminonigral) fibers appear to terminate within clusters of nigrocaudate and nigroputaminal neurons, respectively, indicating the existence of separate reciprocally linked striato-nigro-striatal projections in primates. The present study indicates that in the primate brain, in addition to the segregated reciprocally-linked systems within the caudate nucleus and putamen (Parent et. al., 1984), another reciprocally-linked striato-nigro-striatal system within the striosomal compartment of the caudate nucleus may exist.

**PHA-L labeling in the mesostriatal pathway:** As described previously (see p. 128, chapter two), several studies on rodent striatal afferent systems have indicated that there are morphologically distinct striatal afferent fiber types projecting to either the striosomal or matrix compartments. For example, Wilson and Xu (Wilson and Xu, 1988) have indicated that corticostriatal fibers in the rat which project specifically to either the matrix or striosomal compartments could be distinguished by their fiber morphology and distribution of synaptic boutons. Striosome-projecting fibers appeared to branch extensively in a small region and to contain numerous synaptic boutons. Matrix-projecting fibers were observed to be very long with extended branches and infrequently spaced boutons and to have "en passant" specializations. Olson and coworkers (Olson et. al., 1972) suggested that two types of dopamine nerve terminals exist; fluorescent dopamine-containing terminals in the limbic forebrain of the adult rat and in the dopamine islands of the neonatal rodent striatum were observed to have a "dotted" appearance whereas the majority of the nigrostriatal terminals in the adult had a "diffuse" appearance. The types of fibers and terminals which account for these different fluorescent patterns were not identified.

A study by Gerfen and colleagues (Gerfen et. al., 1987a) with the anterograde tracer *Phaseolus vulgaris*-leucoagglutinin [PHA-L] also suggested that two types of dopamine-containing terminals within the striatum could be distinguished. These authors identified three types of nigrostriatal fibers in the rodent: type A fibers are thin, smooth, have small varicosities and were found exclusively in the matrix compartment; type B fibers are thicker than type A, have more numerous varicosities and were observed within striosomes; type C fibers are very thick, have large, bulbous varicosities and were also exclusively directed towards the matrix compartment. Types A and B were observed to be predominantly dopamine-



containing while type C fibers, more rarely seen, were shown most often to correspond to non-dopaminergic fibers.

In the present study several different kinds of fibers were observed: single fibers with few or no branches and slight swellings (predominantly within the matrix compartment), dense plexuses of fibers with small but frequent varicosities (observed in both the matrix and striosomal compartments) and thick fibers with many terminal branches and large, bulbous bouton-like structures (rarely observed but found only within the matrix compartment). The first and last types of fibers appear very similar to that described by Wilson and Xu (Wilson and Xu, 1988) as the matrix-projecting and striosome-projecting corticostriatal fibers, respectively. However, in the present study these types of fibers were not observed within regions corresponding to striosomes. Due to the apparent density of labeling in many cases of enhanced labeling of striosomes observed following injections of WGA-HRP and  $^{35}\text{S}$ -methionine (chapter two), it seemed a likely hypothesis that striosome-projecting mesostriatal afferents might have a more dense mode of termination than matrix-projecting afferents. However, these fibers (the single, long branching fiber and the fiber with numerous, bulbous swellings) were too rarely observed to account for different patterns of mesostriatal termination. The fibers with large bulbous terminals are more likely to be the primate homologue of the matrix-projecting, type C, non-dopaminergic fiber described by Gerfen and colleagues (Gerfen et. al., 1987a). The other single fiber with slight swellings may be a component of the more commonly observed plexus of fibers.

There were many examples in the material of the present study where a particularly dense plexus of fibers was observed within the caudate nucleus or the putamen. These fibers (which appeared to be consistently of a similar type) were observed in zones identified histochemically as matrix or striosomes; sometimes

groups of fibers appeared to innervate a zone containing both compartments with no apparent regard for the location of compartmental borders. Because the injection sites in these cases were not small enough to be restricted to a small nigral region and likely infiltrated neurons of the pars mixta or cell group A8 as well as the horizontal band of the pars compacta, it is not surprising that fibers were often observed in both compartmental regions. However, if both striosome-projecting and matrix-projecting neurons were infiltrated and if two distinct types of fibers exist (a striosome-projecting type and a matrix projecting type), then one would expect to see these two different types of fibers within the appropriate histochemically identified zones. In the present study two distinct types of fibers analogous to those identified by Gerfen and colleagues (Gerfen et. al., 1987a) as types A and B were not distinguished. It is possible in the primate that two distinct populations do not exist or that the distinction between these types of fibers is extremely difficult to detect. Several smaller, more restricted injections of PHA-L into nigral regions where fairly selective compartmental labeling may be elicited (e.g. cell group A8 and the lateral part of the main horizontal band of the pars compacta) are needed to unequivocally demonstrate whether two types of mesostriatal fibers may be observed in the primate.

If there are no morphological features which distinguish matrix-projecting and striosome-projecting fibers, it remains unclear as to what accounts for the different types of patterned striatal labeling observed. In chapter two, several possibilities were examined (see Fig. 29, chapter two). In light of the current findings, the possibility that within segregated compartments at least two distinct types of fibers (with different types of terminal arbors, specialized terminal endings or additional bouton structures) account for the patterned striatal labeling is much less likely; these distinct morphological features should be pronounced

enough to be detected in the cases described here. Alternatively, if these features are not easily detectable, certain morphological characteristics could have been masked by the particularly dense innervation of fibers in cases with large injections; in cases with small injections there may have been too few labeled fibers to identify discrete morphological features. It should be noted, however, that in the study reported by Gerfen and coworkers (Gerfen et. al., 1987a), the density of fiber labeling apparent in photographic images of regions corresponding to either striosomes or matrix was substantial, often more dense than the labeling observed in the present study.

In summary, the study with PHA-L suggests at least preliminary conclusions regarding the apparent morphological characteristics of mesostriatal fibers. This information may be useful in distinguishing among the the possibilities described in chapter two to account for patterned mesostriatal labeling (Fig. 29, chapter two). It appears most likely that in the nigral complex there exist neurons that project predominantly to striosomes and others that project predominantly to the matrix compartment; however, the evidence does not rule out the possibility that there are yet other neurons that project to both compartments. Most likely the majority of these neurons have similar types of terminal arbors, judging from the fiber labeling observed. In addition, the retrograde cell labeling observed in the present study strongly suggests that in the primate there exist reciprocating striatonigral-nigrostriatal projections and that striosomal cells are prominent among the population of striatonigral projection neurons as a whole. This observation implies that the dopamine-containing projections to striosomes may be tightly regulated by striatal output, a potentially powerful feedback mechanism for the normal dopaminergic regulation of trans-striatal processing within the striatum<sup>2</sup>.

---

<sup>2</sup>See chapter one for a discussion of the other striatal afferents and efferents involved in compartmentalized trans-striatal processing.

## References

- Alexander, G. E., Koliatsos, V. E., Martin, L. J., Hedreen, J., Hamada, I., DeLong, M. R. (1988) Organization of the primate basal ganglia motor circuit: 1. Motor cortex and supplementary motor area project to complementary regions within matrix compartment of putamen. *Soc. Neurosci. Abstr.* **14**, 287.
- Anden, N. E., Carlsson, A., Dahlstrom, A., Fuxe, K., Hillarp, N. A., Larsson, K. (1964) Demonstrating and mapping out nigro-neostriatal dopamine neurons. *Life Sci.* **3**, 523-530.
- Arsenault, M.-Y., Parent, A., Seguela, P. and Descarries L. (1988) Distribution and morphological characteristics of dopamine-immunoreactive neurons in the midbrain of the squirrel monkey [*Saimiri sciureus*]. *J. Comp. Neurol.* **267**, 489-506.
- Azmitia, E. C. and Segal, M. (1978) An autoradiographic analysis of the differential ascending projections of the dorsal and median raphe nuclei in the rat. *J. Comp. Neurol.* **179**, 641-668.
- Ballard, P. A., Tetrud, J. W., Langston, J. W. (1980) Permanent human parkinsonism due to 1-methyl-4-phenyl- 1,2,3,6-tetrahydropyridine (MPTP): Seven cases. *Neurology* **35**, 525-554.
- Barbeau, A. (1986) Parkinson's Disease: Clinical features and etiopathology. In *Handbook of Clinical Neurology*, Vol. 49 (Edited by Vinken, P. J., Bruyn, G. W. and Klawans, H. L.) pp. 87-152. Elsevier Press, Amsterdam.
- Beckstead, R. M. (1985) Complementary mosaic distributions of thalamic and nigral axons in the caudate nucleus of the cat: double anterograde labeling combining autoradiography and wheat germ-HRP histochemistry. *Brain Res.* **335**, 153-159.
- Beckstead, R. M. (1987) Striatal substance P cell clusters coincide with the high density terminal zones of the discontinuous nigrostriatal dopaminergic projection system in the cat. A study by combined immunohistochemistry and autoradiographic axon tracing. *Neuroscience* **20**, 557-576.
- Beckstead, R. M. (1987) The distributions of dopamine D1 and D2 receptors are partially complementary in the cat basal ganglia. *Soc. Neurosci. Abstr.* **13**, 190.

- Beckstead, R. M. and Frankfurter, A. (1982) The distribution and some morphological features of substantia nigra neurons that project to the thalamus, superior colliculus and pedunculopontine nucleus in the monkey. *Neuroscience* **7**, 2377-2388.
- Beckstead, R. M., Domesick, V. B., Nauta, W. J. H. (1979) Efferent connections of the substantia nigra and ventral tegmental area in the rat. *Brain Res.* **175**, 191-217.
- Beckstead, R. M., Wooten, G. F., Trugman, J. M. (1988) Distribution of D1 and D2 dopamine receptors in the basal ganglia of the cat determined by quantitative autoradiography. *J. Comp. Neurol.* **268**, 131-145.
- Beninato, M., Spencer, R. F. (1986) A cholinergic projection from the pedunculopontine tegmental nucleus to the substantia nigra in the rat: a light and electron microscopic immunohistochemical study. *Soc. Neurosci. Abstr.* **12**, 28.
- Besson, M. J., Graybiel, A. M. and Nastuk, M. A. (1988) [3H]-SCH23390 binding to D1 dopamine receptors in the basal ganglia of the cat and primate: delineation of striosomal compartments and pallidal and nigral subdivisions. *Neuroscience* **26**, 101-119.
- Biocom Inc. (1989) *Biocom User's Manual: Photometric Image for Analysis of Autoradiographs*. Biocom, Paris, France.
- Bjorklund, A. and Lindvall, O. (1984) Dopamine-containing systems in the central nervous system. In *Handbook of Clinical Neuroanatomy Vol. 2 Classical Transmitters in the Central Nervous System* (Edited by Bjorklund, A. and Hokfelt, T.) pp. 55-122. Elsevier Press, Amsterdam.
- Bobillier, P., Sequin, S., Petitjean, F., Salvert, D., Touret, M., and Jouvet, M. (1976) The raphe nuclei of the cat brain stem: a topographical atlas of their efferent projections as revealed by autoradiography. *Brain Res.* **113**, 449-486.
- Bouras, C., Taban, C. H., and Constantinidis, J. (1984) Mapping of enkephalin in human brain. An immunofluorescence study on brains from patients with senile and presenile dementia. *Neuroscience* **12**, 179-190.
- Brownstein, M. J., Mroz, E. A., Tappaz, M. L., and Leeman, S. E. (1977) On the origin of substance P and glutamic acid decarboxylase (GAD) in the substantia nigra. *Brain Res.* **135**, 315-323.

- Burns, R. S., Chiueh, C. C., Markey, S. P., Ebert, M. H., Jacobowitz, D. M., Kopin, I. J. (1983) A primate model of parkinsonism: selective destruction of dopaminergic neurons in the pars compacta of the substantia nigra by N-methyl-4-phenyl-1,2,3,6-tetrahydropyridine. *Proc. Natl. Acad. Sci. U.S.A.* **80**, 4546-4550.
- Butcher, L. L. and Marchand, R. (1978) Acetylcholinesterase is synthesized and transported by dopamine neurons in the pars compacta of the substantia nigra: functional significance and histochemical correlations on the same brain section. In *Catecholamines: basic and clinical frontiers*, (Edited by Usdin, L.) pp. 223-240. Pergamon Press, Oxford.
- Carpenter, M. B., Peter, P. (1972) Nigrostriatal and nigrothalamic fibers in the rhesus monkey. *J. Comp. Neurol.* **144**, 93-116.
- Carpenter, M. B. and Strominger, N. L. (1967) Efferent fibers of the subthalamic nucleus in the monkey. A comparison of the efferent projections of the subthalamic nucleus, substantia nigra and globus pallidus. *Amer. J. Anat.* **121**, 41-72.
- Carpenter, M. B., Nakano, K., Kim, r. (1976) Nigrothalamic projections in the monkey demonstrated by autoradiographic technics. *J. Comp. Neurol.* **165**, 401-416.
- Cheramy, A., Romo, R., and Glowinski, J. (1987) Role of corticostriatal glutamatergic neurons in the presynaptic control of dopamine release. In *Neurotransmitter Interactions in the Basal Ganglia*, (Edited by Sandler, M.) pp. 133-141. Raven Press, New York.
- Chesselet, M.-F., and Graybiel, A. M. (1983) Subdivisions of the pallidum and the substantia nigra demonstrated by immunohistochemistry. *Soc. Neurosci. Abstr.* **8**, 9.
- Chesselet, M.-F. and Graybiel, A. M. (1983) Met-enkephalin-like and dynorphin-like immunoreactivity of the basal ganglia of the cat. *Life Science* **33**, 37-40.
- Chesselet, M. F. and Graybiel, A. M. (1986) Striatal neurons expressing somatostatin-like immunoreactivity: evidence for a peptidergic intraneuronal system in the cat. *Neuroscience* **17**, 547-571.
- Cowan, W. M., Gottlieb, D. I., Hendrickson, A. E., Price, J. L., Woolsey, T. A. (1972) The autoradiographic demonstration of axonal connections in the central nervous system. *Brain Res.* **37**, 21-51.

- Crosby, E. C. and Woodburne, R. T. (1943) The nuclear pattern of the non-tectal portions of the midbrain and isthmus in primates. *J. Comp. Neurol.* **78**, 441-482.
- Dahlstrom, A. and Fuxe, K. (1964) Evidence for the existence of monoamine-containing neurons in the central nervous system. I. Demonstration of monoamines in the cell bodies of brain stem neurons. *Acta Physiol. Scand.* **62**, 1-55.
- Davis, R. and Huffman, R. D. (1968) *A Stereotaxic Atlas of the Brain of the Baboon [Papio]*. Univ. Texas Press, Austin.
- Descarries, L., Boser, O., Berthelet, F., and Des Roeirs, M. H. (1980) Dopaminergic nerve endings visualized by high resolution autoradiography in adult rat neostriatum. *Nature* **284**, 620-622.
- Deutch, A. Y., Goldstein, M., Bunney, B. S., and Roth, R.H. (1984) The anatomical organization of the efferent projections of the A8 dopamine cell group. *Soc. Neurosci. Abstr.* **10**, 9.
- Deutch, A. Y., Elsworth, J. D., Goldstein, M., Fuxe, K., Redmond, D. E., Jr., Sladek, J. R., Jr., Roth, R. H. (1986) Preferential vulnerability of A8 dopamine neurons in the primate to the neurotoxin 1-methyl-4-phenyl-1,2,3,6-tetrahydropyridine. *Neurosci. Lett.* **68**, 51-56.
- DiCarlo, V., Hubbard, J. E., and Pate, P. (1973) Fluorescence histochemistry of monoamine-containing cell bodies in the brain stem of the squirrel monkey *Saimiri sciureus*. *J. Comp. Neurol.* **152**, 347-372.
- Domesick, V. B., Stinus, L., and Paskevich, P. A. (1983) The cytology of dopaminergic and nondopaminergic neurons in the substantia nigra and ventral tegmental area of the rat: a light- and electron-microscopic study. *Neuroscience* **8**, 743-765.
- Donoghue, J. P. and Herkenham, M. (1986) Neostriatal projections from individual cortical fields conform to histochemically distinct striatal compartments in the rat. *Brain Res.* **365**, 397-403.
- Dubois, A., Savasta, M., Curet, O., and Scatton, B. (1986) Autoradiographic distribution of the D1 agonist 3H-SKF38393 in the rat brain and spinal cord. Comparison with the distribution of D2 dopamine receptors. *Neuroscience* **19**, 125-137.
- Eadie, M. J. (1963) Pathology of certain medullary nuclei in Parkinsonism. *Brain* **86**, 781-792.

- Emmers, R. and Akert, K. (1963) *A stereotaxic atlas of the brain of the squirrel monkey [Saimiri sciureus]*. Univ. of Wisconsin Press, Madison, WI.
- Emson, P. C., Arregui, A., Clement-Jones, V., Sandberg, B. E. and Rossor, M. (1980) Regional distribution of met-enkephalin and substance P immunoreactivity in normal human brain and in Huntington's disease. *Brain Res.* **199**, 147-160.
- Fallon, J. H. and Loughlin, S. E. (1982) Monoamine innervation of the forebrain: collateralization. *Brain Res. Bull.* **9**, 295-307.
- Fallon, J. H. and Moore, R. Y. (1978) Catecholamine innervation of the basal forebrain. IV. Topography of the dopamine projection to the basal forebrain and neostriatum. *J. Comp. Neurol.* **180**, 545-580.
- Fallon, J. H., Riley, J. and Moore, R. Y. (1978) Substantia nigra dopamine neurons: separate populations project to neostriatum and allocortex. *Neurosci. Letters* **7**, 157-162.
- Fass, B. B., and Butcher, L. L. (1981) Evidence for a crossed nigrostriatal pathway in rats. *Neurosci. Letters* **22**, 108-113.
- Faull, R. L. M., Mehler, W. R. (1978) The cells of origin of nigrotectal, nigrothalamic and nigrostriatal projections in the rat. *Neuroscience* **3**, 989-1002.
- Faull, R. L. M., Dragunow, M. and Villiger, J. W. (1989) The distribution of neurotensin receptors and acetylcholinesterase in the human caudate nucleus: evidence for the existence of a third neurochemical compartment. *Brain Res.* **488**, 381-386.
- Feigenbaum, L. A., and Graybiel, A. M. (1988) Heterogeneous striatal afferent connections from distinct regions of the dopamine-containing midbrain of the primate. *Soc. Neurosci. Abstr.* **14**, 156.
- Ferrante, R. J. and Kowall, N. W. (1987) Tyrosine hydroxylase-like immunoreactivity is distributed in the matrix compartment of normal and Huntington's disease striatum. *Brain Res.* **416**, 141-146.
- Flaherty, A. W., Graybiel, A. M., Sur, M. and Garraghty, P. (1989) Distinctive patterns of projections to striatum from physiologically mapped somatosensory representations in primate cortex. *Soc. Neurosci. Abstr.* **15**, In Press.



- Fonnum, F., Gottesfeld, Z., and Grofova, I. (1978) Distribution of glutamate decarboxylase, choline acetyl-transferase and aromatic amino acid decarboxylase in the basal ganglia of normal and operated rats. Evidence for striatopallidal, striatoentopeduncular and striatonigral gabaergic fibers. *Brain Res.* **143**, 125-138.
- Forno, L. S. and Alvord, E. C. (1974) Depigmentation in the nerve cells of the substantia nigra and locus coeruleus in Parkinsonism. *Adv. Neurol.* **5**, 195-202.
- Fox, C. A. , Andrade, A. Hillman, D. E., and Schwyn, R. C. (1971) The spiny neurons in the primate striatum: a Golgi and electron microscopic study. *J. Hirnforsch* **13**, 181-201.
- Francois, C., Percheron, G., Yelnik, J. and Heyner, S. (1979) Demonstrationh of the existence of small local circuit neurons in the Golgi-stained primate substantia nigra. *Brain Res.* **172**, 160-164.
- Francois, C., Percheron, G. and Yelnik, J. (1984) Localization of nigrostriatal, nigrothalamic and nigrotectal neurons in ventricular coordinates in macaques. *Neuroscience* **13**, 61-76.
- Francois, C., Percheron, G., Yelnik, J., and Heyner, S. (1985) A histological atlas of the macaque *Macaca mulatta* substantia nigra in ventricular coordinates. *Brain Res. Bull.* **14**, 349-367.
- Freund, T. F., Powell, J. F., and Smith, A. D. (1984) Tyrosine hydroxylase immunoreactive synaptic boutons in contact with identified striatonigral neurons, with particular reference to dendritic spines. *Neuroscience* **13**, 1189-1215.
- Gale, K., Hong, J. S., and Guidotti, A. (1977) Presence of substance P and GABA in separate striatonigral neurons. *Brain Res.* **136**, 371-375.
- Garver, D. L. and Sladek, J. R. Jr. (1975) Monoamine distribution in primate brain. I. Catecholamine-containing perikarya in the brain stem of *Macaca speciosa*. *J. Comp. Neurol.* **159**, 289-304.
- Gaspar, P., Berger, B., Gay, M., Hammon, M., Cesselin, F., Vigny, A., Javoy-Agid, R. and Agid, Y. (1983) Tyrosine hydroxylase and methionine-enkephalin in the human mesencephalon. *J. Neurol. Sci.* **58**, 247-267.
- Geneser-Jensen, F. A. and Blackstad, J. W. (1971) Distribution of acetylcholinesterase in the hippocampal region of the guinea pig. *Z. Zellforsch. Mikrosk. Anat.* **114**, 460-481.

- Gerfen, C. R. (1985) The neostriatal mosaic. I. Compartmental organization of projections from the striatum to the substantia nigra in the rat. *J. Comp. Neurol.* **236**, 454-476.
- Gerfen, C. R., Baimbridge, K. G., and Miller, J. J. (1985) The neostriatal mosaic: Compartmental distribution of calcium-binding protein and parvalbumin in the basal ganglia of the rat and monkey. *Proc. Natl. Acad. Sci. USA* **82**, 8780-8784.
- Gerfen, C. R., Herkenham, M., and Thibault, J. (1987) The neostriatal mosaic. II. Patch- and matrix-directed mesostriatal dopaminergic and non-dopaminergic systems. *J. Neurosci.* **7**, 3915-3934.
- Gerfen, C. R., Baimbridge, K. G., and Thibault, J. (1987) The neostriatal mosaic: III. Biochemical and developmental dissociation of patch-matrix mesostriatal systems. *J. Neurosci.* **7**, 39.
- Gergen, J. A. and MacLean, P. D. (1962) *A Stereotaxic Atlas of the Squirrel Monkey's Brain [Saimiri sciureus]*. U. S. Dept. Health, Education and Welfare, Bethesda.
- German, D. C., Dubach, M., Askari, S., Speciale, S. G. and Bowden, D. M. (1988) 1-methyl-4-phenyl-1,2,3,6-tetrahydropyridine-induced parkinsonism syndrome in *Macaca fascicularis*: which midbrain dopaminergic neurons are lost? *Neuroscience* **24**, 161-174.
- Gibb, W. R. G., Fearnley, J. M., and Lees, A. J. (1988) The anatomy and pigmentation of the human substantia nigra in relation to selective neuronal vulnerability. *Ninth Intl. Symp. on Parkinson's Disease Jerusalem*, 6.
- Gimenez-Amaya, J. M. and Graybiel, A. M. (1988) Compartmental origins of the striatopallidal projection in the primate. *Soc. Neurosci. Abstr.* **14**, 156.
- Gimenez-Amaya, J. M. and Graybiel, A. M. (1989) Compartmental origins of the striatopallidal projection in the primate. *Submitted*, .
- Goldman, P. S. and Nauta, W. J. H. (1977) An intricately patterned prefronto-caudate projection in the rhesus monkey. *J. Comp. Neurol.* **177**, 369-386.
- Graybiel, A. M. (1977) Direct and indirect preoculomotor pathways of the brainstem: an autoradiographic study of the pontine reticular formation in the cat. *J. Comp. Neurol.* **175**, 37-78.
- Graybiel, A. M. Neurochemically specified subsystems in the basal ganglia. In *Functions of the Basal Ganglia*. London: Pitman, 1984.

- Graybiel, A. M. (1984) Correspondence between the dopamine islands and striosomes of the mammalian striatum. *Neurosci.* **13**, 1157-1187.
- Graybiel, A. M. (1986) Dopamine-containing innervation of the striatum: subsystems and their striatal correspondents. In *Recent Developments in Parkinson's Disease*, (Edited by Fahn, S.) pp. 1-16. Raven Press, New York.
- Graybiel, A. M. (1986) Neuropeptides in the basal ganglia. In *Neuropeptides in Neurologic and Psychiatric Disease*, (Edited by Martin, J. B. and Barchas, J. D.) pp. 135-161. Raven Press, New York.
- Graybiel, A. M. (1989) Dopaminergic and cholinergic systems in the striatum. In *Neural mechanisms in disorders of movement*, (Edited by Crossman, A. R. and Sambrook, M. A.) pp. 3-15. Libbey, London.
- Graybiel, A. M. and Chesselet, M-F. (1984) Compartmental distribution of striatal cell bodies expressing met-enkephalin-like immunoreactivity. *Proc. Natl. Acad. Sci. USA* **81**, 7980-7984.
- Graybiel, A. M. and Elde, R. P. (1983) Somatostatin-like immunoreactivity characterizes neurons of the nucleus reticularis thalami in the cat and monkey. *J. Neurosci.* **3**, 1308-1321.
- Graybiel, A. M. and Ragsdale, C. W. (1978) Histochemically distinct compartments in the striatum of human, monkey and cat demonstrated by acetylcholinesterase staining. *Proc. Natl. Acad. Sci. USA* **75**, 5723-5726.
- Graybiel, A. M. and Ragsdale, C. W. (1979) Fiber connections of the basal ganglia. *Prog. Brain Res.* **51**, 239-283.
- Graybiel, A. M. and Ragsdale, C. W. (1980) Clumping of acetylcholinesterase activity in the developing striatum of the human fetus and young infant. *Proc. Natl. Acad. Sci. USA* **77**, 1214-1218.
- Graybiel, A. M., and Ragsdale, C. W. (1983) Biochemical anatomy of the striatum. In *Chemical Neuroanatomy*, (Edited by Emson, P. C.) pp. 427-504. Raven Press, New York.
- Graybiel, A. M., Ragsdale, Jr. C. W., Moon-Edley, S. (1979) Compartments in the striatum of the cat observed by retrograde cell labeling. *Exptl. Brain. Res.* **34**, 189-195.
- Graybiel, A. M., Ragsdale, C. W., Yoneoka, E. S., and Elde, R. P. (1981) An immunohistochemical study of enkephalins and other neuropeptides in the striatum of the cat with evidence that the opiate peptides are arranged to form mosaic patterns in register with the striosomal compartments visible by acetylcholinesterase staining. *Neuroscience* **6**, 377-397.

- Graybiel, A. M., Hirsch, E. C., and Agid, Y. A. (1987) Differences in tyrosine hydroxylase-like immunoreactivity characterize the nigrostriatal innervation of striosomes and extrastriosomal matrix. *Proc. Natl. Acad. Sci. U. S. A.* **84**, 303-307.
- Graybiel, A. M., Besson, M-J., and Weber, E. (1989) Neuroleptic-sensitive binding sites in the nigrostriatal system: Evidence for differential distribution of sigma sites in the substantia nigra, pars compacta of the cat. *J. Neurosci.* **9**, 326-338.
- Graybiel, A. M., Flaherty, A. W. and Langer, L. F. (1989) Afferent fiber mosaics in the primate striatum. *Intl. Meeting of the Basal Ganglia Society Sardinia*, .
- Greenfield, J. G. and Bonsaquet, F. D. (1953) The brainstem lesions in Parkinsonism. *J. Neurol. Neurosurg. Psychiatry* **16**, 213-226.
- Groenewegen, H. J. and Russchen, F. T. (1984) Organization of efferent projections of the nucleus accumbens to pallidal, hypothalamic, and mesencephalic structures: a tracing and immunohistochemical study in the cat. *J. Comp. Neurol.* **223**, 347-367.
- Gulley, R. L. and Wood, R. L. (1971) The fine structure of the neurons in the rat substantia nigra. *Tissue Cell* **3**, 675-690.
- Haber, S. and Elde, R. (1982) The distribution of enkephalin immunoreactive fibers and terminals in the monkey central nervous system: An immunohistochemical study. *Neuroscience* **7**, 1049-1095.
- Haber, S. N. and Watson, S. J. (1985) The comparative distribution of enkephalin, dynorphin and substance P in the human globus pallidus and basal forebrain. *Neuroscience* **14**, 1011-1024.
- Hajdu, F., Hassler, R. and Bak, I. J. (1973) Electron microscopic study of the substantia nigra and the strio-nigral projection in the rat. *Z. Zellforsch* **146**, 207-221.
- Hanaway, J., McConnel, J. A., and Netsky, M. G. (1970) Cytoarchitecture of the substantia nigra in the rat. *Am. J. Anat.* **129**, 417-438.
- Hassler, R. (1938) Zur Pathologie der Paralysis Agitans und des post-encephalitischen Parkinsonismus. *J. Psychol. Neurol.* **48**, 387-476.
- Hattori, T., McGeer, P. L., Fibiger, H. C., and McGeer, E. G. (1973) On the source of GABA containing terminals in the substantia nigra. Electron microscopic, autoradiographic and biochemical studies. *Brain Res.* **54**, 103-114.

- Hemphill, M., Holm, G., Crutcher, M., DeLong, M., and Hedreen, J. (1981) Afferent connections of the nucleus accumbens in the monkey. In *Neurobiology of the Nucleus Accumbens*, (Edited by Chronister, R. B. and De France, J. F.) pp. 75-81. Haer Institute, Brunswick, Maine.
- Henderson, Z. (1981) Ultrastructure and acetylcholinesterase content of neurons forming connections between the striatum and substantia nigra of rat. *J. Comp. Neurol.* **197**, 185-196.
- Henderson, Z. and Greenfield, S. A. (1987) Does the substantia nigra have a cholinergic innervation? *Neurosci. Lett.* **73**, 109-113.
- Hendrickson, A., Moe, L., and Nobel, B. (1972) Staining for autoradiography of the central nervous system. *Stain Technol.* **47**, 283-290.
- Hirosawa, K. (1968) Electron microscopic studies on pigment granules in the substantia nigra and locus coeruleus of the Japanese monkey [Macaca fuscata yakui]. *Z. Zellforsch Mikrosk Anat* **88**, 187-203.
- Hirsch, E. C., Graybiel, A. M., Duyckaerts, C, Javoy-Agid, F. (1987) Neuronal loss in the pedunculopontine tegmental nucleus in Parkinson's disease and in progressive supranuclear palsy. *Proc. Natl. Acad. Sci.* **84**, 5976-5980.
- Hirsch, E., Graybiel, A. M., and Agid, Y. A. (1988) Melanized neurons are differentially susceptible to degeneration in Parkinson's disease. *Nature* **334**, 345-348.
- Hokfelt, T., Skirboll, L., Rehfeld, J. F., Goldstein, M., Markey, K., and Dann, O. (1980) A subpopulation of mesencephalic dopamine neurons projecting to limbic areas contains a cholecystokinin-like peptide: Evidence from immunohistochemistry combined with retrograde tracing. *Neuroscience* **5**, 2093-2124.
- Hokfelt, T., Martensson, R., Bjorklund, A., Kleinau, S., and Goldstein, M. (1984) Distributional maps of tyrosine-hydroxylase-immunoreactive neurons in the rat brain. In *Handbook of Chemical Neuroanatomy*, Vol. 2 (Edited by Bjorklund, A. and Hokfelt, T.) pp. 277-379. Elsevier, Amsterdam.
- Hokfelt, T., Everitt, B. J., Theodorsson-Norheim, E., and Goldstein, M. (1984) Occurrence of neurotensin-like immunoreactivity in subpopulations of hypothalamic, mesencephalic and medullary catecholamine neurons. *J. Comp. Neurol.* **222**, 543-559.
- Hong, J. S., Yang, H.-Y. T., Racagni, G., and Costa, E. (1977) Projections of substance P containing neurons from neostriatum to substantia nigra. *Brain Res.* **122**, 541-544.

- Hubbard, J. E. and DiCarlo, V. (1974) Fluorescence histochemistry of monoamine-containing cell bodies in the brain stem of the squirrel monkey *Saimiri sciureus*. *J. Comp. Neurol.* **153**, 369-384.
- Illing, R. B. and Wassle, H. (1979) Visualization of the HRP reaction product using the polarization microscope. *Neurosci. Lett.* **13**, 7-11.
- Inagaki, S. and Parent, A. (1984) Distribution of substance P and enkephalin-like immunoreactivity in the substantia nigra of the rat, cat and monkey. *Brain Res. Bull.* **13**, 319-329.
- Inagaki, S. and Parent, A. (1985) Distribution of enkephalin-immunoreactive neurons in the forebrain and upper brainstem of the squirrel monkey. *Brain Res.* **359**, 267-280.
- Inagaki, S., Kubota, Y. and Kito, S. (1986) Ultrastructural localization of enkephalin immunoreactivity in the substantia nigra of the monkey. *Brain Res.* **362**, 171-174.
- Jellinger, K. (1986) Pathology of parkinsonism. In *Recent Developments in Parkinson's Disease*, (Edited by Fahn, S.) pp. 33-66. Raven Press, New York.
- Jessell, T. M., Emson, P. C., Paxinos, G., and Cuello, A. C. (1978) Topographic projections of substance P and GABA pathways in the striato- and pallido-nigral system: A biochemical and immunohistochemical study. *Brain Res.* **152**, 487-498.
- Jimenez-Castellanos, J. and Graybiel, A. M. (1985) The dopamine-containing innervation of striosomes: nigral subsystems and their striatal correspondents. *Soc. Neurosci. Abstr.* **11**, 1249.
- Jimenez-Castellanos, J. and Graybiel, A. M. (1986) Innervation of striosomes and extrastriosomal matrix by different subdivisions of the midbrain A8-A9-A10 dopamine-containing cell complex. *Soc. Neurosci. Abstr.* **12**, 1327.
- Jimenez-Castellanos, J. and Graybiel, A. M. (1987) Subdivisions of the dopamine-containing A8-A9-A10 complex identified by their differential mesostriatal innervation of striosomes and extrastriosomal matrix. *Neuroscience* **23**, 223-242.
- Jimenez-Castellanos, J. and Graybiel, A. M. (1987) Subdivisions of the primate substantia nigra pars compacta detected by acetylcholinesterase activity. *Brain Res.* **437**, 349-354.

- Jimenez-Castellanos, J. and Graybiel, A. M. (1989) Evidence that histochemically distinct zones of the primate substantia nigra pars compacta are related to patterned distributions of nigrostriatal projection neurons and striatonigral fibers. *Expl. Brain Res.* **74**, 227-238.
- Jimenez-Castellanos, J. and Graybiel, A. M. (1989) Compartmental origins of striatal efferent projections in the cat. *Neuroscience In Press*, .
- Joyce, J. N., Sapp, D. W., and Marshall, J. F. (1986) Human striatal dopamine receptors are arranged in compartments. *Proc. Natl. Acad. Sci. USA* **83**, 8002-8006.
- Juraska, J. M., Wilson, C. J., and Groves, P. M. (1977) The substantia nigra of the rat: A Golgi study. *J. Comp. Neurol.* **172**, 585-600.
- Kanazawa, I., Emson, P. C., and Cuello, A. C. (1977) Evidence for the existence of substance P-containing fibers in the striatonigral and pallidonigral pathways in the rat brain. *Brain Res.* **119**, 447-453.
- Kanazawa, I., Mogaki, S., Muramoto, O., and Kuzuhara, S. (1980) On the origin of substance P-containing fibers in the entopeduncular nucleus and substantia nigra in the rat. *Brain Res.* **184**, 481-485.
- Kemel, M. L., Gauchy, C., Desdab, M. and Glowinski, J. (1989) Striosome and matrix compartments of the cat caudate nucleus: respective roles of muscarinic and nicotinic receptors in the presynaptic control of dopamine release. In *Neural Mechanisms in Disorders of Movement*, (Edited by Crossman, A. and Sambrook, M. A.) pp. (in press). Libbey, London.
- Kent, J. L., Pert, C. B., and Herkenham, M. (1982) Ontogeny of opiate receptors in rat forebrain: visualization by in vitro autoradiography. *Devel. Brain Res.* **2**, 487-504.
- Kim, J. S., Bak, I. J., Hassler, R. and Okada, Y. (1971) Role of gamma-aminobutyric acid (GABA) in the extrapyramidal motor system. 2. Some evidence for the existence of a type of GABA-rich striatonigral neuron. *Exp. Brain Res.* **14**, 95-104.
- Kornhuber J., Kim, J. S., Kornhuber, M. E., and Kornhuber, H. H. (1984) The cortico-nigral projection: Reduced glutamate content in the substantia nigra following frontal cortex ablation in the rat. *Brain Res.* **322**, 124-126.
- Kunkle, H. (1975) Bilateral projections from precentral motor cortex to the putamen and other parts of the basal ganglia. *Brain Res.* **88**, 195-210.

- Kunzle, H. (1978) An autoradiographic analysis of the efferent connections from premotor and adjacent prefrontal regions [areas 6 and 9] in *Macaca fascicularis*. *Brain Behav. Evol.* **15**, 185-234.
- Kusama, T. and Mabuchi, M. (1970) *Stereotaxic Atlas of the Brain of Macaca fuscata*. Univ. Tokyo Press, Tokyo.
- Langer, L. F. and Graybiel, A. M. (1989) Distinct nigrostriatal projection systems innervate striosomes and matrix in the primate striatum. *Brain Res.* **In Press**, .
- Loughlin, S. E. and Fallon, J. H. (1982) Mesostriatal projections from ventral tegmentum and dorsal raphe; cells project ipsilaterally or contralaterally but not bilaterally. *Neurosci. Lett.* **32**, 11-16.
- Loughlin, S. E. and Fallon, J. H. (1983) Dopaminergic and non-dopaminergic projections to amygdala from substantia nigra and ventral tegmental area. *Brain Res.* **262**, 334-338.
- Mai, J. K., Stephens, P. H., Hopf, A. and Cuello, A. C. (1986) Substance P in human brain. *Neuroscience* **17**, 709-739.
- Malach, R. and Graybiel, A. M. (1986) Mosaic architecture of the somatic sensory-reipient sector of the cat's striatum. *J. Neurosci.* **6**, 3436-3458.
- Marshall, J. F., Joyce, J. N., and Sapp, D. W. (1985) Quantitative autoradiography reveals a correlation between heterogeneous distribution of dopamine (D-2) sites and AChE patchiness in the human brain striatum. *Soc. Neurosci. Abstr.* **11**, 207.
- Martres, M. P., Bouthenet, M. L., Sales, N. Sokoloff, P. and Schwartz, J. C. (1985) Widespread distribution of brain dopamine receptors evidenced with [<sup>125</sup>I]iodosulpiride, a highly selective ligand. *Science* **228**, 752-754.
- McLean, S., Skirboll, L. R., and Pert, C. (1985) Comparison of substance P and enkephalin distribution in rat brain: An overview using radioimmunohistochemistry. *Neuroscience* **14**, 837-852.
- Mehler, W. R. and Nauta, W. J. H. (1974) Connections of the basal ganglia and of the cerebellum. *Confin. Neurol.* **36**, 205-222.
- Mesulam, M. M. (1978) Tetramethyl benzidine for horseradish peroxidase neurohistochemistry: a non-carcinogenic blue reaction product with superior sensitivity for visualizing neural afferents and efferents. *J. Histochem. Cytochem.* **26**, 106-117.



- Moon-Edley, S. and Graybiel, A. M. (1983) The afferent and efferent connections of the feline nucleus tegmenti, pedunculopontinus, pars compacta. *J. Comp. Neurol.* **217**, 187-215.
- Moon-Edley, S. and Herkenham, M. (1983) Heterogeneous dopaminergic projections to the neostriatum of the rat: nuclei of origin dictates relationship to opiate receptor patches. *Anat. Rec.* **205**, 120A.
- Mugnaini, E. and Oertel, W. H. (1985) Atlas of the distribution of GABAergic neurons and terminals in the rat CNS as revealed by GAD immunohistochemistry. In *Handbook of Chemical Neuroanatomy*, Vol. 4 (Edited by Bjorklund, A. and Hokfelt, T.) pp. 436-595. Elsevier, Amsterdam.
- Nagai, T., McGeer, P. L. and McGeer, E. G. (1983) Distribution of GABA-T-intensive neurons in the rat forebrain and midbrain. *J. Comp. Neurol.* **218**, 220-238.
- Nagy, J. I., Carter, D. A., and Fibiger, H. C. (1978) Anterior striatal projections to the globus pallidus, entopeduncular nucleus and substantia nigra in the rat: the GABA connection. *Brain Res.* **158**, 15-29.
- Nauta, W. J. H. and Mehler, W. R. (1966) Projections of the lentiform nucleus in the monkey. *Brain Res.* **1**, 3-42.
- Nauta, W. J. H., Smith, G. P., Faull, R. L. M. and Domesick, V. B. (1978) Efferent connections and nigral afferents of the nucleus accumbens septi in the rat. *Neuroscience* **3**, 385-401.
- Newman-Gage, H. and Graybiel, A. M. (1988) Expression of calcium/calmodulin dependent protein kinase in relation to dopamine islands and synaptic maturation of cat striatum. *J. Neurosci.* **8**, 3360-3375.
- Nobin, A. and Bjorklund, A. (1973) Topography of the monoamine neuron systems in the human brain as revealed in fetuses. *Acta Physiol. Scand.* **388**, 1-40.
- Oertel, W. H., Schmechel, D. E., Brownstein, M. J., Tappaz, M. L., Ransom, D. H. and Kopin, I. J. (1981) Decrease of glutamate decarboxylase (GAD)-immunoreactive nerve terminals in the substantia nigra after kainic acid lesion of the striatum. *J. Histochem. Cytochem.* **29**, 977-980.
- Oertel, W. H., Tappaz, M. L., Berod, A., and Mugnaini, E. (1982) Two-color immunohistochemistry for dopamine and GABA neurons in rat substantia nigra and zona incerta. *Brain Res. Bull.* **9**, 463-474.
- Olson, L., Seiger, A., and Fuxe, K. (1972) Heterogeneity of striatal and limbic innervation: highly fluorescent islands in developing and adult rats. *Brain Res.* **44**, 283-288.

- Olszewski, J. and Baxter, D. (1954) *Cytoarchitecture of the Human Brain Stem*. Karger, Basel.
- Palkovits, M., Brownstein, M. J. and Zamir, N. (1984) On the origin of dynorphin and alpha-neo-endorphin in the substantia nigra. *Neuropeptides* **4**, 193-199.
- Parent, A., Descarries, L. and Beaudet, A. (1981) Organization of ascending serotonin systems in the adult rat brain. An autoradiographic study after intraventricular administration of [<sup>3</sup>H]-5-hydroxytryptamine. *Neuroscience* **6**, 115-138.
- Parent, A., Mackey, A., Smith, Y. and Boucher, R. (1983) The output organization of the substantia nigra in primate as revealed by a retrograde double labeling method. *Brain Res. Bull.* **10**, 529-537.
- Parent, A., Mackey, A. and De Bellefeuille, L. (1983) The subcortical afferents to caudate nucleus and putamen in primate: a fluorescence retrograde double labeling study. *Neuroscience* **10**, 1137-1150.
- Parent, A., Bouchard, C. and Smith, Y. (1984) The striatopallidal and striatonigral projections: two distinct fiber systems in primate. *Brain Res.* **303**, 385-390.
- Pert, C. B., Kuhar, M. J., and Snyder, S. H. (1976) Opiate receptors: autoradiographic localization in rat brain. *Proc. Natl. Acad. Sci. USA* **73**, 3729-3733.
- Pickel, V. M., Beckey, S. C., Joh, T. H. and Reis, D. J. (1981) Ultrastructural immunocytochemical localization of tyrosine hydroxylase in the neostriatum. *Brain Res.* **225**, 373-385.
- Poirier, L. J., Giguere, M. and Marchand, R. (1983) Comparative morphology of the substantia nigra and ventral tegmental area in monkey, cat and rat. *Brain Res. Bull.* **11**, 371-397.
- Poitras, D. and Parent, A. (1978) Atlas of the distribution of monoamine-containing nerve cell bodies in the brain stem of the cat. *J. Comp. Neurol.* **179**, 699-718.
- Quirion, R., Gaudreau, P., Martel, J-C., St.-Pierre, S. and Zamir, N. (1985) Possible interactions between dynorphin and dopaminergic systems in rat basal ganglia and substantia nigra. *Brain Res.* **331**, 358-362.
- Ragsdale, C. W. and Graybiel, A. M. (1981) The fronto-striatal projection in the cat and monkey and its relationship to inhomogeneities established by acetylcholinesterase histochemistry. *Brain Res.* **208**, 259-266.

- Ragsdale, C. W. and Graybiel, A. M. (1987) Description of histochemical compartmentation in the cat's ventral striatum. *Unpublished Manuscript* , .
- Ragsdale, C. W. and Graybiel, A. M. (1988) Fibers from the basolateral nucleus of the amygdala selectively innervate striosomes in the caudate nucleus of the cat. *J. Comp. Neurol.* **269**, 506-522.
- Ragsdale, C. W. and Graybiel, A. M. (1988) Multiple patterns of thalamostriatal innervation in the cat. In *Cellular Thalamic Mechanisms*, (Edited by Bentivoglio, M., Macchi, G., and Spreafico, R.) pp. 261-269. Elsevier, Amsterdam.
- Ragsdale, C. W. and Graybiel, A. M. (1989) Corticostriatal projections to striosomes and their affiliation with limbic system subcircuits. *Nature*, *Submitted* , .
- Ragsdale, C. W. and Graybiel, A. M. (1989) The compartmental organization of the thalamostriatal connection in the cat. *Submitted* , .
- Rinvik, E. and Grofova, I. (1970) Observations on the fine structure of the substantia nigra in the cat. *Exp. Brain Res.* **11**, 229-248.
- Rioch, D. McK. (1929) Studies on the diencephalon of carnivora. Part II. Certain nuclear configurations and fiber connections of the subthalamus and midbrain of the dog and cat. *J. Comp. Neurol.* **49**, 121-153.
- Rosner, B. (1986) *Fundamentals of Biostatistics*. Duxbury Press, Boston, Massachusetts.
- Royce, G. J. (1978) Cells of origin of subcortical afferents to the caudate nucleus: a horseradish peroxidase study in the cat. *Brain Res.* **153**, 465-475.
- Royce, G. J. and Laine, E. J. (1984) Efferent connections of the caudate nucleus, including cortical projections to the striatum and other basal ganglia: an autoradiographic and horseradish peroxidase investigation in the cat. *J. Comp. Neurol.* **226**, 28-49.
- Scarnati, E., Proia, A., Campana, E., and Pacitti, C. (1986) A microiontophoretic study on the nature of the putative synaptic neurotransmitter involved in the pedunculopontine-substantia nigra pars compacta excitatory pathway of the rat. *Exp. Brain Res.* **62**, 470-478.
- Schofield, S. P. M. and Everitt, B. J. (1981) The organization of catecholamine-containing neurons in the brain of the rhesus monkey [*Macaca mulatta*]. *J. Anat.* **132**, 391-418.

- Schwyn, R. C. and Fox, C. A. (1974) The primate substantia nigra: a Golgi and electron microscopic study. *J. Hirnforsch* **15**, 95-126.
- Smith, Y. and Parent, A. (1986) Differential connections of caudate nucleus and putamen in the squirrel monkey *Saimiri sciureus*. *Neuroscience* **18**, 347-371.
- Smith, Y., Parent, A., Seguela, P., and Descarries, L. (1987) Distribution of GABA-immunoreactive neurons in the basal ganglia of the squirrel monkey [*Saimiri sciureus*]. *J. Comp. Neurol.* **259**, 50-64.
- Snider, R. S. and Lee, J. C. (1961) *A Stereotaxic Atlas of the Monkey Brain [Macaca mulatta]*. Univ. Chicago Press, Chicago.
- Sternberger, L. A. (1979) *Immunocytochemistry*. Wiley, New York.
- Swanson, L. W. (1982) The projections of the ventral tegmental area and adjacent regions: a combined fluorescent retrograde tracer and immunofluorescent study in the rat. *Brain Res. Bull.* **9**, 321-353.
- Szabo, J. (1979) Striatonigral and nigrostriatal connections. *Appl. Neurophysiol.* **42**, 9-12.
- Szabo, J. (1980) Distribution of striatal afferents from the mesencephalon in the cat. *Brain Res.* **188**, 3-21.
- Szabo, J. (1980) Organization of the ascending striatal afferents in monkeys. *J. Comp. Neurol.* **189**, 307-321.
- Taquet, H., Javot-Agid, F., Cesselin, F., Haman, M., Legrand, J. C. and Agid, Y. (1982) Microtopography of met-enkephalin, dopamine, and noradrenaline in the ventral mesencephalon of human control and parkinsonian brains. *Brain Res.* **235**, 303-314.
- Tennyson, V. M., Barrett, R. E., Cohen, G., Cote, L., Heikkila, R. and Mytilineou, C. (1972) The developing neostriatum of the rabbit: correlation of fluorescence histochemistry, electron microscopy, endogenous dopamine levels and [<sup>3</sup>H]-dopamine uptake. *Brain Res.* **46**, 251-285.
- Thierry, A. M., Deniau, J. M., Herve, D., Chevalier, G. (1980) Electrophysiological evidence for non-dopaminergic mesocortical and mesolimbic neurons in the rat. *Brain Res.* **201**, 210-214.
- Turner, B. H., Wilson, J. S., McKenzie, J. C., Richtand, N. (1988) MPTP produces a pattern of nigrostriatal degeneration which coincides with the mosaic organization of the caudate nucleus. *Brain Res.* **473**, 60-64.

- Uhl, G. R., Hedreen, J. C. and Price, D. L. (1985) Parkinson's disease: loss of neurons from the ventral tegmental area contralateral to therapeutic surgical lesions. *Neurology* **35**, 1215-1218.
- Ungerstedt, U. (1971) Stereotaxic mapping of the monoamine pathways in the rat brain. *Acta physiol. scand.* **197**, 1-48.
- Usunoff, K. G., Hassler, R., Romansky, K., Usunova, P., Wagner, A. (1976) The nigrostriatal projection in the cat. *J. Neurol. Sci.* **28**, 256-288.
- Van der Kooy, D., Coscina, D. V. and Hattori, T (1981) Is there a non-dopaminergic nigrostriatal pathway? *Neuroscience* **6**, 345-357.
- Voorn, P. (1988) The dopaminergic innervation of the striatum in the rat. In *The Dopaminergic Innervation of the Striatum in the Rat*, pp. 5-66. Free University Press, Amsterdam.
- Voorn, P., Kalsbeek, A., Jorritsma-Byham, B. and Groenewegen, H. J. (1988) The pre- and postnatal development of the dopaminergic cell groups in the ventral mesencephalon and the dopaminergic innervation of the striatum of the rat. *Neuroscience* **25**, 857-888.
- Voorn, P., Gerfen, C. R., and Groenewegen, H. J. (1988) The compartmental organization of the ventral striatum of the rat: immunohistochemical distribution of enkephalin, substance P, dopamine and calcium-binding protein. In *The Dopaminergic Innervation of the Striatum in the Rat*, pp. 67-78. Free University Press, Amsterdam.
- Walaas, I. and Fonnum, F. (1980) Biochemical evidence for gamma-aminobutyrate containing fibers from the nucleus accumbens to the substantia nigra and ventral tegmental area in the rat. *Neuroscience* **5**, 63-72.
- Waters, C. M., Peck, R., Rossor, M., Reynolds, G. P., and Hunt, S. P. (1988) Immunocytochemical studies on the basal ganglia and substantia nigra in Parkinson's disease and Huntington's chorea. *Neuroscience* **25**, 419-438.
- White, L. E. (1981) Development and morphology of human nucleus accumbens. In *Neurobiology of the Nucleus Accumbens*, (Edited by Chronister, R. B. and De France, J. F.) pp. 198-209. Haer Institute, Brunswick, Maine.
- Wilson, C. J. and Xu, Z. C. (1988) Morphological differences between corticostriatal fibers terminating in the patch and matrix compartments of the rat neostriatum. *Soc. Neurosci. Abstr.* **14**, 75.
- Wilson, J. S., Turner, B. H., Morrow, G. D., and Hartman, P. J. (1987) MPTP produces a mosaic-like pattern of degeneration in the caudate nucleus of dog. *Brain Res.* **423**, 329-332.

- Wright, A. K. and Arbuthnott, G. W. (1981) The pattern of innervation of the corpus striatum by the substantia nigra. *Neuroscience* **6**, 2063-2067.
- Zaborszky, L., Alheid, G. F., Beinfeld, M. C., Eiden, L. E., Heimer, L. and Palkovits, M. (1985) Cholecystokinin innervation of the ventral striatum: A morphological and radioimmunological study. *Neuroscience* **14**, 427-453.
- Zamir, N., Palkovits, M., Weber, E., Mezey, E., and Brownstein, M. J. (1984) A dynorphinergic pathway of Leu-enkephalin production in rat substantia nigra. *Nature* **307**, 643-645.